People's Democratic Republic of Algeria
Ministry of Higher Education and Scientific Research

University Amar Thelidji- Laghouat
Faculty of Technology
Department of Process Engineering

MASTER'S MANUSCRIT

Presented by:

SEBA Fatheddine

TAOUTI Mohammed Belkacem

DOMAIN: Sciences and Technologies

Branch: Process Engineering

MAJOR: Chemical Engineering

This work is entitled:

Calculation methods investigation, of some thermodynamic & volumetric properties, for some non-ideal fluids.

Supervisory and examining committee:

First and last name	Grade	Quality
Mme. BELHADJ Soraya	MCA	President
Mr. SAIDAT Boubekeur	Full Pr.	Examiner
Mr. BOUREZG Mohammed Tahar	MAA	Supervisor

Promotion: JUNE 2024

Acknowledgment

At the outset, we express our deepest gratitude to 'Allah', for bestowing upon us life, health, and the strength to complete this work.

This thesis research was conducted at the Process Engineering Department of the University of Laghouat Amar Thelidji.

We owe our profound thanks to our supervisor, ***Dr. BOUREZG Mohammed Tahar****, whose unwavering guidance, daily support, and exceptional human qualities were instrumental in the successful completion of this work, both scientifically and morally.*

We extend our sincere thanks to the members of the jury: ***Mr****., president, and* ***Mr.*** *Examiner, for their time and effort in reviewing and evaluating this work.*

We also express our gratitude to the head of the department, ***Mr. Benalia Mokhtar****, and his deputy,* ***Mr. Tounsi Aissa****, along with all the faculty members of the Process Engineering Department, for their continuous support.*

We are deeply thankful to all the teachers in the Process Engineering Department who have provided us with knowledge and guidance throughout our academic journey.

Lastly, we extend our heartfelt thanks to our colleagues and to everyone who has been a part of our lives and contributed significantly to the successful completion of this work in the best possible conditions.

Dedication

I dedicate this work

*To **my dear honorable**, **strong mother**, you are the epitome of strength, kindness, and unwavering devotion. Your love has been a constant source of encouragement throughout my life. Your prayers and blessings fueled my studies in a way no words can express. No dedication could ever truly repay the sacrifices you've made for me, from my childhood to this day.*

*To **my dear father**, words can't express the depth of my love, respect, and gratitude for you. This achievement wouldn't be possible without the sacrifices you made for my education. I dedicate it to you, a token of my immense love. May God bless you with continued health, happiness, and a long life.*

*To **my dear sister**, I am truly blessed to have you as my sister. Your friendship, loyalty, and love are treasures I hold dear. With every passing day, my admiration for you grows stronger. You are an epitome of grace, resilience, and compassion, and I am forever grateful for your positive influence on my life. I dedicate this work to you with my best wishes for happiness, health and success.*

*And **my dear friends**, words seem to fall short when I try to express how much your friendship means to me. The bond we share and the memories we've created together are truly irreplaceable. Please know that I cherish each and every one of you. With all my love*

SEBA FATHEDDINE

Dedication

With the grace of Allah Almighty, who has blessed me with the courage, determination, and strength to complete this thesis,

I dedicate this humble work:

*To my dear father **Brahim**,*

whose patience, understanding, and encouragement have provided me with immense comfort and strength. His fatherly warmth has been my steadfast support throughout this journey.

*To my dear mother **Souad**,*

whose unwavering efforts and endless sacrifices have guided me to this achievement. Her boundless love and dedication, despite all hardships, have been my constant source of inspiration.

*To my wonderful sisters: **Maria**, **Soumaya**, and **Sarah**, and to her delightful children, **Khadidja**, **Amani**, and **Yahia**,*

whose presence brings joy and motivation to my life.

*To my esteemed uncle, **Professor Taouti Med Benabdallah**,*

whose scholarly wisdom and teaching have profoundly shaped my academic path.

To my cherished extended and immediate family, whose love and support have been a cornerstone in my life.

*To my dear friends I mean my brothers: **Saad**, **Rahim**, **Hmaida**, and **Fethi** and my cousin and my brother **Med Bachir**,*

whose camaraderie and encouragement have been invaluable.

To all my friends from the class of 2024, whose shared experiences and support have enriched my academic journey.

And to all those who have offered their help and support during my work. Your contributions have been instrumental in completing this thesis, and I am deeply grateful for your presence in my life.

TAOUTI MED BELKACEM

List of abbreviations & symbols

EOS: Equation of state.

PVT: Pressure-molar volume-temperature.

P-V: Pressure-molar volume

P-T : Pressure- temperature.

VLE: Vapor–liquid equilibrium.

RMSE: Root Mean Squared Error.

RE: Relative Error.

NIST: National Institute of Standards and Technology.

VdW: Van der Waals.

RK: Redlich-Kwong.

SRK: Soave-Redlich-Kwong.

PR: Peng-Robinson.

CSP: Corresponding States Principle.

ω: Acentric Factor**.**

Pc: Critical pressure.

Tc: Critical temperature.

Vc: Critical molar volume.

Pr: Reduced pressure.

Tr: Reduced temperature.

Vr: Reduced molar volume.

Table of figures

List of tables

Table of Contents

General Introduction

Ever wondered how engineers predict the volume a fluid occupies when it transforms between liquid and vapor? This crucial property, known as saturation volume, plays a vital role in countless industrial processes, from designing efficient power plants to optimizing desalination units. Traditionally, measuring saturation volume has been a cumbersome affair, requiring specialized equipment and meticulous procedures. But what if there was a more efficient and cost-effective way? (1) (2).

Equation-of-State models, a powerful tool for predicting fluid properties based on readily measurable parameters. By harnessing the power of these models, we can potentially unlock a new level of accuracy and efficiency in calculating saturation volumes. Imagine being able to estimate this crucial property with just a temperature and pressure reading, bypassing the complexities of traditional methods. This not only saves time and resources but also opens doors to explore the behavior of fluids under extreme conditions or those with complex properties, previously inaccessible through direct measurement.

The Potential of EOS Models Goes Beyond Efficiency: While the ability to calculate saturation volume quickly and cost-effectively is a game-changer, the true power of EOS models lies in their potential to unlock entirely new realms of understanding. These models aren't just about replicating known behavior; they can help us predict how fluids might behave under previously unimaginable conditions. Imagine designing next-generation heat engines that operate at extreme pressures or formulating advanced refrigerants for unexplored temperature ranges. EOS models, coupled with our ever-evolving understanding of intermolecular interactions, can pave the way for groundbreaking discoveries in the field of thermodynamics and beyond. By embracing this new approach, we can not only optimize existing processes but also push the boundaries of what's possible in the world of fluid mechanics.

Studies like [Twu et al., 1999] demonstrated the effectiveness of the Peng-Robinson PR model for hydrocarbon fluids. The PR model excels at predicting PVT relationships due to its ability to account for non-idealities in these fluids, including molecular shape and attractive forces. This translates to accurate predictions of density, compressibility, vapor pressure, and ultimately, liquid saturation volume - a key parameter in designing equipment for processes like distillation and refrigeration.

The findings of this study will contribute to a better understanding of EOS model selection for accurately representing the behavior of CO2 and water across various applications. This knowledge is valuable in fields like thermodynamics, chemical engineering, and environmental science. (3)

This research aims to investigate, how accurately do EOS models, particularly cubic EOS, predict the phase behavior of CO2 and water compared to Experimental data, here we will try to explore, if this kind of EOS, are going to be able to model the phase properties of these two real fluids

To find an answer for those questions, we embark on a two-chapter journey. Chapter 1, titled "**PVT Relations & Equations of State Evolution,**" lays the groundwork by delving into the theoretical foundations of these models. This chapter will establish a robust understanding of PVT relationships and how EOS models have evolved to represent them.

Chapter 2, titled "**Evaluation of Cubic EOS Ability to Represent PVT Relations for Carbon Dioxide & Water,**" delves deeper into the heart of the investigation. Here, we unveil the methodology employed to assess the performance of cubic EOS models for both CO2 (a non-polar fluid) and water (a polar fluid). This chapter will showcase the meticulous process of plotting experimental isotherms, followed by the critical step of calculating and superimposing these calculated isotherms over the experimental data. This visualization will serve as a powerful tool for evaluating the prediction accuracy of the EOS models. We will then delve into the quantitative analysis using established metrics like RMSE calculations. These calculations, along with insightful interpretations, will expose the accuracy levels and limitations of the models. Additionally, we explore how molecular shape affects the behavior of polar fluids as described by cubic EOS models. This analysis leverages the concept of Reduced Coordinates (Back to Zero Parameters Model), a simplified thermodynamic approach where properties are expressed in terms of dimensionless quantities like Pr and Tr. By plotting actual pressure PR versus Tr for water and co2 with different (ω), we can gain a deeper understanding of this relationship. The acentric factor, a key parameter reflecting molecular shape, plays a crucial role in this analysis. Finally, the general conclusion will bring all the findings together, drawing clear insights and deductions from our exploration. This comprehensive analysis will focus on the potential of cubic EOS models for polar fluids and provide valuable forward-looking perspectives for future research and model development.

Chapter I

PVT Relations & Equations of State Evolution.

I.1. Introduction

Predicting the behavior of real-world substances under various conditions is a cornerstone of numerous scientific and engineering disciplines. At the heart of this lies the relationship between pressure, volume, and temperature (PVT) for pure substances. EOS capture these crucial PVT relationships, providing a powerful tool to unlock the secrets of a substance's thermodynamic properties and phase behavior.

However, accurately modeling real-world fluids requires venturing beyond the limitations of basic EOS models. These limitations stem from the inherent simplicity of treating molecules as perfect spheres. In our exploration, we will delve into the concept of the acentric factor, a key parameter that bridges the gap between idealized and real gas behavior. The acentric factor accounts for a molecule's shape and size, allowing us to refine cubic EOS models and achieve a more comprehensive description of real fluids. Furthermore, by employing RMSE analysis, we can objectively compare the effectiveness of different cubic EOS models for a specific fluid.

This journey through PVT relations for pure substances will begin with foundational concepts, laying the groundwork for understanding idealized gas behavior. We will then progressively explore more advanced topics, investigating the intricacies of various EOS models and their limitations. By incorporating the acentric factor and utilizing RMSE analysis, we will equip ourselves to navigate the complexities of real gas behavior and identify the most accurate EOS model for a given system. This comprehensive approach will ultimately lead to a deeper understanding and more reliable predictions of real gas behavior in practical applications.

So, get ready, and let's hit the road!

I.2. PVT relations for pure substance

A substance that has a definite chemical composition throughout is called a pure substance. Even though it may exist in multiple phases, its chemical composition must remain constant in all phases.

Understanding the intricate relationship between pressure, volume, and temperature for pure substances is crucial across various scientific and engineering fields.

PVT relations serve as powerful tools for analyzing and visualizing how a substance behaves under different conditions. These relations offer insights into thermodynamic properties, phase transitions, and critical points, enabling the design and optimization of processes in fields like chemical engineering, thermodynamics, and material science.

Common PVT diagrams, like Pressure-Volume (PV) and Pressure-Temperature (PT), provide valuable visual representations of how a substance's volume changes with pressure (at constant temperature) or how its pressure varies with temperature (at constant volume). These diagrams are invaluable assets for predicting a substance's behavior and troubleshooting processes across diverse scientific and engineering endeavors (4).

I.2.a. P-V diagram

The PV diagram is a valuable tool for understanding the behavior of a pure substance under different pressure and volume conditions at constant temperatures. It can be used to predict phase transitions, such as boiling, and to determine the thermodynamic properties of the substance.

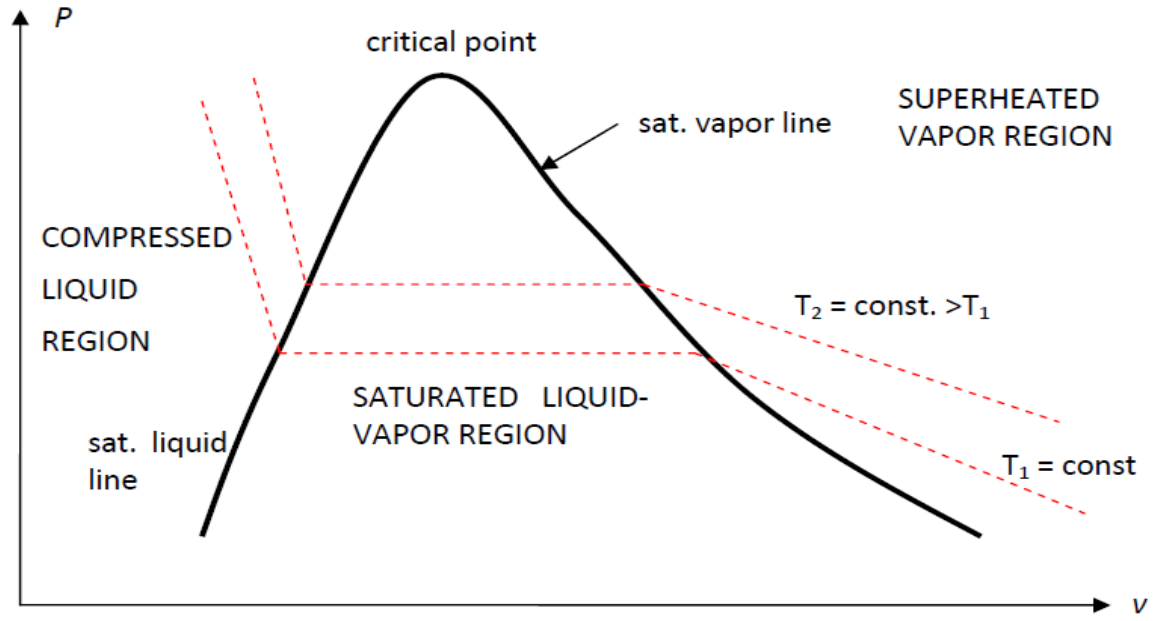

Figure I. 1: P-v diagram of a pure substance. (5)

- **Examples of some p-v diagrams of pure substances like (Carbon dioxide & water):**

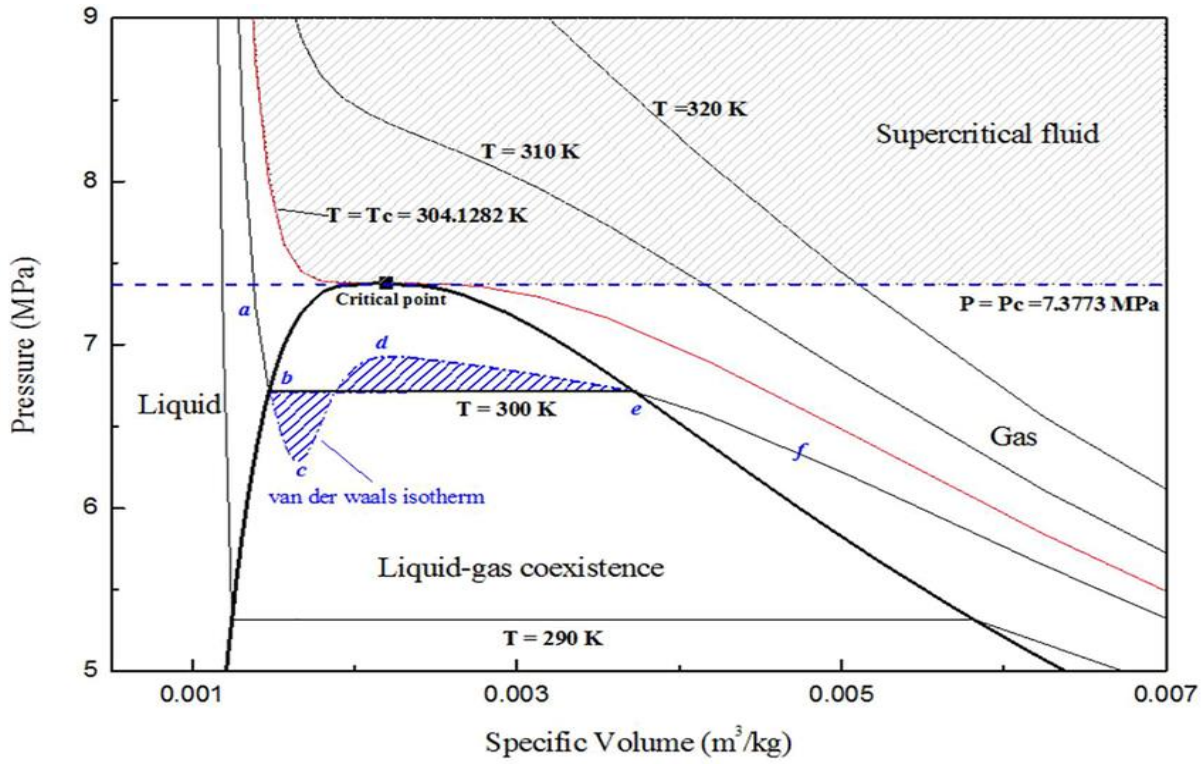

Figure I. 2: P-V diagram of CO2. (6)

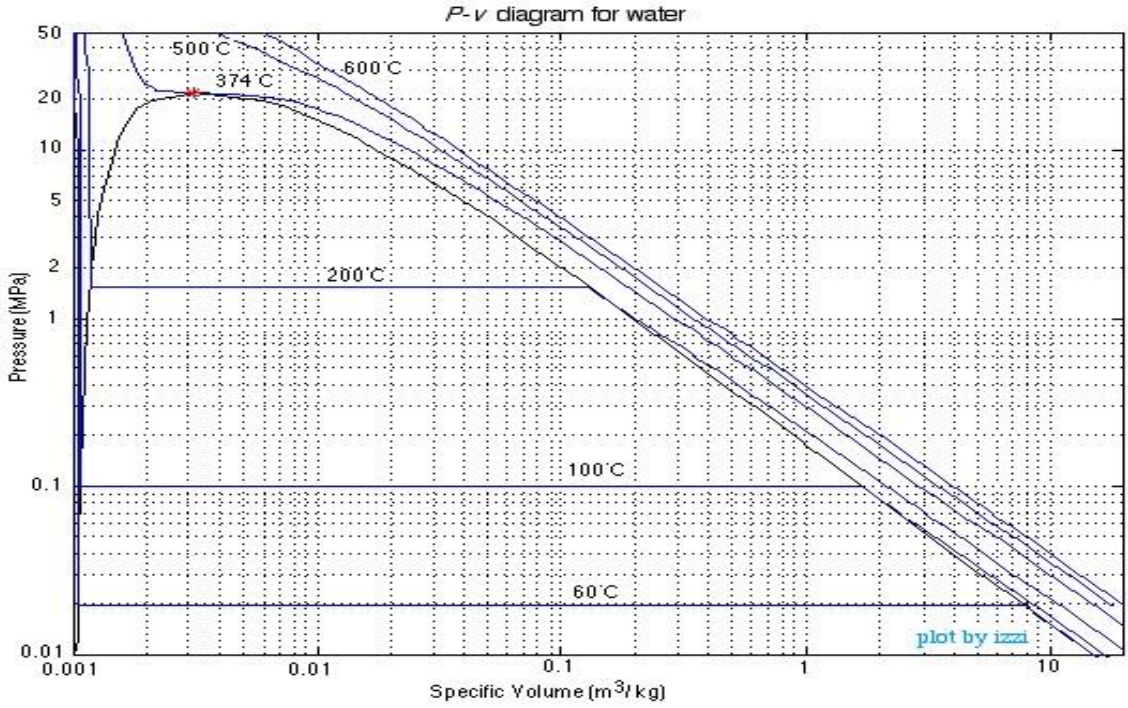

Figure I. 3: P-V diagram of H2O. (7)

I.2.b. P-T diagram (phase change)

A phase diagram shows the distinct phases of a substance at different temperatures and pressures. Most pure substances have three lines showing the solid, liquid, and gas phases. Matter (like CO2) which has a triple point above 1 atm sublimates under atmospheric conditions (dry ice). Water behaves differently and expands during freezing. This property has significant implications in various scientific and engineering fields, making it an interesting topic to explore. (5)

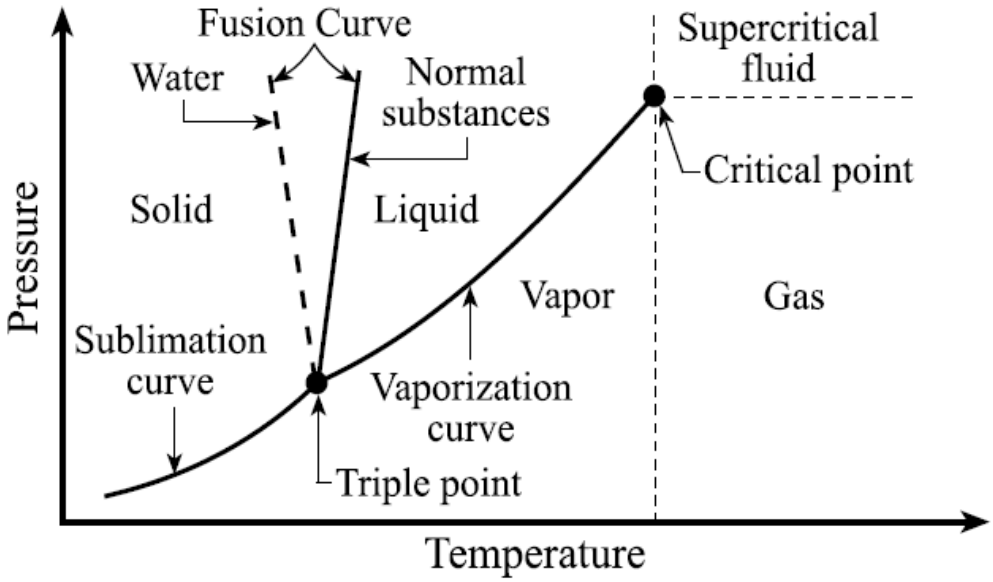

Figure I. 4: Phase diagram for a pure substance. (4)

Note:

The term "vapor" is often used to describe a gas that is close to its condensation point, the temperature at which it will condense into a liquid. In the diagram, the saturated vapor region is the region where the vapor exists close to its condensation point. On the other hand, the superheated vapor region refers to the region where the vapor is at a higher temperature and is not close to condensing. (8)

- **Examples of some P-T diagrams of pure substances like (Carbon dioxide & water):**

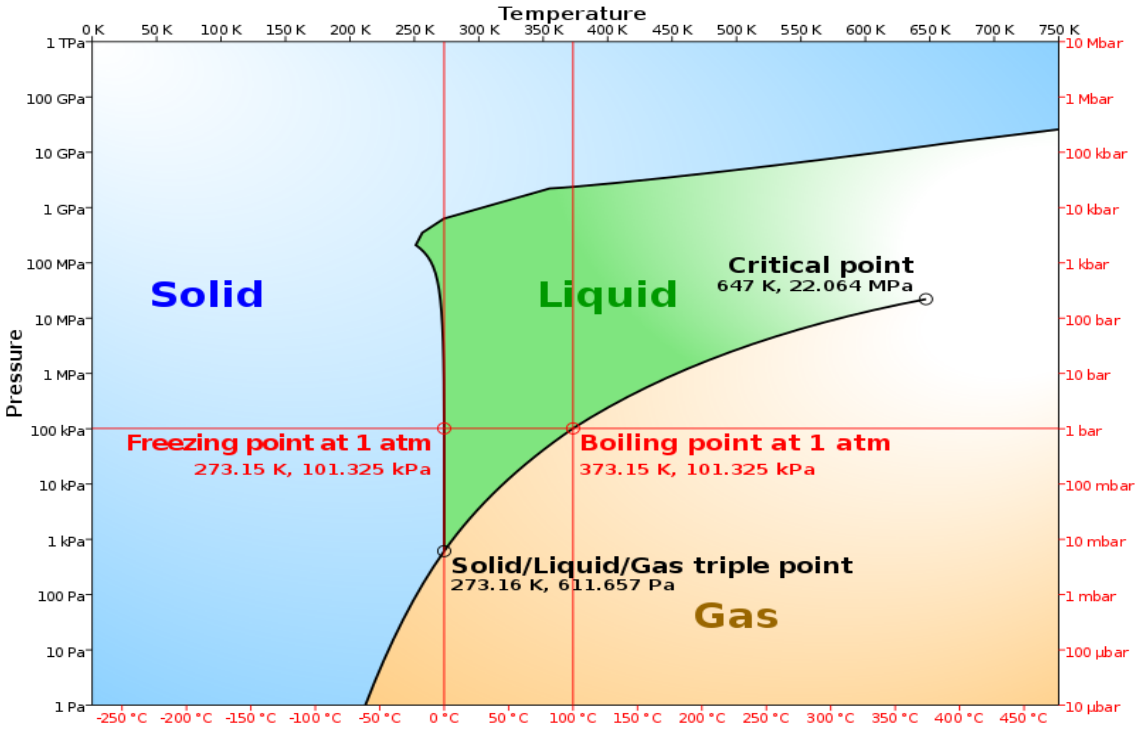

Figure I. 5:Phase diagram of water. (9)

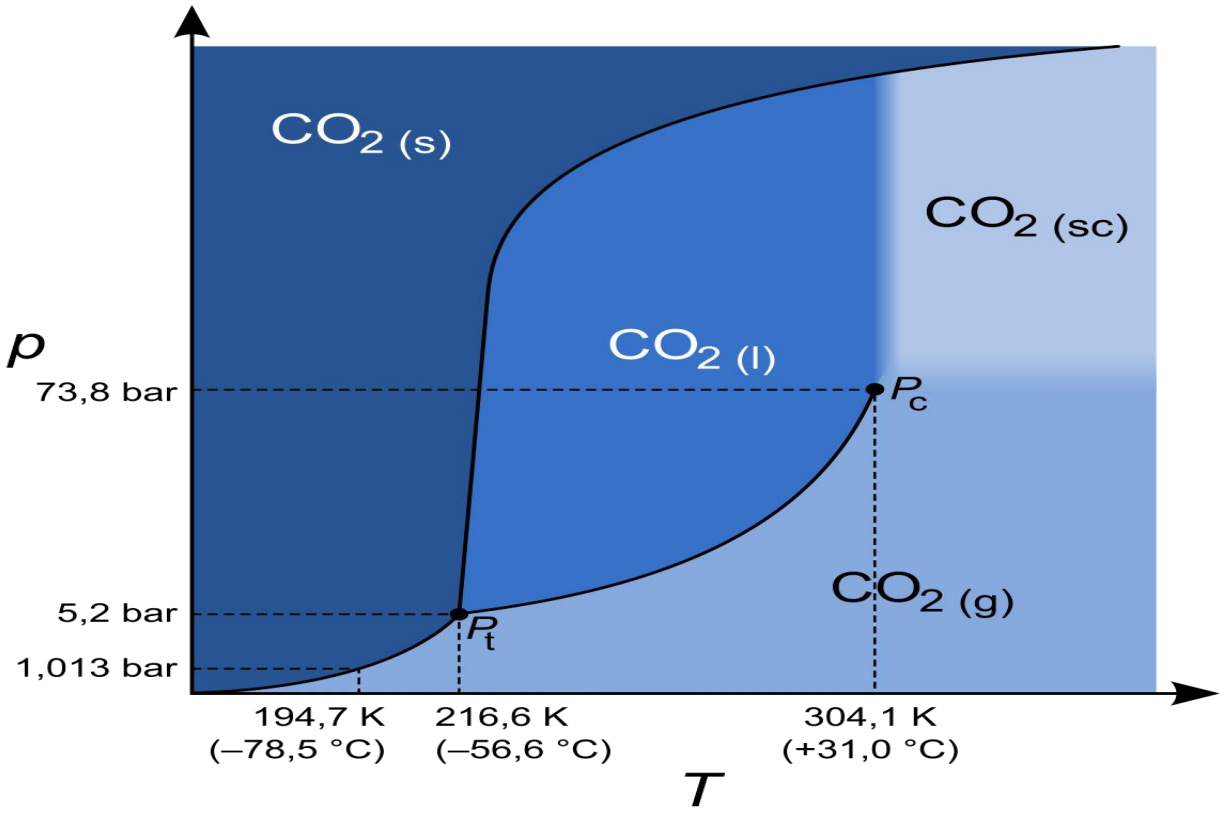

Figure I. 6:Phase diagram of carbon dioxide. (10)

- The behavior of a substance can often be represented by EOS, which are mathematical equations that correlate the PVT properties of a substance. Some well-known equations of state include the Ideal Gas Law, VdW equation, RK equation, and PR equation, among others. This is what we will see in the next part.

I.3. PVT relations & equations of state EOS

"Consider a closed system, in a vessel so equipped that the pressure, volume, and temperature may be easily measured. If the volume is set at some arbitrary value and the temperature is maintained at a specific value, then the pressure will be fixed at a definite value. Once the V and T are chosen, then the value of P at equilibrium is fixed. That is, of the three thermodynamic coordinates P, V, and T, only two are independent variables. There exists an equation of equilibrium which connects the thermodynamic coordinates and which robs one of them of its independence."

"Such an equation, called an EOS, is a mathematical function relating the appropriate thermodynamic coordinates of a system in equilibrium. Every thermodynamic system has its own EOS, although in some cases the relation may be so complicated that it cannot be expressed in terms of simple mathematical functions. For a closed system, the EOS relates the temperature to two other thermodynamic variables."

"An EOS expresses the individual peculiarities of one system as compared with another system and must, therefore, be determined either by experiment or by molecular theory. A general theory like thermodynamics, based on general laws of nature, is incapable of generating an EOS for any substance. An EOS is not a theoretical deduction from the theory of thermodynamics, but is an experimentally derived law of behavior for any given pure substance. It expresses the results of experiments in which the thermodynamic coordinates of a system were measured as accurately as possible, over a range of values. An EOS is only as accurate as the experiments that led to its formulation, and holds only within the range of values measured. As soon as this range is exceeded, a different form of EOS may be required." (11). (12)

- In this part, we aim to explore the EOS more comprehensively and understand why there is a requirement for an alternative form of state equations. We will delve deeper into the intricacies of these equations and gain a better understanding of their significance, so let's go.

I.3.a. Kinetic theory for ideal gases (zero parameters)

In the context of kinetic theory for ideal gases with "zero parameters," it doesn't literally mean there are zero properties considered. Instead, it refers to a simplified model that ignores certain factors to make it easier to understand the basic principles.

"Any equation that relates the pressure, temperature, and specific volume of a substance is called an EOS. There are many equations of state, some simple and others very complex. The simplest and best-known EOS for substances in the gas phase is the Ideal Gas EOS." (11). (12)

An ideal gas is an imaginary gas that satisfies the following conditions:

- Negligible interactions between the molecules,
- Its molecules occupy no volume (negligible molecular volume),
- Collisions between molecules are perfectly elastic — this is, no energy is lost after colliding.

We recognize that this fluid is imaginary because — strictly speaking — there are no ideal gases. In any fluid, all molecules are attracted to one another to some extent. However, the ideal approximation works best at some limiting conditions, where attraction forces can be considered to be weak. In fact, ideal behavior may be approached by real gases at low pressures (close to atmospheric) and high temperatures. Note that at low pressures and high temperatures, the distance between any pair of gas molecules is great. Since attraction forces weaken with distance, we have chosen a condition where attraction forces may be neglected. In conclusion, we consider a gas ideal when each molecule behaves as if it were alone molecules are so far apart from each other that they are not affected by the existence of other molecules. (13)

$$PV = nRT \tag{1}$$

The behavior of ideal gases has been studied exhaustively and can been extensively described by mathematical relationships.

- P: Absolute pressure
- V: Volume of gas
- n: Number of moles of the gas
- R: Universal Gas Constant
- T: Absolute temperature in degrees Rankine or Kelvins

If we construct the P-v diagram for an ideal gas at a given temperature, we end up with the isotherm shown in Figure I.7.

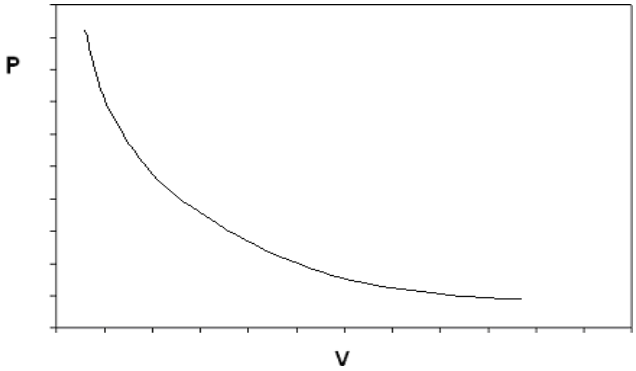

Figure I. 7: Isotherm for an Ideal Gas. (13)

The ideal gas model predicts two distinct behaviors for fluids under extreme conditions. First, as pressure approaches zero, the volume of the gas expands infinitely, which aligns with our real-world experience. Second, as pressure tends towards infinity, the volume of the gas also approaches infinity, suggesting that matter essentially disappears under extremely high pressure. These predictions arise from the foundational assumptions of the ideal gas model. (13)

- Transitioning from the ideal gas law to the VdW equation becomes necessary when dealing with gases under conditions where the ideal gas assumptions no longer hold, such as when pressures are high or temperatures are low. By accounting for particle volume and intermolecular forces, the VdW equation provides a more realistic description of gas behavior in these situations. In the upcoming part, we will delve deeper into it.

I.3.b. Van der WAALS theory (two parameters EOS)

Even though (VdW EOS) has been around for more than one hundred years, we still recognize VdW' achievements as crucial in revolutionizing our thinking about EOS. We talk about VdW EOS because of pedagogical reasons, not because it finds any practical application in today's world. In fact, VdW EOS is not used for any practical design purposes. However, most of the EOS being used widely today for practical design purposes have been derived from VdW EOS.

The contributions of VdW EOS can be summarized as follows:

- It radically improved predictive capability over ideal gas EOS,
- It was the first to predict continuity of matter between gas and liquid,
- It formulated the Principle of Corresponding States (PCS),
- It laid foundations for modern cubic EOS.

In his PhD thesis in 1873, VdW proposed to semi-empirically remove the main key "weaknesses" that the ideal EOS carried with it. Essentially, what he did was to look again at the basic assumptions that underlie the ideal EOS, which we have listed above.

VdW accounted for the non-zero molecular volume and non-zero force of attraction of a real substance. He realized that there is a point at which the volume occupied by the molecules cannot be neglected. One of the first things VdW recognized is that molecules must have a finite volume, and that volume must be subtracted from the volume of the container. At the same time, he modified the pressure term to acknowledge the fact that molecules do interact with each other though cohesive forces. These are the two main valuable recognitions that he introduced.

The ideal EOS states

$$(P)(\bar{v}) = RT \tag{2}$$

VdW focused his attention on modifying the terms "P" and "$\bar{v}$" in the original ideal gas law by introducing an appropriate correction. Looking back at the inequality of equation (1), VdW proposed that the difference of both pressures is the result of the attraction forces — cohesive forces — neglected in the ideal model (2) and thus,

$$P_{ideal} = P_{real} + \frac{a}{\bar{v}^2} \tag{3}$$

Next, VdW took care of the inequality in equation (1) .Any particle occupies a physical space; hence, the space available to the gas is less than the total volume of its container. Let us say we can experimentally determine the actual physical space that all the molecules in the container occupy, and that we call it "b", or the co-volume. VdW then proposed:

$$\bar{v}_{available} = \bar{v}_{total} - b \tag{4}$$

The inclusion of a parameter "b" (co-volume) recognizes the role of repulsive forces. Repulsive forces prevent molecules from "destroying" one another by not letting them get too close. In a condensed state, there is a maximum allowable "closeness" among molecules. Therefore, it is because of repulsive forces that we cannot compress the volume of a fluid beyond its co-volume value "b". If the molecules get too close to each other, repulsion forces take over to prevent their self-destruction.

In summary, VdW proposed to correct the pressure and volume terms of the ideal model represented by equation (2). The "new" modified-ideal EOS becomes:

$$P = \frac{RT}{\bar{v}-b} - \frac{a}{\bar{v}^2} \tag{5}$$

where:

- $\bar{v}$ = molar volume
- "a" and "b" are constants that are specific to each component. However, the numerical value of "R" depends on the system of units chosen.

Now let's learn how to find the equation of "a" and "b"

We saw in our discussion of critical phenomena that the mathematical definition of the critical point is:

$$\left(\frac{\partial P}{\partial \bar{v}}\right)_{Cr\ Pt} = 0 \tag{6}$$

$$\left(\frac{\partial^2 P}{\partial \bar{v}^2}\right)_{Cr\ Pt} = 0 \tag{7}$$

In other words, the critical isotherm on a p-$\bar{v}$ diagram has a point of inflection. Equations (6) and (7) constitute a set of two equation in two unknowns, $\bar{v}$, and T. One can test to see if an approximate EOS gives a critical point by calculating these two derivatives for the EOS and trying to solve the pair of equations. If a solution exists (and T and V are neither zero or infinity) then we say that the EOS has a critical point.

Let's use this test to see if a VdW gas has a critical point. First, we have to solve the VdW EOS for pressure P (eqt 5), which become (5)'at the critical point:

$$P_c = \frac{RT_c}{v_c - b} - \frac{a}{v_c^2} \tag{5}'$$

Now we can take the derivatives in Equations 6 and 7 and set them (independently) equal to zero.

$$-\frac{nRT_c}{(v_c - b)^2} + \frac{2a}{v_c^2} = 0 \tag{8}$$

And

$$-\frac{2nRT_c}{(v_c-b)^3}+\frac{6a}{v_c^4}=0 \quad (9)$$

After resolution of this system of equation for a, b & Vc, we obtain:

$$a=\frac{27}{64}.\frac{(RT_c)^2}{P_c} \quad (10)$$

$$b=\frac{1}{8}.\frac{RT_c}{P_c} \quad (11)$$

$$v_c=3.b=\frac{3}{8}.\frac{RT_c}{P_c} \quad (12)$$

As can be inferred from their definitions, “a” and “b” are different for different substances

With

- a: attractive forces between molecules
- b: the volume occupied by one mole of the molecules of a gas)

- By accounting for these factors, the VdW equation provides a more accurate description of real gas behavior compared to the ideal gas law. But still found some limitations. (14)

➢ **limitations of the VDW Equation:**

- **Accuracy at High Pressures and Low Temperatures:** The VdW equation struggles at high pressures and low temperatures, where real gases start to condense into liquids. It doesn't capture the behavior of gases near their critical point, the point where gas and liquid phases become inseparable.
- **Oversimplified Interactions:** The VdW model treats gas molecules as attractive spheres with a fixed volume. This is a good starting point, but real molecules can have more complex shapes and attractions like water & carbon dioxide.
- **Limited to Single Component Systems:** The VdW equation applies well to single-component gases, but not to mixtures where the interactions between different gas molecules become important. (15)
  - Overall, the VdW equation is a valuable tool for understanding real gases, but it's important to remember its limitations, especially when dealing with gases at low temperatures and high pressures. For better accuracy in these regimes, more complex equations of state are

needed. Which prompts us in the next part to learn about these equations including the RK (Redlich & Kwong) equation.

I.3.c. Redlich & Kwong EOS

The VdW equation, formulated in 1873 by Johannes Diderik VdW, is generally regarded as the first somewhat realistic EOS (beyond the ideal gas law) equation 05

However, its modeling of real behavior is not sufficient for many applications, and by 1949, had fallen out of favor, with the Beattie–Bridgeman and Benedict–Webb–Rubin equations of state being used preferentially, both of which contain more parameters than the VdW equation. The Redlich–Kwong equation was developed by Redlich and Kwong while they were both working for the Shell Development Company at Emeryville, California. Kwong had begun working at Shell in 1944, where he met Otto Redlich when he joined the group in 1945. The equation arose out of their work at Shell - they wanted an easy, algebraic way to relate the pressures, volumes, and temperatures of the gasses they were working with - mostly non-polar and slightly polar hydrocarbons (the Redlich–Kwong equation is less accurate for hydrogen-bonding gases). It was presented jointly in Portland, Oregon at the *Symposium on Thermodynamics and Molecular Structure of Solutions* in 1948, as part of the 14th Meeting of the American Chemical Society. The success of the Redlich–Kwong equation in modeling many real gases accurately demonstrate that a cubic, two-parameter EOS can give adequate results, if it is properly constructed. After they demonstrated the viability of such equations, many others created equations of similar form to try to improve on the results of Redlich and Kwong. (16)

The Redlich–Kwong equation is formulated as:

$$P = \frac{RT}{\bar{v}-b} - \frac{a}{\sqrt{T}\bar{v}(\bar{v}+b)} \tag{13}$$

where:

- *a* is a constant that corrects for attractive potential of molecules,
- *b* is a constant that corrects for volume.

The constants are different depending on which gas is being analyzed. The constants can be calculated from the critical point data of the gas:

$$a = 0.42748\,\frac{R^2 T_c^{2.5}}{P_c} \tag{14}$$

$$b = 0.08554\ \frac{RT_c}{P_c} \tag{15}$$

Where:

- T_c is the temperature at the critical point
- P_c is the pressure at the critical point. (17)

But also, the RK equation have limitations specially in liquid state

- **Limited Accuracy for Complex Fluids:** The RK EOS struggles to accurately predict the behavior of highly polar or complex fluids like hydrocarbons. These molecules have intricate structures and non-central forces that the two-parameter RK EOS cannot fully capture.
- **Overestimation of Pressure:** The EOS tends to overestimate pressure, especially at low temperatures and high pressures. While this might be acceptable for preliminary calculations, it can lead to inaccurate predictions in certain applications.

- Following the VdW equation, which provides a basic framework for real gas behavior, the RK EOS offers a more sophisticated theoretical approach. RK incorporates temperature-dependent terms $\sqrt{T}$ to account for attractive intermolecular forces, potentially improving the description of real fluids compared to VdW. However, limitations likely persist, particularly in capturing the complexities of real gas interactions at different temperatures and pressures. To address these limitations, the SRK EOS builds upon the RK model. SRK introduces volume-shift functions, theoretically allowing for a more accurate representation of co-volume and the size of molecules. This refinement aims to provide a more comprehensive understanding of real gas behavior, especially in regimes where the VdW equation struggles.

I.3.d. Soave Redlich & Kwong EOS

The RK equation was designed largely to predict the properties of small, non-polar molecules in the vapor phase, which it generally does well. However, it has been subject to various attempts to refine and improve it. In 1975, Redlich himself published an EOS adding a third parameter, in order to better model the behavior of both long-chained molecules, as well as more polar molecules. His 1975 equation was not so much a modification to the original equation as a re-inventing of a new EOS, and was also formulated so as to take advantage of

computer calculation, which was not available at the time the original equation was published.[7] Many others have offered competing equations of state, either modifications to the original equation, or equations quite different in form. It was recognized by the mid 1960s that to significantly improve the equation, the parameters, especially *a*, would need to become temperature dependent. As early as 1966, Barner noted that the Redlich–Kwong equation worked best for molecules with an acentric factor (ω) close to zero. He therefore proposed a modification to the attractive term:

$$a = \alpha + \gamma\, T^{-1.5} \tag{16}$$

Where:

- α is the attractive term in the original RK equation
- γ is a parameter related to ω, with γ = 0 for ω = 0 (17)

It soon became desirable to obtain an equation that would also model well the VLE properties of fluids, in addition to the vapor-phase properties. Perhaps the best known application of the Redlich–Kwong equation was in calculating gas fugacities of hydrocarbon mixtures, which it does well, that was then used in the VLE model developed by Chao and Seader in 1961.However, in order for the RK equation to stand on its own in modeling vapor–liquid equilibria, more substantial modifications needed to be made. The most successful of these modifications is the **Soave modification** to the equation, proposed in 1972. Soave's modification involved replacing the $T^{1/2}$ power found in the denominator attractive term of the original equation with a more complicated temperature-dependent expression. He presented the equation as follows:

$$P = \frac{RT}{\bar{v}-b} - \frac{a\,\alpha}{\bar{v}(\bar{v}+b)} \tag{17}$$

Where:

- $\alpha = \left(1 + (0.480 + 1.574\,\omega - 0.176\,\omega^2)\left(1 - \sqrt{T_r}\right)\right)^2$ (18)
- $a = 0.42748\ \frac{R^2 T_c^2}{P_c}$ (19)
- $b = 0.08554\ \frac{RT_c}{P_c}$ (20)
- T_r is the reduced temperature of the compound

- ω is the acentric factor (18)

Next, a brief introduction about the acentric factor will be given.

Acentric Factor (ω)

The acentric factor (ω) is a term used in thermodynamics and fluid dynamics to describe the deviation of a substance from ideal behavior, particularly in terms of its vapor pressure. It is a dimensionless factor introduced by Kenneth Pitzer in 1955 as part of the corresponding states theory, which helps in predicting the thermodynamic properties of fluids. The acentric factor is defined based on the vapor pressure of a substance at a temperature that is 70% of its Tc.

Mathematically, the acentric factor is defined as:

$$\omega = -log_{10}(P_r^{Sat}) - 1 \qquad (20)'$$

where P_r^{Sat} is the reduced vapor pressure at a Tr, Tr =0.7 The reduced vapor pressure is the actual vapor pressure divided by the critical pressure of the substance.

The acentric factor provides a measure of the "shape" or "complexity" of a molecule in terms of how its vapor pressure deviates from that of a simple spherical molecule. For simple, spherical molecules (like noble gases), the ω is close to zero. For more complex molecules, the ω is greater than zero, reflecting increased deviation from ideal behavior.

- The SRK builds upon the RK model by introducing volume-shift functions. While this offers a more accurate representation of co-volume and molecular size compared to RK, limitations can still arise, particularly when dealing with complex mixtures or highly non-ideal fluids. The Peng-Robinson PR EOS seeks to address these limitations by taking a different theoretical approach. PR incorporates temperature-dependent terms for both attractive and repulsive intermolecular forces. This broader consideration, compared to SRK's focus on volume-shift functions, has the potential to provide a more comprehensive description of real gas behavior, especially for complex systems. Which prompts us in the next part to learn about these attractive and repulsive force terms and how they are incorporated in the PR EOS.

I.3.e. Peng–Robinson EOS

The Peng–Robinson EOS (PR EOS) was developed in 1976 at The University of Alberta by Ding-Yu Peng and Donald Robinson in order to satisfy the following goals:

- The parameters should be expressible in terms of the critical properties and the acentric factor.
- The model should provide reasonable accuracy near the critical point, particularly for calculations of the compressibility factor and liquid density.
- The mixing rules should not employ more than a single binary interaction parameter, which should be independent of temperature, pressure, and composition.
- The equation should be applicable to all calculations of all fluid properties in natural gas processes.

The equation is given as follows:

$$P = \frac{RT}{\bar{v}-b} - \frac{a\,\alpha}{\bar{v}(\bar{v}+b)+b(\bar{v}-b)} \tag{21}$$

Where:

- $\alpha = \left(1 + (0.37464 + 1.54226\,\omega - 0.26992\,\omega^2)\left(1 - \sqrt{T_r}\right)\right)^2$ (22)
- $a = 0.45742\,\frac{R^2 T_c^2}{P_c}$ (23)
- $b = 0.07780\,\frac{RT_c}{P_c}$ (24)

The PR EOS represents a significant advancement in modeling the behavior of real fluids, particularly complex molecules and mixtures. Its ability to handle a wider range of fluids with improved accuracy makes it a valuable tool for engineers across various disciplines. While the added complexity compared to simpler EOS models needs consideration, the PR EOS remains a powerful choice for applications demanding a more nuanced understanding of real gas behavior. (19)

- After delving into all these equations, we now have a very good view of their positive aspects, and this is what we will conclude in the next part.

I.3.f. Advantages of using cubic equations of state

All cubic equations of state have their foundation in VdW EOS. The use of cubic EOS has become widespread because of their advantages:

- Simplicity of application
- Only a few parameters need to be determined
- Low computational overhead is required to implement them. This was a critical issue, particularly in the early stages of computers; it is not really anymore. Nevertheless, this feature is still a "plus."

While cubic equations of state offer a balance between simplicity and accuracy, they do have limitations. One key drawback is their potential for reduced accuracy, especially when dealing with complex systems like mixtures containing diverse components. In such cases, it might be necessary to refine the predictions by incorporating additional, system-specific information.

- Cubic EOS offer a simple way to predict real gas behavior. However, their accuracy suffers for complex fluids because they treat molecules as perfect spheres. The concept of "acentric factor" tackles this limitation. This factor accounts for a molecule's shape and size, going beyond the spherical picture. By incorporating the acentric factor, cubic EOS models become more versatile, allowing them to describe a wider range of real fluids with improved accuracy. This increased complexity necessitates further exploration of how molecular interactions are incorporated into these models.

I.4. Acentric factor and corresponding states principle (CSP)

It is important to point out that the CSP that we have just discussed was originally outlined by VdW. In reality, it is the simplest version of the principle of corresponding states, and it is referred to as the *two-parameter CSP*. This is because it relies on two parameters (Pr and Tr) for defining a "corresponding state."

With the passing of time, more accurate CSP formulations have made use of more than two parameters. For instance, the three-parameter CSP affirms that two substances are in corresponding states not only when they are at the same reduced conditions (Pr and Tr), but also when they have the same "acentric factor" value. In any case, the general statement of CSP remains untouched:

"Substances at corresponding states behave alike."

What makes the difference is the definition of "*what a corresponding state is.*"

The acentric factor "ω" is a concept that was introduced by Pitzer in 1955, and has proven to be very useful in the characterization of substances. It has become a standard for the proper characterization of any single pure component, along with other common properties, such as molecular weight, Tc, Pc, and Vc.

Pitzer came up with this factor by analyzing the vapor pressure curves of various pure substances. From thermodynamic considerations, the vapor pressure curve that we studied in our first modules for pure components can be mathematically described by the Clausius Clapeyron equation:

$$\frac{1}{P}\frac{dP}{dT} = \frac{\Delta H_{vap}}{RT\,\Delta Z} \tag{25}$$

The use of the integrated version of equation is very common for the mathematical fitting of vapor pressure data. The integrated version of equation (25) shows that the relationship between the logarithm of vapor pressure and the reciprocal of absolute temperature is approximately linear. That is, in terms of reduced conditions, vapor pressure data approximately follows a straight line when plotted in terms of "logPr" versus "1/Tr", or, equivalently:

$$log_{10}P_r = a\left(\frac{1}{T_r}\right) + b \tag{26}$$

If the two-parameter corresponding state principle were to hold true for all substances, the parameters "a" and "b" should be the same for all substances. That is, all vapor pressure curves of all imaginable substances should lie on top of each when plotted in terms of reduced conditions. Stated in another way, if the plot is of the form "logPr" versus "1/Tr", all lines should show the same slope (a) and intercept (b).

The bad news is that, as you may imagine, this is not always true. Vapor pressure data for different substances do follow different trends. The good news is that some gases follow the expected trend. Which are they? The noble gases. Noble gases (such as Ar, Kr and Xe) happen to follow the two-parameter corresponding states theory very closely. Hence, they yield themselves amenable to acting as a reference to evaluate "compliance" with the two-parameter EOS.

Pitzer wanted to come up with a reliable way of quantifying the deviation of substances with respect to two-parameter corresponding state predictions. He decided to use noble gases as the base for comparison. Analyzing vapor pressure data for noble gases, Pitzer showed that a value of logPr = – 1 was achieved at approximately Tr = 0.7. So, He thought: if the vapor

pressure data of a substance show that logPr = – 1 at Tr = 0.7, it behaves as the noble gases and thus complies with the two-parameter corresponding states. If not, we are to compute the difference:

$$Difference = -log_{10}(P_r)\,T_{r=0.7} - 1 \qquad (27)$$

Pitzer called this difference the "acentric factor, ω " of the substance. Noble gases, being the reference themselves, have an acentric factor value of zero (ω=0). Substances with an ω of zero are called "simple" substances. The acentric factor is said to be a measure of the non-sphericity (a centricity) of the molecules. Therefore, the three-parameter corresponding state theory of Pitzer reads: "Fluids that have the same value of ω will behave alike at the same conditions of reduced pressure and temperature." (20) (21)

- The figure I-8, explains the corresponding state principle:

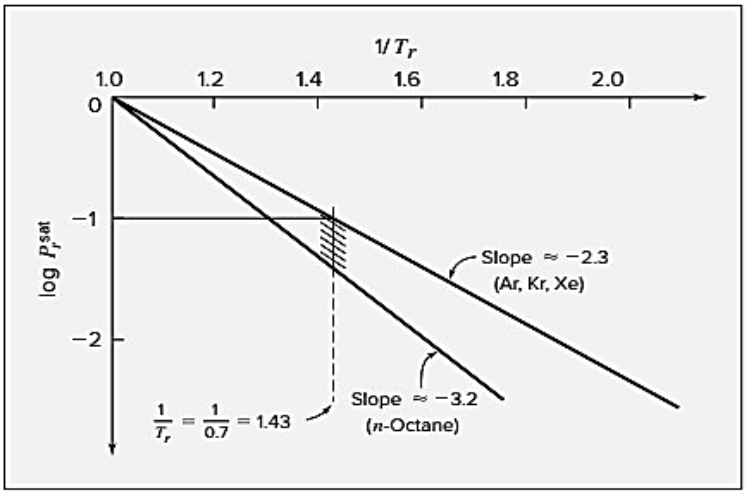

Figure I. 8: Approximate temperature dependence of the reduced vapor pressure. (22)

- Cubic EOS offer a simple framework for real gas behavior, but their accuracy suffers for complex fluids due to their inherent simplicity. The "ω" addresses this by accounting for molecular shape, improving the applicability of cubic EOS models. However, discrepancies between predicted and actual behavior can still exist. Metrics like RMSE help quantify these discrepancies and guide the selection of the most accurate cubic EOS model for a specific fluid.

The RMSE can be expressed as:

$$RMSE = \sqrt{\frac{\sum_{i=1}^{N}(y(i) - y''(i))^2}{N}} \qquad (28)$$

Were,

N is the number of data points

y(i) is the i-th measurement,

and y"(i) is its corresponding prediction.

I.5. Conclusion

While cubic EOS offer a convenient approach to model real gas behavior, their inherent simplicity can lead to limitations, particularly when dealing with complex fluids. These limitations arise because cubic EOS often treat molecules as perfect spheres, neglecting the influence of their actual shapes and sizes. Fortunately, the concept of the acentric factor steps in to address this very issue. By incorporating this factor, we can refine cubic EOS models to account for molecular non-ideality and achieve a more comprehensive description of real fluid behavior. However, even with this refinement, discrepancies between predicted and actual behavior can still exist. This is where the powerful tool of RMSE comes into play. By analyzing RMSE, we can quantify these discrepancies and objectively compare the effectiveness of different cubic EOS models for a specific fluid. In our practical work, this interplay between acentric factor, cubic EOS selection, and RMSE analysis becomes crucial. We will delve deeper into the impact of the acentric factor on various cubic EOS models and utilize RMSE analysis to meticulously evaluate their accuracy for our specific system. Through this comprehensive approach, we aim to identify the most accurate cubic EOS model, enabling us to achieve a deeper understanding and more reliable predictions of real gas behavior in our chosen system.

Chapter II

Evaluation of Cubic EOS Ability to Represent PVT Relations, for CO2 & Water.

II.1. Introduction

Water and carbon dioxide (CO2) are two of the most encountered fluids in engineering applications. Their behavior under varying pressure and temperature conditions significantly impacts processes in power generation, desalination, refrigeration, and carbon capture. While the ideal gas law provides a basic understanding, it falls short for these real fluids.

This practical investigation delves into the effectiveness of four established cubic equations of state : VdW, RK, SRK, and PR, for accurately representing the behavior of water and carbon dioxide (CO2) under varying pressure and temperature conditions. Our focus will be two-fold: firstly, by generating pressure-volume isotherms, we will visually compare the predicted behavior from these models to actual experimental data. Secondly, we will specifically assess the performance of each EOS in predicting cubic EOS saturation volume, which refers to the volume occupied by a fluid in a two-phase region (e.g., liquid-vapor coexistence). By employing metrics like percentage error, we aim to identify the strengths and limitations of these models for water and CO2. Additionally, this work will explore the role of the corresponding states principle and the acentric factor in these EOS models, ultimately providing valuable insights for selecting the most appropriate EOS for engineering applications involving these ubiquitous fluids.

II.2. Experimental PVT data for carbon dioxide and water

Underpinning our evaluation of the EOS models is a foundation of reliable experimental data. This section delves into the PVT data collected for both carbon dioxide (CO2) and water as individual components. This data serves as the benchmark against which we will compare the EOS predictions.

II.2.a.Experimental PV diagrams plotting for carbon dioxide and water

To visualize the relationship between pressure (P) and volume (V) for CO2 and water, we'll create pressure-volume (PV) diagrams. These diagrams will be based on reliable experimental data obtained from the NIST.

By plotting the P and V values from the NIST data on a graph, we can analyze how pressure changes as volume varies for each fluid. This graphical representation will provide valuable

insights into their behavior under different pressure and volume conditions. (see figures II-1 & II-2).

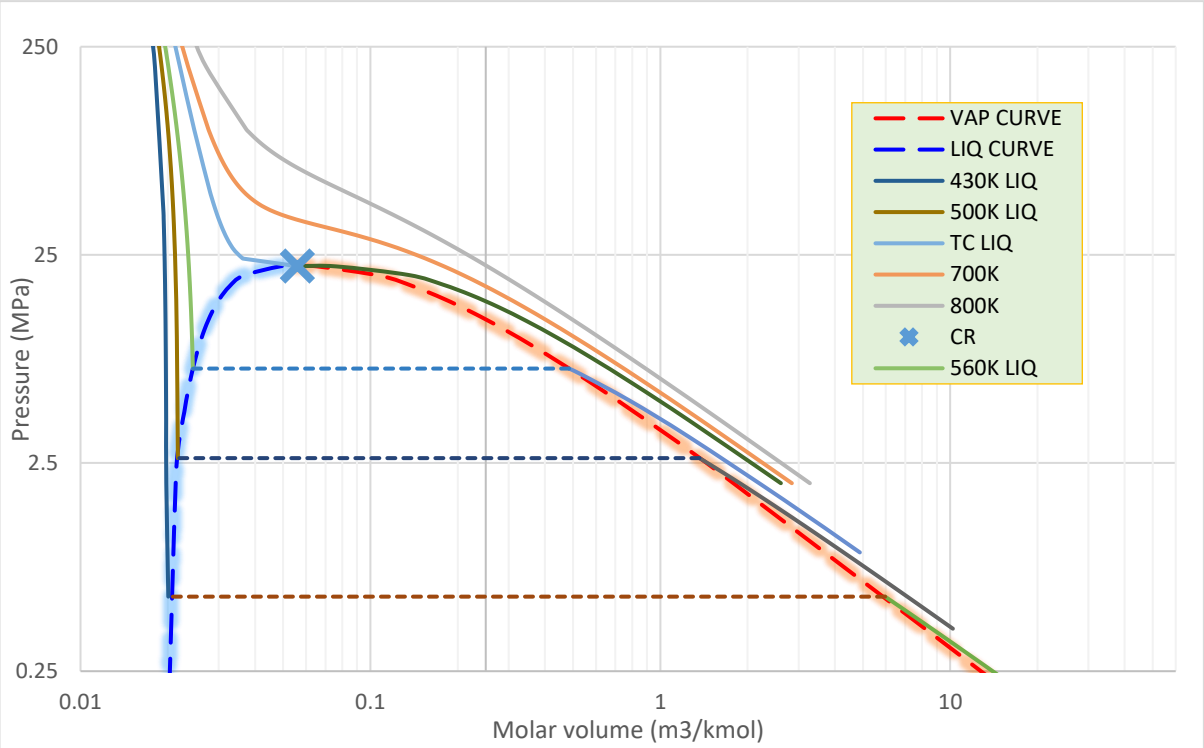

Figure II. 1: Experimental PV diagram plotting for Water.

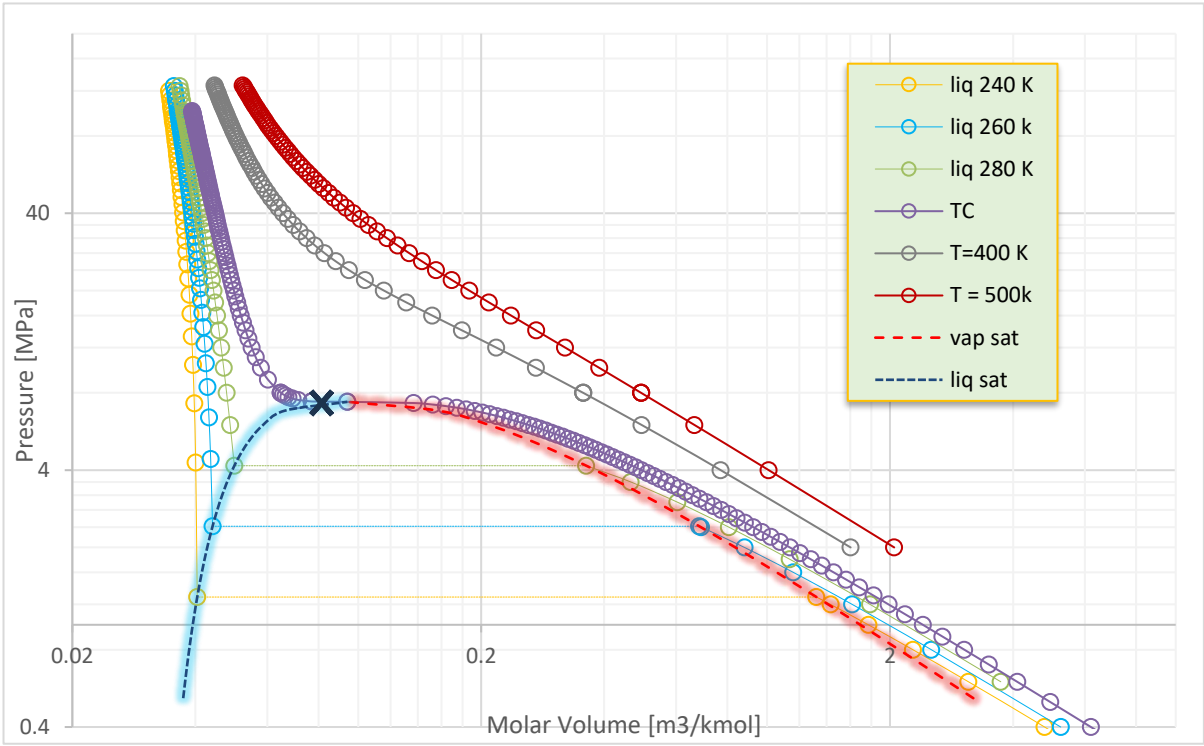

Figure II. 2: Experimental PV diagram plotting for CO2

The PV diagrams, constructed using reliable experimental data from the NIST, serve as a crucial foundation for our work. These diagrams depict isotherms, lines representing constant temperatures, for both water and CO2. We will specifically, just as example focus, on isotherms plotted for:

- Water: 430K, 500K, 560K , 647.096K (Tc), 700K, and 800K.
- CO2: 240K, 250K, 280K, 304.1282 (Tc), 400K, and 500K.

- By analyzing the slope and shape of these isotherms for each fluid, we can observe how pressure changes with respect to volume at various temperatures. This in-depth understanding of their behavior under different pressure and volume conditions will be instrumental later when we begin by comparing this experimental data with predictions from the VdW EOS EOS and subsequently with other, more complex EOS models.

II.3. Van Der WAALS VdW isotherms plotting:

The VdW EOS has been a cornerstone in the modeling of fluid behavior for decades. However, its simplicity often falls short in accurately predicting the properties of real fluids, particularly at high pressures and temperatures or near the critical point. So, let's get to know this equation.

II.3.a. Parametrization

To unlock the secrets of real gas behavior, we embark on finding the VDW constants (a and b). These constants, like a gas's fingerprint, encode the influence of molecular attractions and finite volume in the VdW EOS.

Table II. 1: Additional water and co2 properties.

Additional fluid properties	Value (Water)	Value (CO2)
Critical temperature (Tc) in K	647.096	304.1282
Critical pressure (Pc) in MPA	22.064	7.3773
Critical density (Dc) in kg/m3	322	467.6
critical molar volume Vc in m^3/mol	0.055948	0.094119
Normal boiling point in K	373.1243	194.686
Dipole moment in Debye	1.855	0
Gas Constant , R in m^3. MPA / Kmol. K	0.008314	0.008314

The VdW parameters, a and b, were determined specifically for water and CO2 using equations 10 and 11

Table II. 2: VdW a and b values of water and co2 properties.

VdW Parameters	Water	CO2
a $(\mathbf{MPa}.(\frac{\mathbf{m3}}{\mathbf{kmol}})^{\mathbf{2}})$	0.55342	0.36565
b $(\frac{\mathbf{m3}}{\mathbf{kmol}})$	0.0305	0.04284

Having established the VdW EOS parameters for water and CO2, we can now put its predictions to the test. We'll calculate pressure values across a range of volumes and chosen temperatures (isotherms). Plotting these calculated isotherms alongside the NIST data will be our first step in comparing the VdW EOS with reality.

II.3.b. Calculating isotherms using the VdW EOS

For the pressure calculation using VdW EOS, implemented using MS EXCEL, we follow those steps, for both water and carbon dioxide:

1. **Selecting the Isotherm Temperature:**

- We confirm the chosen temperature (T) for the isotherm. This temperature will be used consistently throughout the calculations.

2. **Selecting the Initial Molar Volume:**

- We pick an initial value for the molar volume (V) within the range we want to explore for the isotherm.

3. **Plugging and Solving:**

- We use the VdW equation and substitute the following:
    - The chosen temperature (T)
    - The previously determined VdW constants (a & b) for the specific gas
    - The selected molar volume (V)

- We solve the VdW equation to find the pressure (P) corresponding to the chosen volume (V).

4. **Repeating the Steps:**

- We repeat steps 2 and 3 for multiple volume (V) values, effectively creating a grid of pressure (P) and volume (V) points across the desired range for the isotherm.

5. **Plot generation:**

- Finally, we plot the calculated pressure (P) values on the y-axis against the corresponding molar volume (V) values on the x-axis. This visualization yields the theoretical isotherm predicted by the VdW EOS for the chosen temperature.

II.3.c. Plotting

And this is the final plotting results is presented in the figure II.3 and figure II.4:

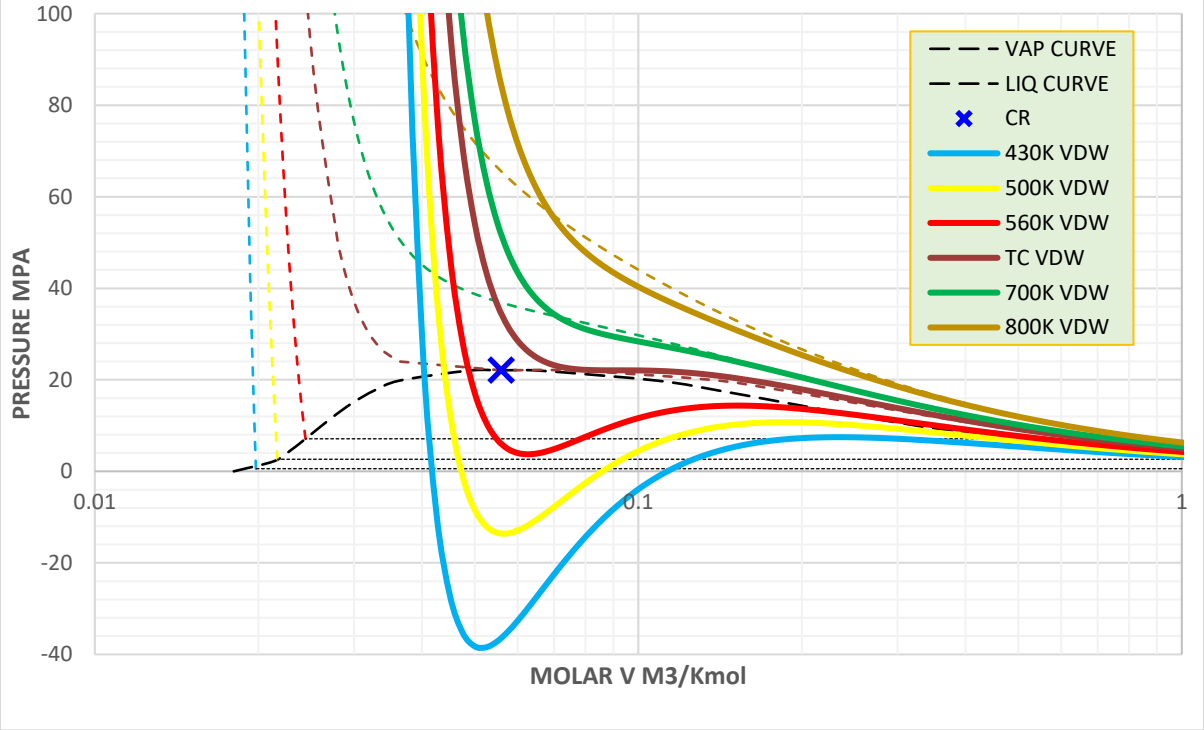

Figure II. 3: VdW and Experimental PV diagram plotting for Water

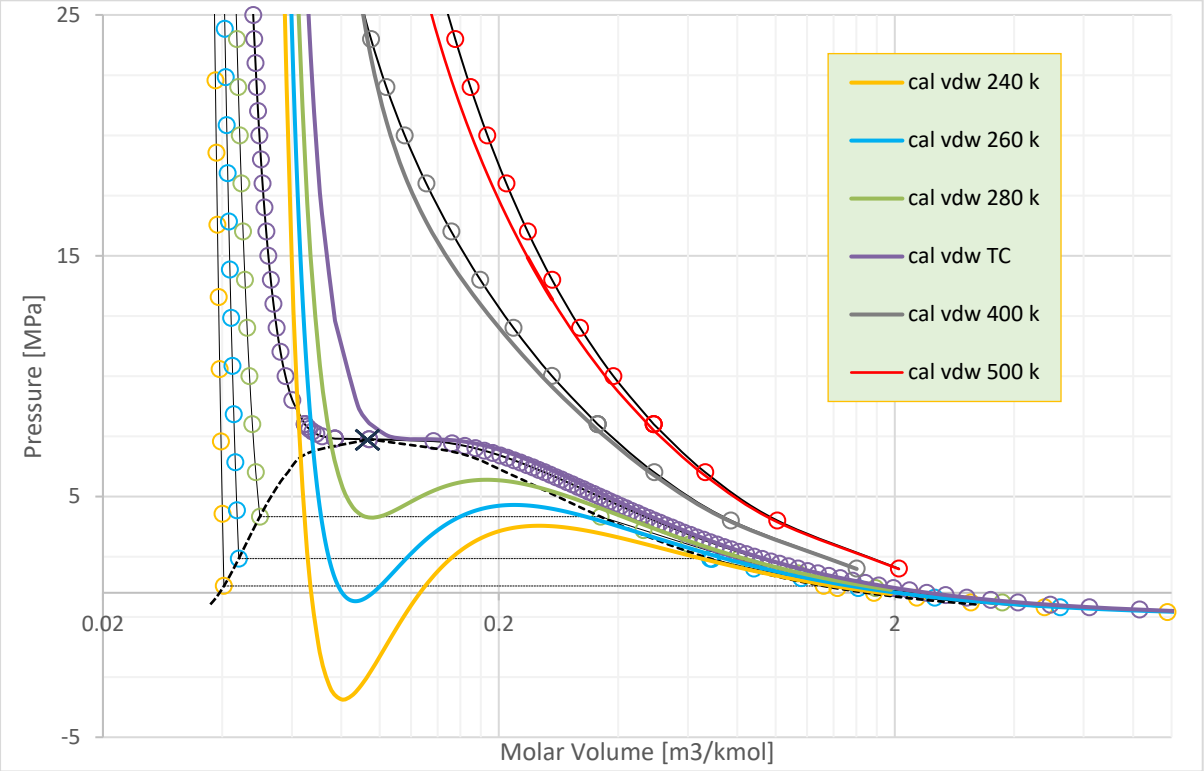

Figure II. 4: VdW and Experimental PV diagram plotting for CO2.

The figures II.3 & 4 showcases a comparison of water and CO2 behavior at different constant temperatures (isotherms) predicted by the chosen EOS with the actual experimental observations. It displays a series of curves, each representing a specific temperature, for both the EOS model and the experimental data.

These curves depict the crucial relationship between pressure (P) and molar volume (V) for water at those specific temperatures. By analyzing the alignment (or misalignment) of these isotherms, we can evaluate the EOS's accuracy in predicting water and CO2 behavior under varying pressure and volume conditions.

Following the visual comparison of the isotherms, the next step involves calculating the RMSE for each isotherm to quantify the discrepancy between the EOS predictions and the experimental data.

II.3.d. VdW EOS performance evaluation:

The RMSE is a widely used metric to assess how well a model's predictions match real-world observations. It quantifies the average magnitude of deviations between predicted and actual values.

When analyzing the behavior of fluids using EOS models, the concept of the critical point Vc plays a crucial role. The critical point represents a specific temperature and pressure above which the distinction between liquid and gas phases disappears. Fluid properties in this region exhibit significant deviations from ideal gas behavior and become challenging to predict accurately using EOS models.

Dividing the curve into "after Vc" and "before Vc" segments acknowledges this limitation.

The table II.3and table II.4 represents the RMSE results using the VdW EOS:

Table II. 3:RMSE results for water VdW.

VdW	***RMSE***	
Temperature	***VAPOR***	***LIQ***
430K	0.007417353	1795.120766
500K	0.0496062	1765.058876
560K	0.2748583	1736.512166
	Before Vc	***After Vc***
Tc	8095.73704	2.668189
700K	783.4054774	1.336401434
800K	226.6251818	3.784304238

Table II. 4:RMSE results for CO2 VdW.

VdW	***RMSE***	
Temperature	***VAPOR***	***LIQ***
240K	0.038358778	700.7717565
260K	0.103989967	6491.09619
280K	0.170515364	3677.920852
/	***Before Vc***	***After Vc***
Tc	7184.566299	0.151682208
400K	557.0831176	0.91055142
500K	79.58900929	1.788516982

The table below summarizes the RMSE results for both water and CO2. The table presents the calculated RMSE values for each isotherm temperature. This allows for a direct comparison of the EOS's accuracy across different temperature conditions for each fluid.

- **Note:**

After Tc we have just one phase (gaseous phase).

- With the graphs and RMSE calculations providing valuable data, we can now interpret the accuracy of the VdW EOS for water and CO2.

II.3.e. Results description & interpretation

Our investigation into water's and carbon dioxide's behavior using the VdW EOS reveals its limitations in capturing the molecule's intricacies. While VdW isotherms (pressure vs. volume at constant temperature) offer a basic visual representation, they deviate significantly from experimental data, particularly at lower temperatures.

This discrepancy becomes even clearer when analyzing the RMSE values. Significantly higher RMSE in the liquid phase (below the Tc) compared to the gas phase but we got best RMSE in carbon dioxide compared to water's RMSE. This highlights the VdW model's struggle to account for the strong intermolecular forces present in liquid water, especially hydrogen bonding (a polar molecule).

On the opposite side the CO2 molecule has London dispersion forces, also known as VdW forces, for intermolecular interactions, and it has polar covalent bonds between the carbon and

oxygen atoms. However, the molecule is linear and symmetrical. This means the individual bond dipoles cancel each other out, resulting in no net dipole moment for the entire CO2 molecule. This bond is weaker than the hydrogen bond found in water, which confirms our results that the RMSE of carbon dioxide is better than the RMSE of water. despite all this the VDW equation also fails to capture the London dispersion forces.

At high temperatures, the molecules move rapidly and have high kinetic energy. This kinetic energy tends to overcome the attractive forces between molecules. As a result, the a/Vm2 term in the VDW equation becomes relatively small compared to the RT/Vm term, making the VDW equation effectively reduce to the ideal gas law:

$$a/Vm^2 \approx 0 \quad ; \quad p = \frac{RT}{vm-b} - 0$$

When a term is negligible, the VDW equation essentially behaves like the ideal gas law This is expected behavior for gases at high temperatures and low pressures. These forces become less influential.

$$P(V_m - b) = RT \quad \approx \quad PV_m = RT$$

This is reflected in the lower RMSE values observed for gas phase isotherms, indicating a better overall fit for the model and aligning with water's and carbon dioxide's behavior approaching an ideal gas state. However, the potential trend of higher RMSE before the Vc and lower after Vc suggests an additional challenge near the critical point, where liquid and gas properties blur. And that's why we decided to analyze our curve into 2 segments (before and after Vc).

- This emphasizes the need for more advanced EOS models that can effectively handle these critical regions and account for the complexities of water's and carbon dioxide's intermolecular interactions, Further exploration of advanced EOS models and their performance near critical points would be crucial for a more comprehensive understanding of water's and carbon dioxide's behavior under various pressure and temperature conditions.

II.4. Redlich-Kwong RK isotherms plotting:

The VdW EOS laid the groundwork for real gas modeling, but its limitations in capturing complex behavior at high pressures and low temperatures are well established. In an effort to improve upon the VdW, the RK was developed. The RK incorporates additional

considerations, such as the temperature dependence of attractive forces between molecules. This enhanced model offers a more accurate representation of real gas behavior compared to the VdW EOS, particularly for specific gas types and pressure-temperature ranges.

II.4.a. Parametrization

The equation of RK is also have parameters "a" & "b" The same thing about VDW parameters. they were determined specifically for water and CO2 using equation 14 and 15

Table II. 5:RK a and b values for water and CO2

RK Parameters	Water	CO2
a $(MPa.(\frac{m3}{kmol})^2)$	14.26664	6.46142
b $(\frac{m3}{kmol})$	0.02112	0.02969

With the RK EOS EOS parameters determined for water and CO2, we can now evaluate its predictive capabilities. We'll embark on a comparison with real-world behavior by calculating pressure values across a range of volumes and chosen isotherms (constant temperature lines). Plotting these calculated RK isotherms alongside the reliable experimental data obtained from NIST will be our initial step in assessing the accuracy of the RK EOS in representing the PVT relationships of water and CO2 under varying pressure and volume conditions.

II.4.b. Calculating isotherms using the RK EOS

The same steps were taken in the VDW equation, but of course we changed the equation by using the RK equation which is equation 23

II.4.c. Plotting

And this is the final plotting results is presented in the figure II.5 and figure II.6:

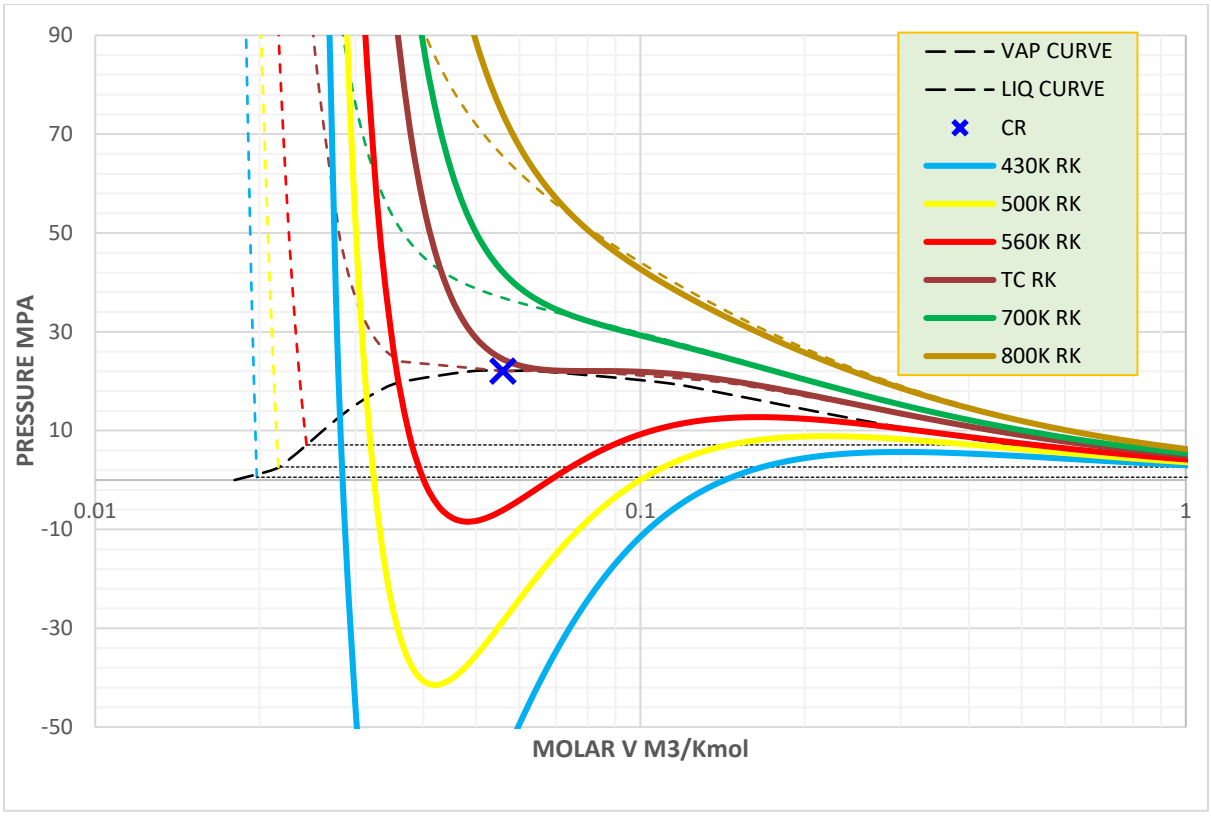

Figure II. 5:RK and Experimental PV diagram plotting for Water

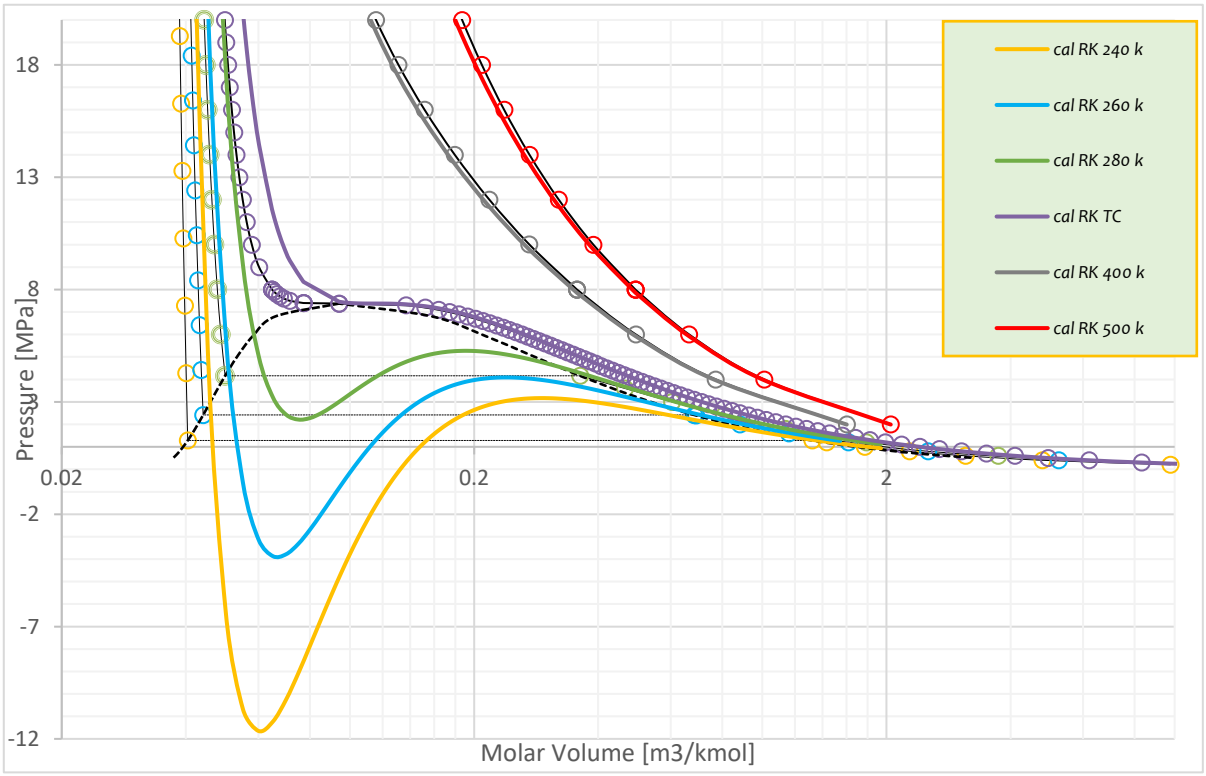

Figure II. 6:RK and Experimental PV diagram plotting for CO2

These figures II.5&6 visualizes the RK EOS's EOS predictions for water and CO2 behavior at various constant temperatures (isotherms). It presents these predictions alongside actual experimental data. We see a series of curves for each substance, depicting both the RK model's calculations and the corresponding experimental measurements. These curves represent the crucial link between pressure (P) and molar volume (V) for water and CO2. By analyzing the degree of overlap between the predicted and measured isotherms, we can evaluate the RK EOS's effectiveness in capturing the true behavior of these fluids under varying pressure and volume conditions. While the RK EOS might offer some improvement over simpler models, a visual comparison alone has its limitations. To quantify any remaining discrepancies, we'll calculate the RMSE for each isotherm.

II.4.d. RK performance evaluation

The table II.6 and table II.7 represents the RMSE results using the RK EOS :

Table II. 6:RMSE results for water RK.

RK	***RMSE***	
Temperature	***VAPOR***	***LIQ***
430K	0.005304743	2991.674106
500K	0.032142612	15024.84348
560K	0.164012714	3341.637864
	Before Vc	***After Vc***
Tc	289.4357831	0.543209046
700K	220.5114766	0.54225444
800K	45.04685713	1.929583489

Table II. 7: RMSE results for CO2 RK.

RK	***RMSE***	
Temperature	***VAPOR***	***LIQ***
240K	0.015723947	69.40786255
260K	0.039118041	46.87942794
280K	0.058248134	32.56872003
/	***Before Vc***	***After Vc***
Tc=304.1	18.66082784	0.031756455
400K	1.359171131	0.330660102
500K	5.569292152	0.959935007

The table II.6&7 below summarizes the RMSE results for both water and CO2. The table presents the calculated RMSE values for each isotherm temperature. This allows for a direct comparison of the EOS's accuracy across different temperature conditions for each fluid.

- With the graphs and RMSE calculations providing valuable data, we can now interpret the accuracy of the RK EOS for water and CO2.

II.4.e. Results description & interpretation

The RK EOS demonstrates a visually better fit to isotherm data compared to the VdW EOS, especially for non-polar substances like CO2 at lower temperatures. This suggests an improved ability to account for some aspects of their intermolecular interactions. However, the quantitative analysis using RMSE reveals a persistent challenge: a significant difference in RMSE between the liquid and gas phases for both water and CO2.

This discrepancy highlights the inherent difficulty of capturing strong intermolecular forces, particularly hydrogen bonding in water. Water's polar nature and hydrogen bonding lead to significantly stronger intermolecular interactions (represented by W) compared to CO2. This is reflected in the higher RMSE values for water, even with the RK EOS's attempt to account for these forces. The complex network of hydrogen bonds in water might not be fully captured by the RK EOS, leading to an underestimation of its attractive forces in the liquid state.

Despite these limitations, the RK EOS offers advantages. Like VdW, it might show a decrease in RMSE in the gas phase (above the Tc) for both substances. However, the trend of higher RMSE before the Vc and lower afterwards might still persist, indicating limitations in modeling the critical point region.

The RK equation's strength lies in its refined treatment of attractive forces compared to simpler models. This allows for a better approximation of the critical point conditions and a more accurate representation of real gas behavior, particularly in the liquid phase where intermolecular attractions are significant. This is evident in the lower RMSE values for CO2 in the vapor phase at lower temperatures, where the "a" term becomes negligible and the RK equation behaves similarly to the ideal gas law. The RK equation modifies the attractive term by incorporating a temperature dependence into the 'a' parameter: $\mathbf{a}/\sqrt{\mathbf{T}}$. This adjustment helps to better represent the behavior of real gases, especially at higher pressures and lower temperatures where intermolecular attractions are more significant. These improvements enable the RK equation to better capture the complexities of the liquid phase, where intermolecular forces play a significant role, leading to more accurate predictions and lower RMSE values compared to simpler equations.

In conclusion, while the RK EOS offers some visual improvement and a better approximation of critical points compared to VdW, it faces similar challenges in capturing the complexities of water and CO2 behavior, especially regarding strong intermolecular forces and the critical region. The significant difference in RMSE between water and CO2 highlights the limitations of the RK EOS in capturing the nuances of hydrogen bonding. Analyzing the RMSE across different phases and the critical point region remains crucial for understanding the model's performance for each substance.

- Further exploration of more sophisticated EOS models specifically designed for complex molecules like water is necessary for a more accurate depiction of their behavior under various conditions.

II.5. Soave-Redlich-Kwong SRK isotherms plotting:

The SRK builds upon the foundation laid by the RK EOS, pushing real gas modeling to a new level. While the RK EOS represented a significant leap forward by incorporating temperature dependence into attractive forces, it couldn't fully capture the complexities of real gas behavior. The SRK EOS tackles this limitation by introducing the acentric factor. This

parameter accounts for the asymmetry and shape variations among gas molecules, providing a more nuanced description. Compared to the RK EOS and even simpler models, the SRK EOS offers a more refined understanding of real gas behavior, especially for a broader range of gas types and operating conditions. However, this work will delve deeper to explore the inherent limitations of the SRK EOS.

II.5.a. Parametrization

The equation of SRK is also have parameters "a" & "b" The same thing about RK parameters. but we add the parameter α This parameter, ranging from 0 to 1, accounts for the asymmetry and shape of gas molecules. Spherical molecules, with weaker attractive forces, have an α close to 0. Conversely, elongated molecules, with stronger attractive forces due to their shape, possess a higher α value. a and b were determined specifically for water and CO2 using equation 18,19 and 20

Table II. 8: SRK a,b and ω values for water and co2. **(23)**

SRK Parameters	Water	CO2
a (MPa. $(\frac{m3}{kmol})^2$)	0.56078	0.37051
b $(\frac{m3}{kmol})$	0.02112	0.02969
$\boldsymbol{\omega}$	0.344	0.224

Having determined the SRK EOS EOS parameters for water and CO2, we can now leverage its enhanced capabilities compared to the RK EOS. We'll embark on a rigorous evaluation by calculating pressure across a range of volumes and chosen isotherms (constant temperature lines). Plotting these calculated SRK isotherms alongside the trusted NIST experimental data will be our initial step. This visual comparison will provide valuable insights into the accuracy of the SRK EOS in representing the behavior of water and CO2 under varying pressure and volume conditions.

II.5.b. Calculating isotherms using the SRK EOS

The same steps were followed with the SRK equation as were taken with the VDW equation. However, instead of using the VDW equation, we applied the SRK equation to modify the approach. Which is equation 27

II.5.c. Plotting

And this is the final plotting results is presented in the figure II.7 and figure II.8:

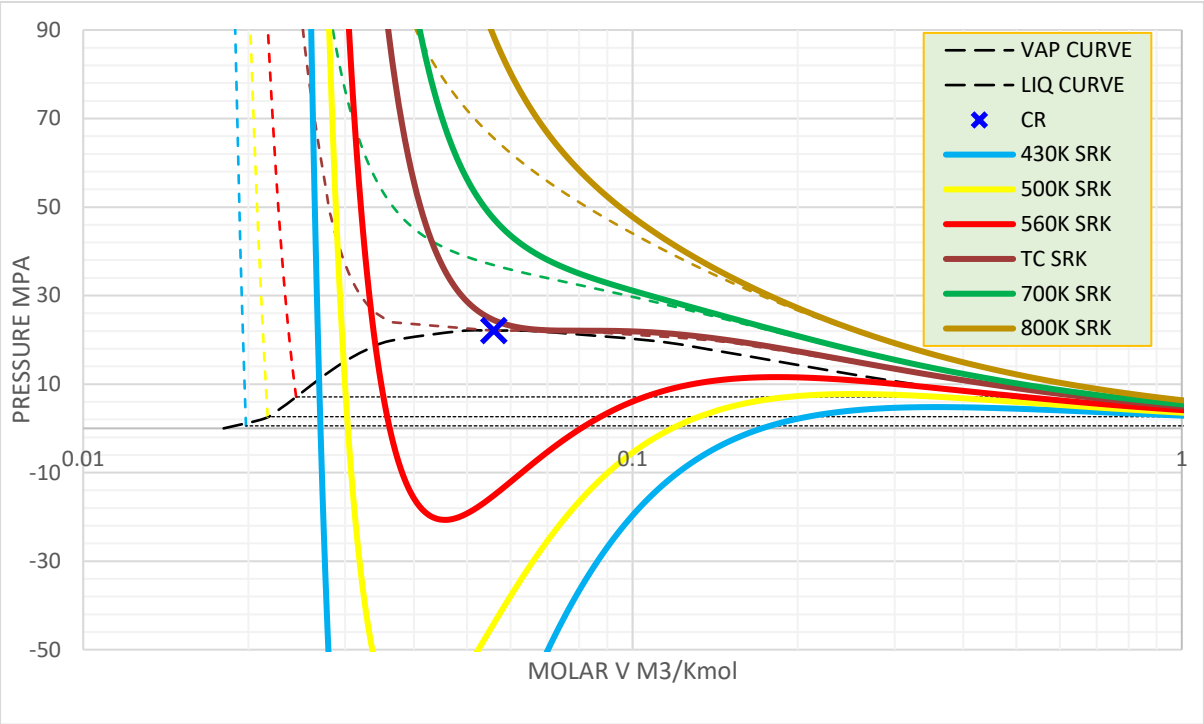

Figure II. 7: SRK and Experimental PV diagram plotting for Water.

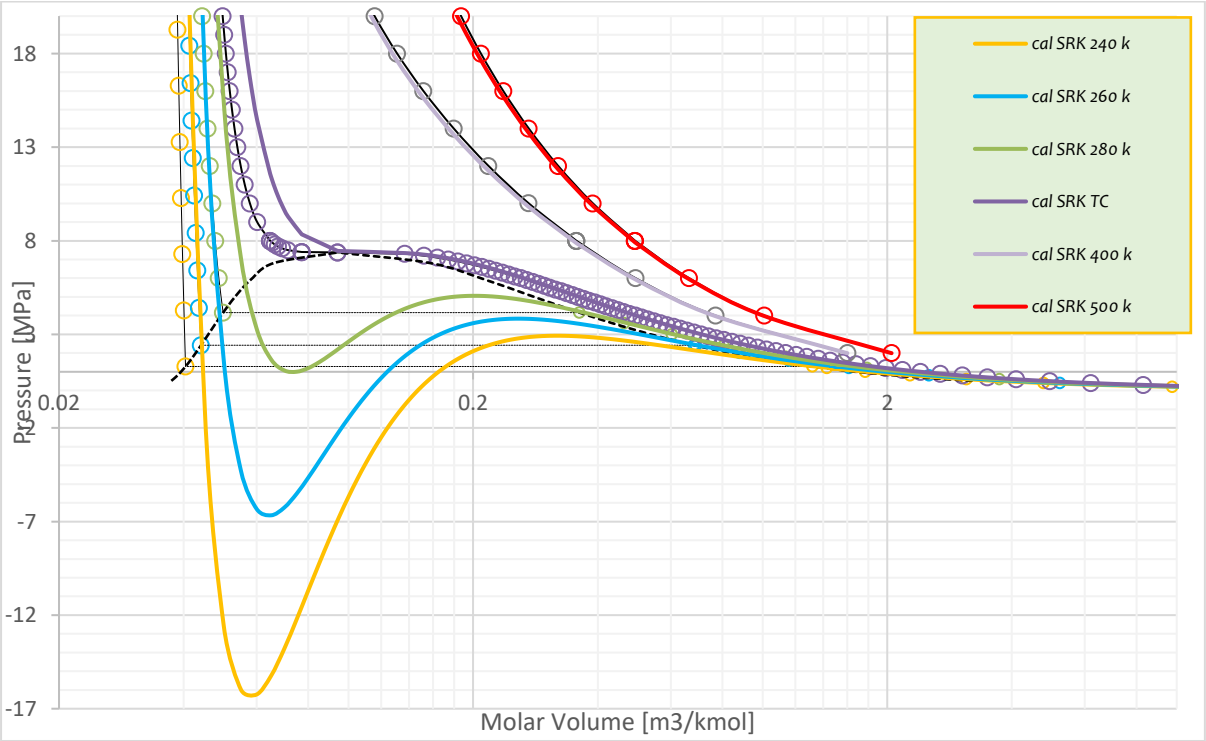

Figure II. 8: SRK and Experimental PV diagram plotting for CO2.

Building upon the limitations identified with the RK and VdW models, the figures II.7&8 delves into the performance of the SRK EOS . It directly compares the SRK's predicted behavior of water and CO2 at various constant temperatures (isotherms) with actual experimental data. Similar to the RK EOS graph, it shows curves for each substance, representing both the SRK model and the measured values. These curves reveal the critical relationship between pressure (P) and molar volume (V) for water and CO2. By analyzing how closely these curves align, we can assess the accuracy of the SRK EOS. Compared to the RK and VdW models, the SRK EOS demonstrates a significant improvement in capturing the true behavior of these fluids. This is evident in the much better agreement between the predicted SRK isotherms and the experimental data. However, a visual comparison is just the first step. To quantify any remaining discrepancies, the next step involves calculating the RMSE for each isotherm.

II.5.d. SRK performance evaluation

The table II.9 and table II.10 represents the RMSE results using the RK EOS:

Table II. 9: RMSE results for water SRK.

SRK	***RMSE***	
Temperature	***VAPOR***	***LIQ***
430K	0.004043485	3238.919393
500K	0.02223143	15050.38024
560K	0.108095941	3308.636624
	Before Vc	***After Vc***
Tc	289.4357831	0.543209046
700K	233.1547078	1.479528293
800K	66.73753951	7.076215147

Table II. 10: RMSE results for CO2 SRK.

SRK	***RMSE***	
Temperature	***VAPOR***	***LIQ***
240K	0.007969042	59.54893988
260K	0.018027824	40.45626332
280K	0.026447524	29.27587498
/	***Before Vc***	***After Vc***
Tc=304.1	18.66082784	0.031756455
400K	2.014839652	0.232974089
500K	3.489870515	0.486045188

The table II.9&10. below summarizes the RMSE results for both water and CO2. The table presents the calculated RMSE values for each isotherm temperature. This allows for a direct comparison of the EOS's accuracy across different temperature conditions for each fluid.

Notably, the RMSE values for water are consistently higher than those obtained for CO2 when using the SRK EOS

- With the graphs and RMSE calculations providing valuable data, we can now interpret the accuracy of the SRK EOS for water and CO2.

II.5.e. Results description & interpretation

The SRK represents a significant advancement over the RK EOS, particularly when dealing with non-polar substances like CO2. Its success lies in its ability to model the behavior of CO2 across different phases. In the vapor phase at lower temperatures, the SRK EOS aligns well with the ideal gas law, as indicated by the low RMSE values. This makes sense because the attractive forces, represented by the "a" term in the equation, become negligible at these conditions. It demonstrates reasonable performance even in the liquid phase for CO2, with slightly higher but still acceptable RMSE values. This improvement can be attributed to the introduction of a temperature-dependent function (α(T)) within the equation. This function allows the SRK EOS to better account for the variation in intermolecular forces. The α(T) function also incorporates the acentric factor (ω), which provides a measure of a molecule's non-sphericity. This inclusion helps the SRK EOS better represent the real behavior of liquids.

The SRK EOS further demonstrates its effectiveness at the critical point and beyond. It accurately predicts the behavior of CO2 at its critical point, where the distinction between liquid and gas properties diminishes. Furthermore, the SRK EOS excels at describing the continuous property shift observed in supercritical fluids, a state where traditional phase boundaries disappear. This capability is evident in the consistently low RMSE values for CO2 across these regions. These findings support the notion that the SRK EOS is a powerful tool for understanding the behavior of non-polar substances transitioning beyond their critical points.

However, the story becomes more complex when we consider a molecule like water. Quantitative analysis using RMSE across different phases is crucial for a more comprehensive understanding. Here, the significant difference in RMSE between water's liquid and gas phases persists, highlighting the limitations of the SRK EOS in capturing the complexities of water's strong intermolecular forces, especially hydrogen bonding. Hydrogen bonding creates a network of interactions significantly stronger than London dispersion forces, and the current formulation of the SRK EOS might not fully capture these complexities.

In conclusion, the SRK EOS represents a significant advancement over the RK EOS, particularly for non-polar substances. It offers a more accurate description of their behavior across various phases, including the critical point and supercritical region. However, for complex molecules like water, the challenge of capturing strong and intricate intermolecular forces remains.

- Moving forward, exploring even more advanced EOS models specifically designed for complex molecules and potentially incorporating factors beyond the acentric factor is crucial for achieving a truly accurate depiction of water's behavior under various pressure and temperature conditions.

II.6. Peng-Robinson PR isotherms plotting

Building on the RK EOS, the Peng-Robinson equation offers a more refined approach to real gas modeling. While the RK EOS advanced the field by introducing temperature-dependent attractive forces, it struggled to fully capture real gas behavior. The PR EOS improves on this by incorporating a more complex term for attractive forces, accounting for both size and shape effects of gas molecules. This enhancement will probably allow the PR

EOS to more accurately represent real gas behavior across a wider range of gases and conditions.

II.6.a. Parametrization

The equation of PR is also have parameters “a” & “b” The same thing about SRK parameters. they were determined specifically for water and CO2 using equation 21,22,23 and 24

Table II. 11: PR a, b and ω values for water and co2.

PR Parameters	Value (Water)	Value (CO2)
a $(MPa.(\frac{m3}{kmol})^2)$	0.59982	0.396304063
b $(\frac{m3}{kmol})$	0.01897	0.02666
$\boldsymbol{\omega}$	**0.344**	**0.224**

With the PR EOS EOS parameters established for water and CO2, we can now unlock its predictive power. We'll embark on a comprehensive comparison with real-world behavior by calculating pressure values across a range of volumes and chosen isotherms (constant temperature lines). Plotting these calculated PR isotherms alongside the reliable NIST experimental data will be our initial step in assessing the accuracy of the PR EOS. This visual comparison will provide valuable insights into how effectively the PR model captures the thermodynamic properties of water and CO2 under varying pressure and volume conditions.

II.6.b. Calculating Isotherms using the PR EOS

The same steps were followed with the PR equation as were taken with the VDW equation. However, instead of using the VDW equation, we applied the PR equation to modify the approach which is equation 32.

II.6.c. Plotting

And this is the final plotting results is presented in the figure II.9 and figure II.10:

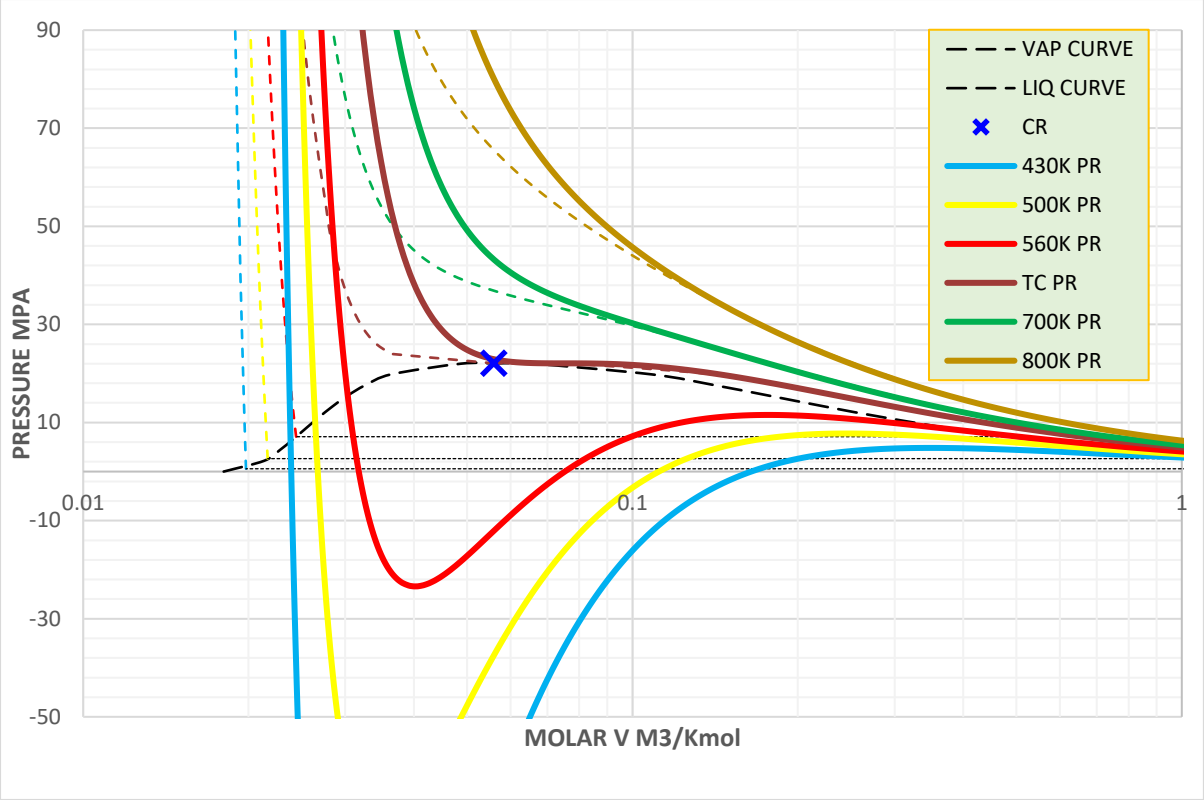

Figure II. 9: PR and Experimental PV diagram plotting for Water.

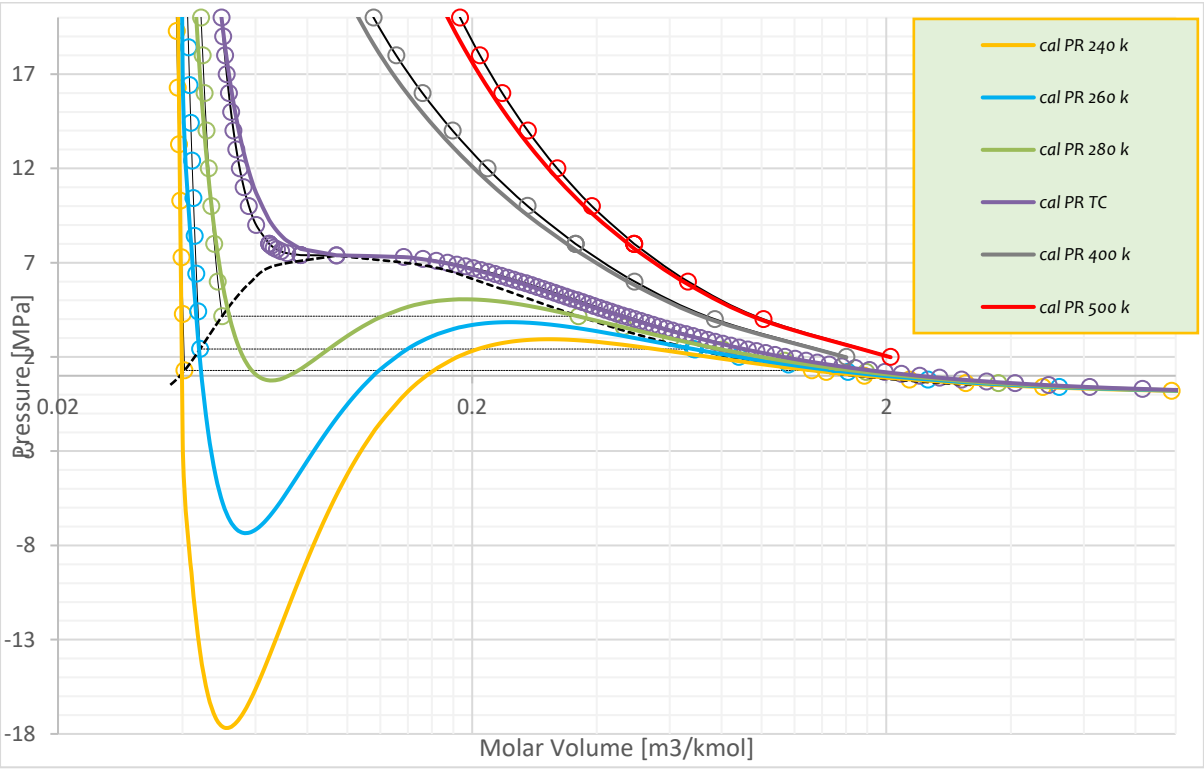

Figure II. 10: PR and Experimental PV diagram plotting for CO2.

The figures II.9&10 showcases a comparison of water and CO2 behavior at different constant temperatures (isotherms) predicted by the Peng-Robinson PR EOS EOS with the actual experimental observations. Similar to the SRK EOS graph, it displays a series of curves for each substance, representing both the PR model and the experimental data. These curves depict the crucial relationship between pressure (P) and molar volume (V) for water and CO2. By analyzing the alignment (or misalignment) of these isotherms, we can evaluate the PR EOS's accuracy.

While the PR EOS is known to excel in capturing the behavior of CO2, as evidenced by a potentially very good agreement between the calculated PR isotherms and the CO2 experimental data, it might require further investigation for water. The visual comparison of the isotherms, particularly for water, might reveal limitations of the PR model in representing its behavior across different temperature and volume conditions. Following this analysis, the RMSE calculation will provide quantitative insights into the discrepancies between the PR predictions and the experimental measurements for both water and CO2.

II.6.d. PR performance evaluation

The table II.12 and table II.13 represents the RMSE results using the RK EOS:

Table II. 12: RMSE results for water PR.

PR	***RMSE***	
Temperature	***VAPOR***	***LIQ***
430K	0.003695538	5662.247642
500K	0.017831981	1728.34833
560K	0.072324069	618.7008729
/	***Before Vc***	***After Vc***
Tc	117.2856835	0.19194491
700K	111.1668698	0.883179225
800K	40.01510041	4.336682931

Table II. 13: RMSE results for CO2 PR.

PR	***RMSE***	
Temperature	***VAPOR***	***LIQ***
430K	0.00263593	37.54868156
500K	0.002886194	31.10466978
560K	0.017480705	26.30448345
/	***Before Vc***	***After Vc***
Tc	0.051371725	17.32572421
700K	0.933519873	20.14955921
800K	1.852352552	17.1570239

The table II.12&13. below summarizes the RMSE results for both water and CO2. The table presents the calculated RMSE values for each isotherm temperature. This allows for a direct comparison of the EOS's accuracy across different temperature conditions for each fluid.

Notably, the RMSE values for water are consistently higher than those obtained for CO2 when using the PR EOS.

- With the graphs and RMSE calculations providing valuable data, we can now interpret the accuracy of the PR EOS for water and CO2.

II.6.e. Results description & interpretation

In general, we obtained improved results compared to the SRK equation, particularly in the gaseous and liquid states (below the critical point). We also achieved excellent values, especially at the critical point. In our view, these improvements are due to the changes in the following three equations:

- Correction of pressure from this:

$$P = \frac{RT}{V_m - b} - \frac{a\,\alpha}{V_m\,(V_m + b)}\ \ SRK$$

to this:

$$P = \frac{RT}{V_m - b} - \frac{a\,\alpha}{V_m\,(V_m + b) + b\,(V_m - b)}\,PR$$

by adding the terms ***(+b(Vm-b))*** to the equation of pressure.

- Correction of "a" and "b" equations from this:

$$a = \mathbf{0.42748}\,\frac{R^2 T_c^2}{P_c} \qquad b = \mathbf{0.08554}\,\frac{RT_c}{P_c}$$

to this:

$$a = \mathbf{0.45742}\,\frac{R^2 T_c^2}{P_c} \qquad b = \mathbf{0.07780}\,\frac{RT_c}{P_c}$$

By changing the constants of "a" and "b" in the PR equation.

- Correction of "α" equation from this:

$$\alpha = \left(1 + (\mathbf{0.480 + 1.574\,\omega - 0.176\,\omega^2})\left(1 - \sqrt{T_r}\right)\right)^2 \text{ SRK}$$

To this:

$$\alpha = \left(1 + (\mathbf{0.37464 + 1.54226\,\omega - 0.26992\,\omega^2})\left(1 - \sqrt{T_r}\right)\right)^2 \text{ PR}$$

The Peng-Robinson PR EOS offers a potential improvement over the SRK equation, particularly when considering complex molecules like water. Visually, PR isotherms (pressure vs. volume at constant temperature) might exhibit a closer resemblance to experimental data, especially at lower temperatures, compared to SRK and even simpler models like CO2. This suggests a potentially superior ability to capture the nuances of intermolecular interactions, including hydrogen bonding in water due to the changes in the previous three equations. However, a critical observation emerges, the visual improvement might feel somewhat inadequate, especially for water. While PR might outperform simpler models like CO2, it might still leave a lingering sense that it doesn't fully capture the complexities, particularly in water. This intuitive feeling finds further support in quantitative metrics like RMSE.

Even though PR might offer a much better visual fit for CO2 compared to SRK across various phases, a closer look at RMSE reveals a persistent discrepancy between the liquid and gas phases for both water and CO2. This difference highlights the challenge of capturing the intricate dance of intermolecular forces, especially hydrogen bonding in water. The transition to the gas phase (above the Tc) might still show a decrease in RMSE, suggesting a better overall

fit for the model. However, the potential trend of higher RMSE before the Vc and lower after Vc might remain. This highlights the limitations of even advanced models near the critical point, where the distinction between liquid and gas properties becomes blurred.

In conclusion, the PR EOS offers a significant improvement over simpler models in visually representing isotherms, particularly at lower temperatures, for both water and CO2. However, the results for CO2 are demonstrably better than for water. The limitations in fully capturing the complexities of intermolecular forces, especially hydrogen bonding in water, remain evident. Analyzing RMSE across different phases and the critical point region is still crucial.

- Further exploration of even more advanced EOS models that go beyond the PR model's framework and potentially incorporate additional factors specific to water's unique interactions might be necessary for a truly accurate representation of both water and CO2 behavior under various pressure and temperature conditions.

II.7. Cubic EOS performances evaluation

This investigation delves into the performance of a specific category – Cubic EOS models. We'll be exploring their effectiveness in capturing the nuances of real gas behavior and uncovering their limitations. By evaluating these models, we gain valuable insights that can guide us towards more accurate predictions and ultimately, a deeper understanding of real gas systems.

II.7.a. Experimental isotherm

In the realm of thermodynamics, accurately describing the behavior of real gas molecules like carbon dioxide (CO2) and water is crucial. Unlike ideal gases, these real molecules exhibit deviations due to intermolecular forces that become more prominent at different temperatures. This analysis will compare the performance of four common EOS models: VdW, RK, SRK, and PR. We will focus on CO2 and water as our molecules of interest, and analyze their behavior at three distinct temperature regimes:

- **Critical Temperature (Tc)**
- **Above Critical Temperature (T > Tc)**
- **Below Critical Temperature (T < Tc)**

To assess the accuracy of each model, we will not only visualize and analyze isotherms (pressure vs. volume at constant temperature) generated by each model alongside experimental data, but we will also calculate the RMSE for each comparison. The RMSE provides a quantitative measure of the difference between the predicted and observed values. By comparing both the visual representations and the RMSE values, we can determine which EOS model exhibits the closest agreement with reality for CO2 and water under these specific temperature conditions.

II.7.a.a. Critical Temperature (Tc)

We will examine the model's performance at the Tc, where the distinction between liquid and gas phases blurs.

The following analysis explores the performance of various EOS models for CO2 and water. We will evaluate their accuracy through both visual comparisons of isotherm plots and quantitative RMSE calculations presented in the table below.

For water:

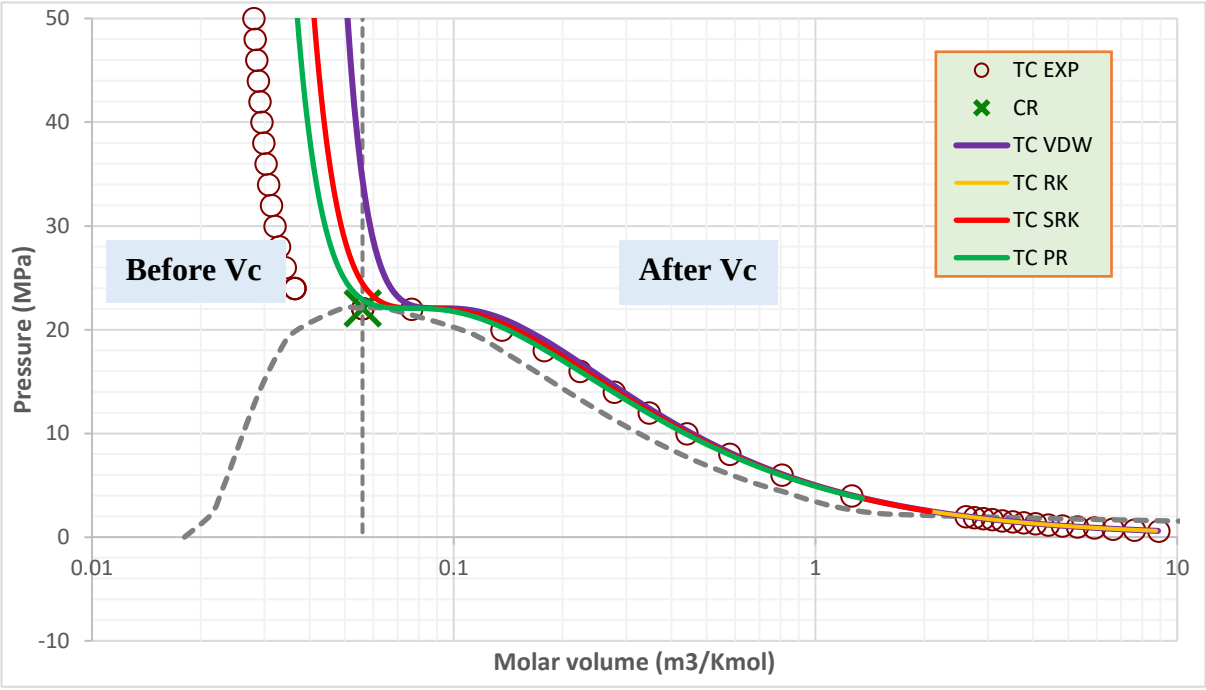

Figure II. 11: Cubic EOS isotherms Superposition over Experimental at T=Tc for water.

- **Result's description**

An analysis of P-V diagrams generated using the VdW, RK, SRK, PR EOS revealed that the PR equation exhibited superior performance in representing the behavior of water at its critical temperature (T=TC).

At the critical point, water exists as a single-phase fluid (gas). The PR equation more accurately captured the P-V relationship compared to VdW, RK, and SRK before and after the Vc was reached. This suggests that the PR EOS provides a more reliable description of water's properties near its critical state.

Table II. 14: RMSE results for cubic EOS isotherms at T=Tc for water .

T=Tc	*VDW*	*RK*	*SRK*	*PR*
RMSE (after Vc)	2.668189	0.543209	0.543209	0.191945
RMSE (before Vc)	8095.737	289.4358	289.4358	117.2857

- **Result's Description**

RMSE calculations show the Peng-Robinson PR equation best describes water behavior at Tc. PR exhibits better accuracy before and after the Vc compared to VdW, RK, and SRK. Additionally, RMSE values are consistently higher before Vc for all equations.

For carbon dioxide:

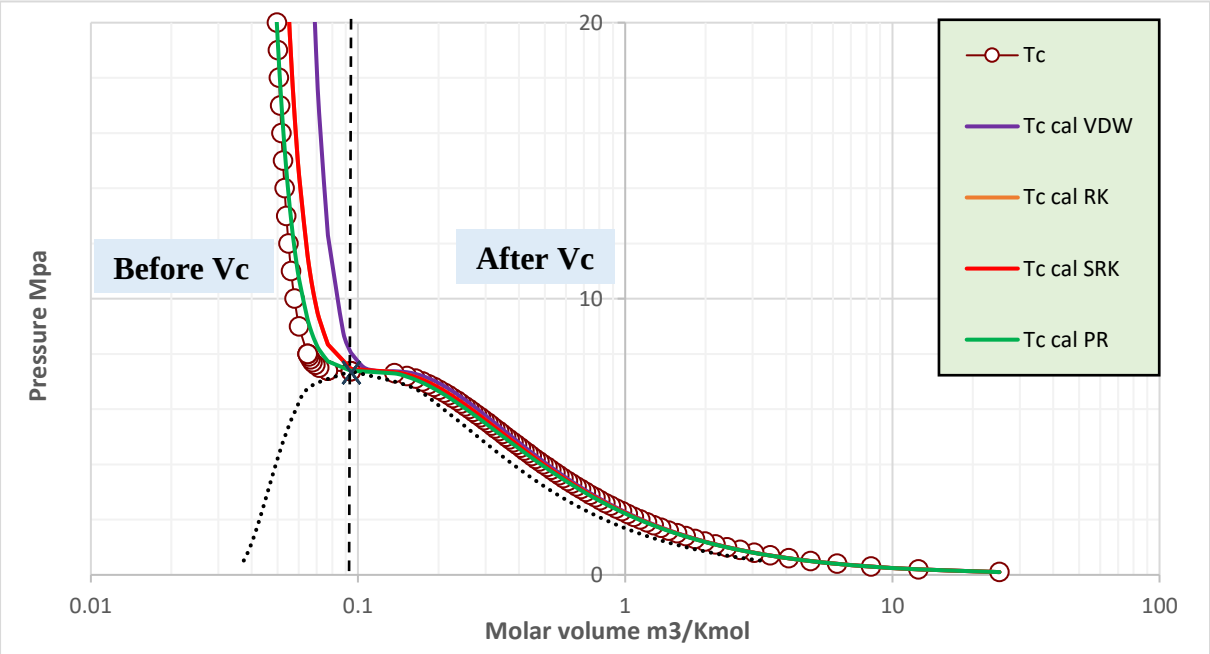

Figure II. 12: Cubic EOS isotherms Superposition over Experimental at T=Tc for CO2.

- **Result's description**

Similar to the findings for water at its Tc, analysis of P-V diagrams for CO2 reveals the Peng-Robinson PR EOS EOS outperforms VdW, RK, and SRK equations. Interestingly, EOS exhibits a generally better match for CO2's behavior compared to water.

Table II. 15: RMSE results for cubic EOS isotherms at T=Tc for CO2.

T=Tc	*VDW*	*RK*	*SRK*	*PR*
***RMSE** (After Vc)*	0.151682	0.031756	0.031756	0.051372
***RMSE** (Before Vc)*	7184.566	18.66083	18.66083	17.32572

- **Result's description**

Building on the P-V isotherm analysis, the root-mean-square error RMSE calculations further solidify the superiority of the Peng-Robinson PR EOS EOS for CO2. Compared to water, the RMSE values for all four EOS (VdW, RK, SRK, and PR) are demonstrably lower for CO2.

II.7.a.a.1 Result's interpretation (general)

Analysis of P-V isotherms and root-mean-square error RMSE calculations for water and CO2 consistently demonstrate the superiority of the PR EOS compared to VdW, RK, and SRK equations. Both the visual agreement between PR and the P-V graphs and the lower RMSE values for CO2 compared to water support this conclusion.

This finding suggests that PR is particularly well-suited for fluids with well-defined attractive and repulsive intermolecular forces, like CO2. Water molecules (H2O) have a bent structure and exhibit hydrogen bonding, creating a complex network of interactions. CO2 molecules (CO2) are linear and have weaker intermolecular forces dominated by simpler attractive and repulsive interactions. PR's formulation likely captures these simpler forces in CO2 more effectively compared to the complex hydrogen bonding network in water.

In summary, PR emerges as the most reliable EOS for both water and CO2, with a clear advantage for CO2 due to its well-defined intermolecular forces. The alignment of graph results with lower RMSE values for CO2 reinforces this observation. These results highlight the importance of selecting an EOS that aligns with the specific intermolecular forces of the fluid,

with PR being a strong choice for applications involving fluids dominated by simpler attractive and repulsive interactions.

II.7.a.b. Above critical temperature (T > Tc)

Here, the molecules behave more like an ideal gas, and we will evaluate how well the models capture this transition.

For water:

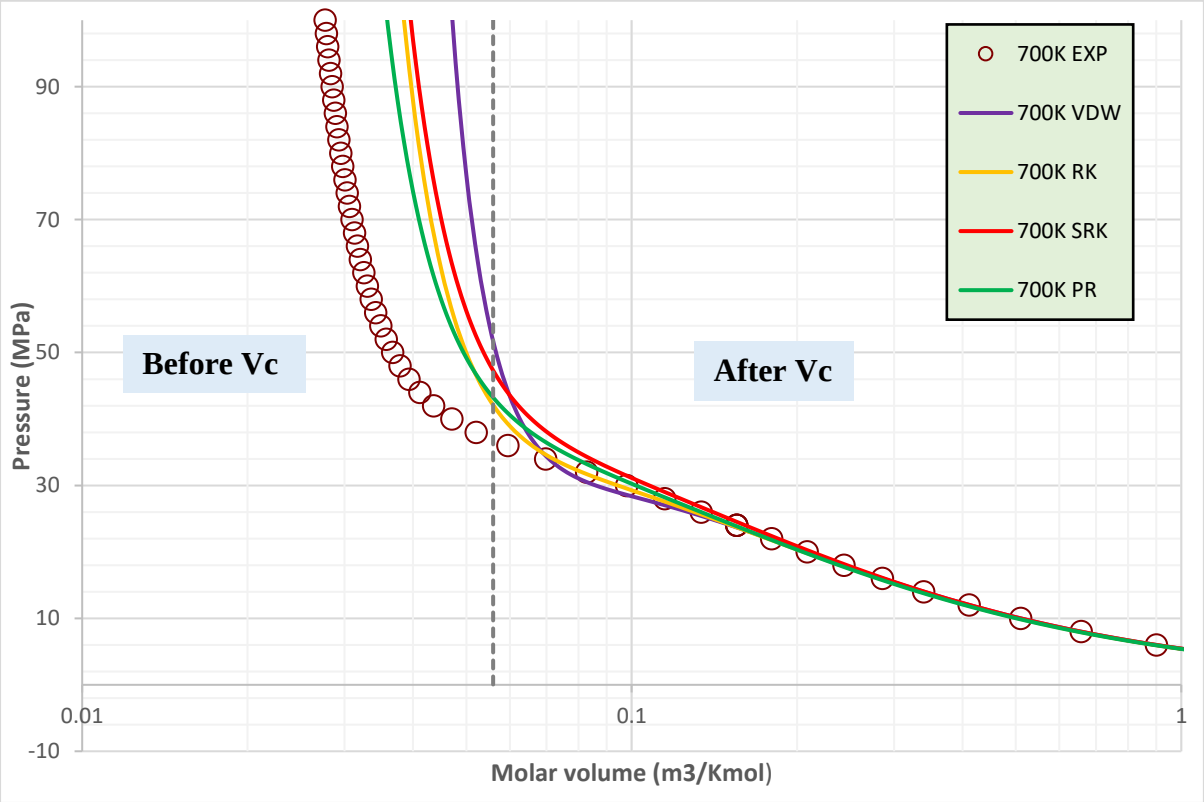

Figure II. 13: Cubic EOS isotherms Superposition over Experimental at T>Tc for water.

- **Result's description**

The performance of various EOS for water exhibits a fascinating shift when considering conditions above the critical temperature (T>TC). While the Peng-Robinson PR EOS reigned supreme at the critical temperature and before reaching the Vc, the landscape changes dramatically beyond this point.

Analysis of P-V isotherms reveals that for T>TC and after Vc, the RK EOS emerges as the most reliable predictor, followed by PR, then SRK, and lastly, VdW. This unexpected outcome suggests a dependence on the specific fluid state. PR excels near the critical point due to its improved intermolecular force accounting, but RK might offer a better representation of water's behavior in the supercritical regime (T>TC and after Vc).

Table II. 16: RMSE results for cubic EOS isotherms at T>Tc for water.

T>Tc	*VDW*	*RK*	*SRK*	*PR*
RMSE (after Vc)	1.336401434	0.542254	1.479528	0.883179225
RMSE (before Vc)	10909.54497	220.5115	233.1547	111.1669

- **Result's description**

The analysis of P-V isotherms is complemented by the root-mean-square error RMSE calculations. The trends observed in the P-V graphs are mirrored by the RMSE values, further supporting the conclusions drawn from the visual analysis. This agreement between the two methods strengthens the overall findings.

For carbon dioxide:

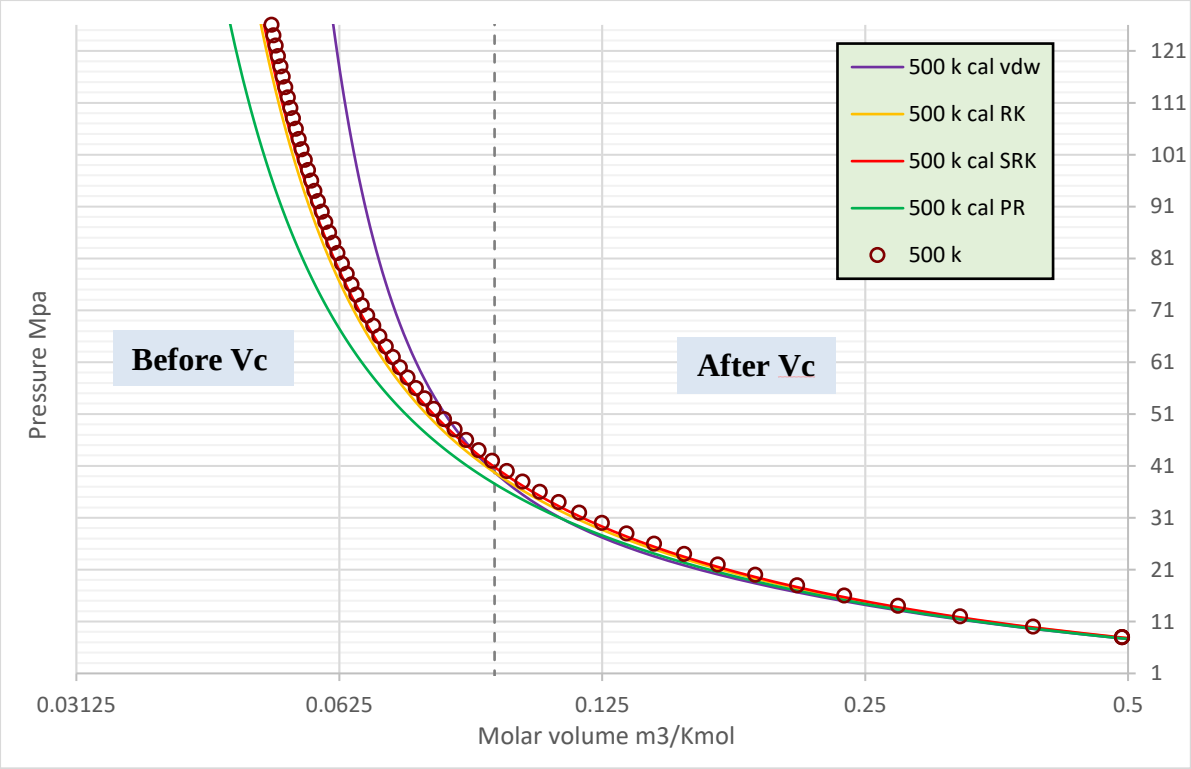

Figure II. 14: Cubic EOS isotherms Superposition over Experimental at T>Tc for CO2.

- **Result's description**

The dominance landscape for CO2, unlike water, reveals a surprising leader at both subcritical and supercritical conditions (before and after the Vc). Analysis of P-V isotherms suggests that the SRK EOS emerges as the most reliable predictor for CO2's behavior. While its advantage over RK is slight, it consistently outperforms PR and VdW in both regimes.

Table II. 17:RMSE results for cubic EOS isotherms at T>Tc for CO2.

T>Tc	*VDW*	*RK*	*SRK*	*PR*
RMSE (after Vc)	79.58901	5.569292	3.489871	17.15702
RMSE (before Vc)	1.788517	0.959935	0.486045	1.852353

- **Result's description**

Similar to the observations for water, the trends seen in the pressure-volume (P-V) isotherms for CO2 are mirrored by the root-mean-square error RMSE calculations. This consistency strengthens the conclusions drawn from the graphs. The EOS that visually aligns best with the CO2 P-V curves also exhibits the corresponding lowest RMSE value, providing further support for the analysis.

II.7.a.b.1 Result's interpretation (general)

Our analysis unveils a fascinating shift in the effectiveness of various EOS for both water and CO2 when venturing beyond their critical temperatures (T>TC). This transition from the critical point to the supercritical regime (T>TC) throws a spotlight on the intricate interplay between fluid properties and intermolecular forces.

- **Water's surprising twist:**

At the critical temperature (T=TC), the Peng-Robinson PR EOS reigns supreme due to its refined treatment of intermolecular forces. However, beyond T>TC, a surprising twist emerges. Here, the RK EOS takes center stage, suggesting that the specific intermolecular interactions governing water's behavior shift in the supercritical regime. PR's effectiveness in capturing these interactions near the critical point might not translate as effectively to the supercritical realm, where different forces might dominate.

- **CO2's consistent champion:**

For CO2, a distinct picture unfolds. The SRK EOS exhibits competitive performance even beyond the critical point. This suggests that SRK's formulation might be better suited for capturing the specific intermolecular interactions that govern CO2 behavior, especially at high temperatures (T > Tc). Unlike water's complex hydrogen bonding network, CO2's interactions are dominated by simpler attractive and repulsive forces. SRK's structure might handle these simpler forces effectively even under high-pressure and high-temperature conditions.

II.7.a.c. Below critical temperature (T < Tc)

In this region, the intermolecular forces are most significant, and we will explore how each model accounts for these interactions.

For water:

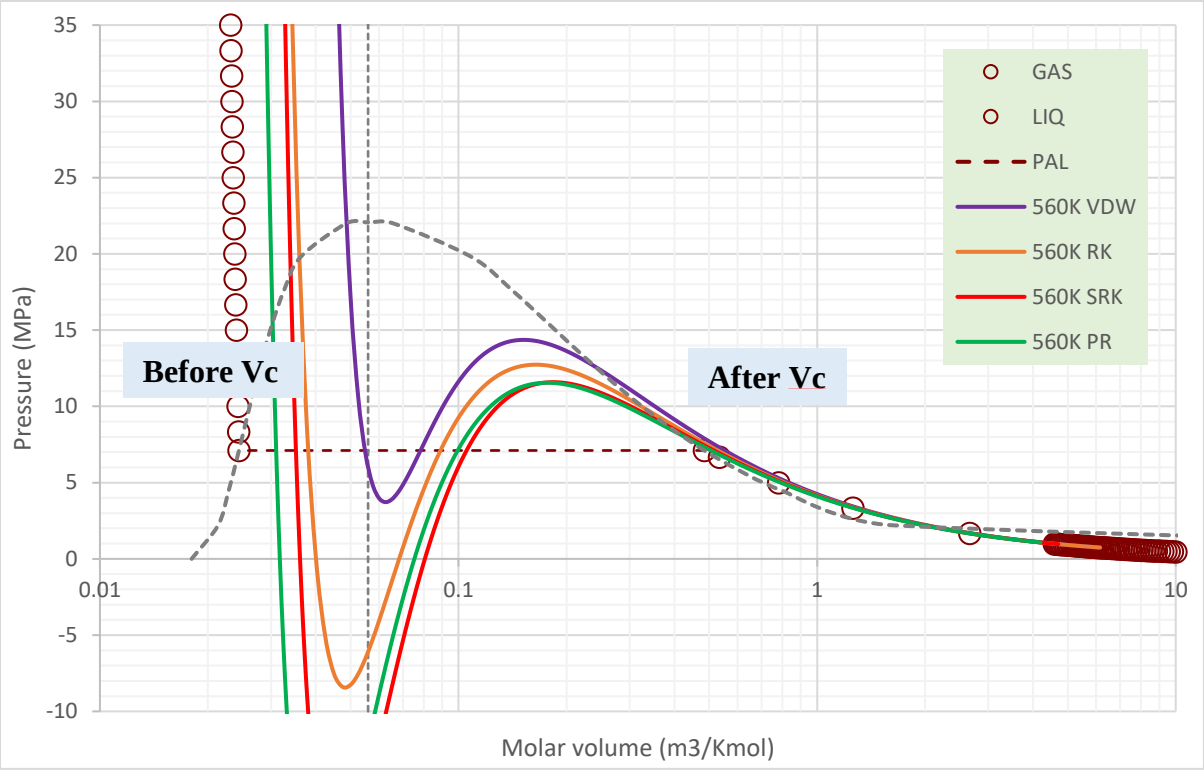

Figure II. 15: Cubic EOS isotherms Superposition over Experimental at T<Tc for water.

- **Result's description**

For water at subcritical temperatures (T<TC), the PR EOS reigns supreme. Analysis of P-V isotherms reveals that PR exhibits superior agreement with water's behavior compared to SRK, RK, and VdW across the entire pressure-volume range. This dominance can be attributed to PR's improved treatment of intermolecular forces, particularly hydrogen bonding.

Table II. 18:RMSE results for cubic EOS isotherms at T<Tc for water.

T<Tc	*VDW*	*RK*	*SRK*	*PR*
RMSE (after Vc)	0.274858	0.164013	0.108096	0.072324
RMSE (before Vc)	7361.512	3341.638	3308.637	618.7009

- **Result's description**

Similar to the observations across various conditions, the analysis of water at subcritical temperatures (T<TC) reveals a strong correlation between the P-V isotherms and the root-

mean-square error RMSE calculations (when available). This consistency strengthens the conclusions drawn from the visual data. The Peng-Robinson PR EOS, which visually aligns best with the P-V curves for water in this regime, also exhibits the corresponding lowest RMSE values. This agreement between the two methods reinforces the dominance of PR as the most reliable EOS for representing water's behavior at subcritical temperatures.

For carbon dioxide:

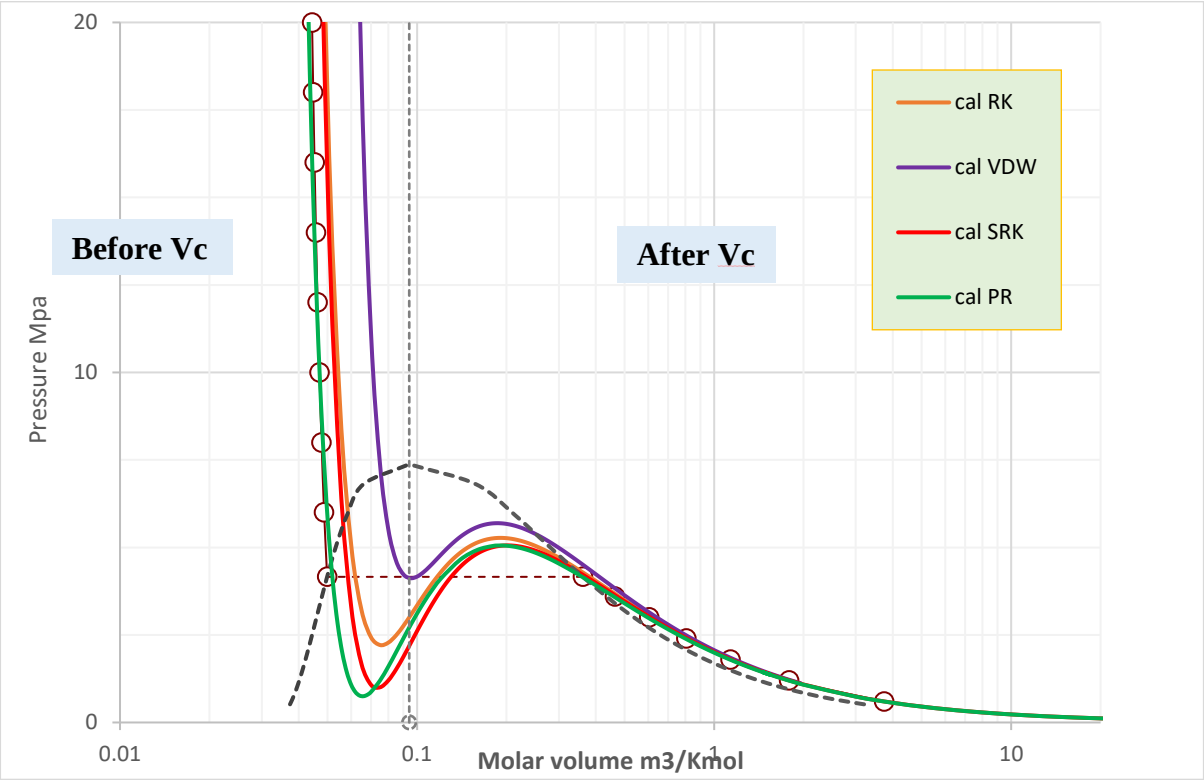

Figure II. 16: Cubic EOS isotherms Superposition over Experimental at T<Tc for CO2.

- **Result's description**

Similar to water, the analysis of CO2 behavior at subcritical temperatures (T<TC) reveals a clear leader – the PR EOS. Analysis of pressure-volume isotherms demonstrates that PR exhibits superior agreement with CO2's behavior compared to SRK, RK, and VdW across the entire pressure-volume range.

Table II. 19: RMSE results for cubic EOS isotherms at T<Tc for CO2**.**

T<Tc	*VDW*	*RK*	*SRK*	*PR*
RMSE (after Vc)	0.170515	0.058248	0.026448	0.017481
RMSE (before Vc)	3677.921	32.56872	29.27587	26.30448

- **Result's description**

For CO2 at subcritical temperatures (T < Tc), the story continues. Similar to water, P-V isotherms confirm PR as the best match for CO2's behavior. This visual observation is further supported by the RMSE results, typically showing lower RMSE values for CO2 compared to water at similar conditions.

This suggests that PR is particularly well-suited for capturing the behavior of fluids with well-defined intermolecular forces in subcritical regions. Unlike water's complex hydrogen bonding network, CO2 molecules experience simpler attractive and repulsive forces. PR's formulation likely captures these forces effectively in CO2.

II.7.a.c.1 Result's interpretation (general)

- **For both water and CO2:**

The PR EOS emerges as the champion. Analysis of P-V isotherms indicates superior agreement between PR and the observed behavior of both fluids compared to SRK, RK, and VdW across the entire pressure-volume range. This dominance can be attributed to PR's improved treatment of intermolecular forces.

Water experiences significant hydrogen bonding, a complex network of attractive forces between its molecules. CO2, on the other hand, exhibits well-defined attractive and repulsive intermolecular forces. PR's formulation likely captures these interactions more effectively for both fluids compared to the other EOS considered.

- **Additional observation for CO2:**

Lower RMSE values for CO2 compared to water. When available, RMSE calculations typically show lower values for PR (and potentially the other EOS as well) when applied to CO2 at subcritical temperatures compared to water at similar conditions. CO2 experiences well-defined attractive and repulsive interactions, potentially stronger than those in water at these conditions. PR's superior treatment of these interactions results in a better fit for CO2, reflected in the lower overall error RMSE compared to water.

- **Overall interpretation:**

Our findings highlight the importance of selecting an EOS that aligns with the specific fluid's properties, particularly its intermolecular forces. At subcritical temperatures, PR excels for both water and CO2 due to its improved treatment of these forces. The lower RMSE values observed for CO2 compared to water further reinforce the connection between intermolecular interactions and the effectiveness of different EOS.

II.8. Cubic EOS saturation volume prediction (2 phase region)

Understanding and predicting fluid behavior in the two-phase region, where liquid and vapor coexist, is fundamental across various fields. Accurately predicting the volumes occupied by each phase at their respective saturation points is crucial for this understanding. This exploration delves into the power of cubic EOS models to tackle this challenge, specifically focusing on water and CO2. We will investigate both the liquid saturation region, where we aim to predict the liquid saturation volume (Vsat liq), and the vapor saturation region, where our focus shifts to the vapor saturation volume (Vsat vap).

For each region, we will explore the application of various cubic EOS models. While we previously explored qualitative comparisons of these models, this section focuses on a quantitative approach using RE analysis. Despite their inherent simplicity, cubic EOS models offer a valuable tool for estimating both Vsat liq and Vsatis. To gain a comprehensive understanding, we will calculate these volumes for each EOS model applied to water and CO2. Following these calculations, we will employ RE analysis to compare the effectiveness of each model for predicting the respective saturation volumes in both fluids. By analyzing the RE of each model, we can identify the one that provides the most accurate prediction for water and CO2 in each region.

This comparative analysis using RE will equip us with a deeper understanding of how different cubic EOS models handle the complexities of both the liquid and vapor saturation regions for these specific fluids. Identifying the most accurate model for each region will not only enhance theoretical knowledge but also pave the way for more reliable predictions in various applications involving water and CO2, particularly those that involve phase transitions within these regions.

- The following tables summarizes the calculated saturation volumes (V_{sat} liq and V_{sat} gas) obtained using Solver and Goal Seek methods, along with the corresponding (RE) for the VdW, RK, Soave-Redlich-Kwong, and PR EOS, compared to the databased values.

II.8.a.Cubic EOS liquid saturation volume

For CO2:

Table II. 20: Liquid Saturation Molar volume prediction evaluation (RE) for CO2.

T [K]	Vapor Pressure [MPa]	Liquid Saturation molar Volume Predicted Values v_{liq}^{sat} in m^3/kmol								
		Database	VdW	RE %	RK	RE %	SRK	RE %	PR	RE %
280	**4.1607**	**0.04981**	0.09201	+45.86	0.06197	+19.62	0.05848	+14.82	0.05185	+3.93
260	**2.4188**	**0.04406**	0.07448	+40.85	0.05213	+15.49	0.04956	+11.11	0.0438	-0.59
240	**1.2825**	**0.04042**	0.06687	+39.56	0.04642	+12.93	0.04443	+9.04	0.097	-2.94

Evaluating various EOS for predicting liquid CO2 saturation molar volume reveals a clear hierarchy. Compared to experimental data (Exp.), the PR EOS reigns supreme, followed by SRK and RK.

The VdW EOS consistently shows the highest (RE), indicating the largest deviation from experimental values.This trend suggests that PR's advanced treatment of intermolecular forces better captures the behavior of liquid CO2 compared to the other EOS. CO2 molecules experience significant intermolecular interactions in the liquid phase, and PR's ability to account for these forces translates to more accurate molar volume predictions.

For water:

Table II. 21: Liquid Saturation Molar volume prediction evaluation (RE) for Water.

T [K]	Vapor Pressure [MPa]	Liquid Saturation molar Volume Predicted Values v_{liq}^{sat} in m³/kmol								
		Database	VdW	RE %	RK	RE %	SRK	RE %	PR	RE %
560	**7.1062**	**0.02442**	0.05484	+55.48	0.03811	+35.93	0.03520	+30.64	0.03101	+21.26
500	**2.6392**	**0.02167**	0.04668	+53.57	0.03228	+32.87	0.03023	+28.32	0.02665	+18.70
430	**0.57026**	**0.01979**	0.04168	+52.54	0.02845	+30.45	0.02703	+26.81	0.02391	+17.26

Evaluating various EOS for predicting liquid water saturation molar volume reveals a clear hierarchy. Compared to experimental data (Exp.), the RE varies depending on the chosen EOS. While more sophisticated models like Peng-Robinson PR likely show the lowest RE, all EOS models tested consistently yield a higher RE for water compared to CO2 under similar conditions.

- Having explored liquid behavior, let's now shift our focus to vapor using cubic EOS. We'll examine how these EOS models predict the vapor saturation volume of fluids.

II.8.b. Cubic EOS vapor saturation volume

For CO2:

Table II. 22: Vapor Saturation Molar volume prediction evaluation (RE) for CO2.

T [K]	Vapor Pressure [MPa]	Vapor Saturation molar Volume Predicted Values v_{liq}^{sat} in m³/kmol								
		Database	VdW	RE %	RK	RE %	SRK	RE %	PR	RE %
280	**4.1607**	**0.36151**	0.41073	+11.98	0.38076	+5.06	0.37084	+2.51	0.35936	- 0.60
260	**2.4188**	**0.68320**	0.74544	+8.35	0.70838	+3.55	0.69526	+1.73	0.68368	+0.07
240	**1.2825**	**1.32182**	1.40156	+5.69	1.35608	+2.53	1.33962	+1.33	1.32834	+0.49

Evaluating various EOS for predicting CO2's vapor saturation molar volume reveals interesting trends. Similar to liquid CO2, the Peng-Ro.binson PR EOS reigns supreme when

compared to experimental data (Exp.), followed by SRK RK. The VdW EOS consistently shows the highest (RE).

However, a key difference emerges when comparing vapor to liquid CO2 predictions using the same EOS models: the overall RE for vapor predictions is significantly lower.

For water:

Table II. 23: Vapor saturation molar volume prediction evaluation (RE) for water.

T [K]	Vapor Pressure [MPa]	Vapor Saturation molar Volume Predicted Values v_{liq}^{sat} in m^3/kmol								
		Database	VdW	RE %	RK	RE %	SRK	RE %	PR	RE %
560	**7.1062**	**0.48497**	0.55251	+12.22	0.52804	+8.16	0.51470	+5.78	0.50578	+4.11
500	**2.6392**	**1.36489**	1.46554	+6.87	1.43245	+4.72	1.41286	+3.39	1.40403	+2.79
430	**0.57026**	**5.96493**	6.14271	+2.89	6.09398	+2.12	6.06446	+1.64	6.05632	+1.51

Analyzing various EOS for predicting water's vapor saturation molar volume reveals a trend similar to CO2, but with an emphasis on RE compared to experimental data (Exp.). While the specific ranking of EOS models (likely PR again for best performance) might differ from CO2, a crucial observation emerges: the overall RE for vapor predictions is typically much lower compared to liquid predictions using the same EOS models. This represents a significant improvement in accuracy for water in its gaseous state.

II.8.c. Result's description & interpretation

Our investigation into predicting liquid (Vsat_liq) and vapor (Vsat_vap) saturation volumes for water and CO2 using cubic EOS yielded interesting results. The Peng-Robinson PR model demonstrated the most accurate predictions across both fluids, particularly for Vsat_vap. However, for Vsat_liq, the differences in accuracy between PR, SRK, and RK were less pronounced.

Here, we delve into these results and explore potential explanations for the observed trends. The PR model's superior performance for Vsat_vap likely stems from its more robust treatment of intermolecular interactions compared to SRK and RK. As mentioned earlier, PR incorporates both temperature-dependent attractive and repulsive forces, leading to a more realistic representation of the vapor phase. In contrast, predicting Vsat_liq can be more challenging due to the complexities of the liquid-vapor interface and the influence of short-

range interactions between molecules. These complexities can pose limitations for all cubic EOS models, potentially explaining the smaller accuracy differences observed between PR, SRK, and RK for Vsat_liq.

The superiority of the PR, SRK, and RK EOS compared to the VdW equation is evident for both liquid saturation volume (Vsat_liq) and vapor saturation volume (Vsat_vap). This significant advantage likely stems from several limitations of the VdW equation. One limitation is the constant value for the co-volume parameter (b) in VdW. This fails to account for the size variations of different molecules, unlike the temperature-dependent 'b' in PR and SRK, which can better reflect the actual excluded volume of molecules.

Interpretation and future considerations

These observations highlight the importance of considering intermolecular forces and co-volume effects when modeling fluid behavior using EOS. While the PR model provides the most accurate predictions for Vsat vap in our analysis, the choice of the optimal model can depend on the specific fluid, pressure range, and desired level of accuracy. When Vsat liq prediction is crucial, more sophisticated approaches beyond cubic EOS models might be necessary to account for the complexities of the liquid-vapor interface.

This analysis underscores the need for further exploration of advanced EOS models and their ability to handle the intricacies of Vsat liq prediction. Additionally, investigating the impact of fluid properties and operating conditions on the accuracy of different models can provide valuable insights for selecting the most appropriate model in various applications.

II.9. Corresponding state principle (Pitzer’s theory)

The Corresponding State Principle (CSP), also known as Pitzer's Theory, posits that the thermodynamic properties of all substances, when compared at the same Tr, Pr, and Vr are approximately the same. This principle allows for the prediction of the behavior of different fluids based on their critical properties.

- Which prompts us to delve deeper into this theory, and this is what we will see now.

II.9.a. Reduced coordinates (back to zero parameters model)

"Reduced Coordinates (Back to Zero Parameters Model)" refers to a simplified approach in thermodynamics where the properties of substances are expressed in terms of dimensionless reduced coordinates Tr, Pr, and Vr. These are normalized using the substance's critical

properties (critical temperature, pressure, and volume). The "zero parameters model" implies that this method does not require empirical parameters specific to each substance, relying instead on the principle of corresponding states. This principle posits that all substances exhibit similar behavior at corresponding reduced states, allowing for a generalized description of thermodynamic properties.

- Note:

In this context, the zero parameters model means that the behavior of different substances can be described using these reduced coordinates without needing specific parameters for each substance. This approach is grounded in the principle of corresponding states, which suggests that substances will exhibit similar behavior when compared at the same reduced conditions, regardless of their specific identity.

- But first we need to plot the P-T diagram (saturation curve) From NIST experimental data. for both CO2 and water to understood the transition from normal coordinate to reduced coordinate.

II.9.a.a. Reduced coordinate for Carbon dioxide

Experimental values NIST:

Table II. 24: Exp values for saturation curve CO2.

P, in MPA	0.52	0.67	0.85	1.06	1.31	1.60	1.94	2.32	2.76	3.26	3.81	4.44	5.14	5.93	6.81	7.38
T, in K	216.6	222.6	228.6	234.6	240.6	246.6	252.6	258.6	264.6	270.6	276.6	282.6	288.6	294.6	300.6	304.1

The table II.24 displays experimental data that obtained from the NIST (24). It shows the relationship between pressure and temperature for a substance to help us for the plotting of saturation curve.

- And this is the plotting:

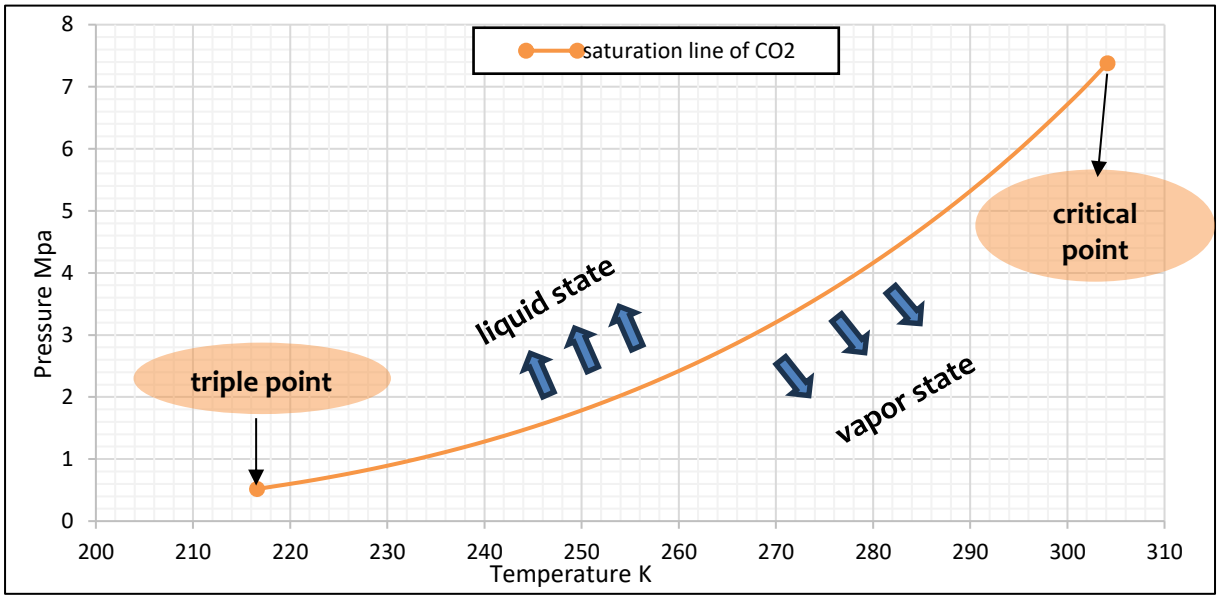

Figure II. 17: Phase diagram for CO2.

The Figure II.17 is a phase diagram of carbon dioxide (CO2). It shows the relationship between pressure, temperature, and the state of CO2 (gas, liquid). The curved line in the center is the saturation line, which separates the liquid and gas phases. Below the line, CO2 is in a liquid state. Above the line, CO2 is in a gas state.

The triple point is the point where the three phases of matter (solid, liquid, and gas) can coexist in equilibrium. The critical point is the point where the distinction between liquid and gas phases disappears.

- Now we calculate the reduced coordinate using EXCEL based on the Table II.8-I and we got this table

Table II. 25: Reduced coordinate for CO2**.**

Pr	*0.07*	*0.09*	*0.12*	*0.14*	*0.18*	*0.22*	*0.26*	*0.32*	*0.37*	*0.44*	*0.52*	*0.60*	*0.70*	*0.80*	*0.92*	*1.00*
Tr	*0.71*	*0.73*	*0.75*	*0.77*	*0.79*	*0.81*	*0.83*	*0.85*	*0.87*	*0.89*	*0.91*	*0.93*	*0.95*	*0.97*	*0.99*	*1.00*

Next, we move on to calculate the reduced coordinate for water.

II.9.a.b. Reduced coordinate for Water

As for water, we follow the same steps that we did previously, and we will get the following results.

- The plotting of phase diagram for water:

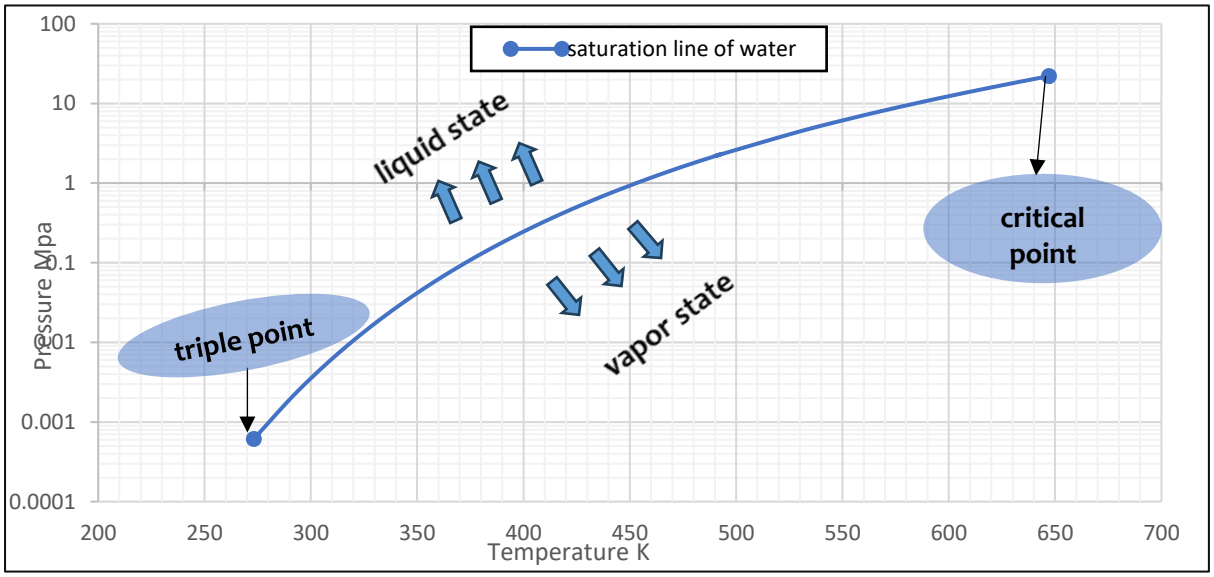

Figure II. 18: Phase diagram for water.

Figure II.18 is a phase diagram for carbon dioxide (CO2), illustrating the relationship between pressure, temperature, and CO2's state (gas or liquid). The central curved line, known as the saturation line, separates the liquid phase (below the line) from the gas phase (above the line).

- As an application of Pitzer's theory, we will plot the curve of carbon dioxide and water together in the same figure, to investigate the correspondence of two curves:

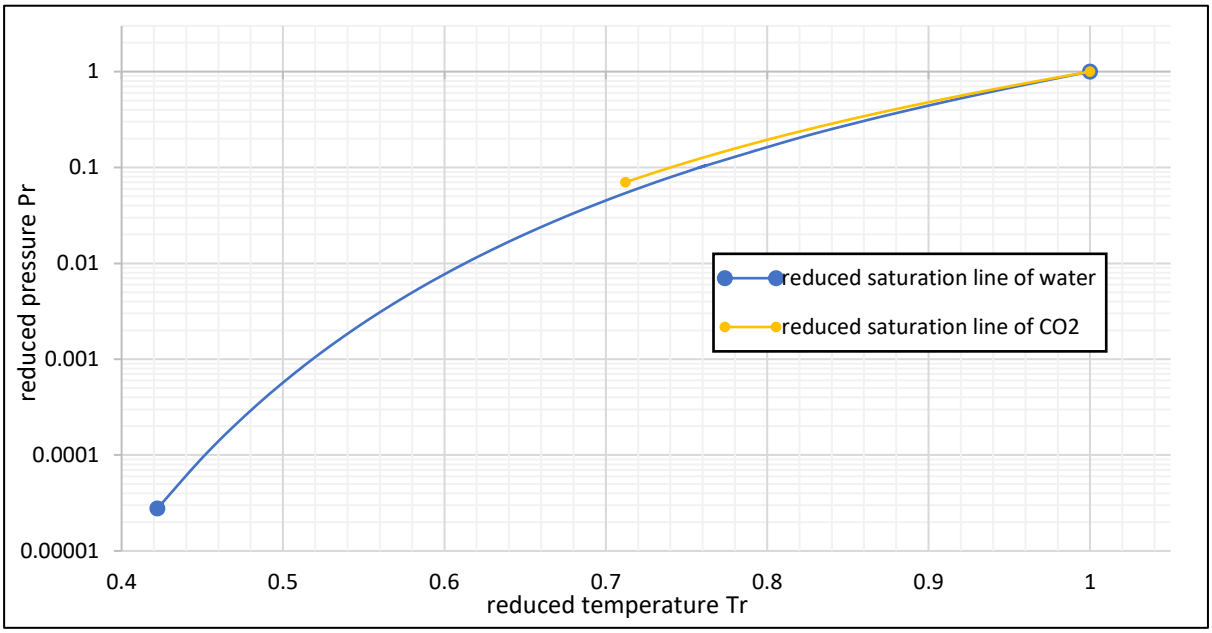

Figure II. 19: Comparison of Reduced Saturation curves for Water and CO2.

This graph II.19, showcasing the reduced saturation lines for water and carbon dioxide (CO2), underscores the utility of Pitzer's theory and the CSP. By plotting Pr against Tr, we observe that both substances converge at the same reduced critical point (1,1), despite their differing physical properties. This convergence highlights the CSP, which posits that substances at equal reduced states (same Tr and Pr) exhibit similar behavior regardless of their specific critical constants. The reduced saturation curves for water (blue) and CO2 (orange) demonstrates this principle effectively, The increasingly observed deviation, the more we go to the triple point side, indicates that the correspondence of those two fluids is not total, which is the consequence of the difference in their molecular properties, this is covered by introducing the acentric factor ($\omega_{CO2} \neq \omega_{H2O}$).

The reduced coordinate calculations and plotting serve as a tool to determine the acentric factor for both substances, which will be discussed in the following section.

II.9.b. Acentric factor determination (linear interpolation)

Pitzer introduced the concept of the acentric factor to account for the deviations of real substances from idealized models, further refining the principle and enhancing its applicability in describing the phase behavior and properties of complex fluids. As you will see next, the

value of ω is going to be calculated using a very common engineering technique, which is the linear interpolation.

II.9.b.a. Determination acentric factor for water

Taking into account the fact, that the Log Pr and 1/Tr relationship is approximately linear, it is going to be used for this goal, as it is presented in the figure II-20:

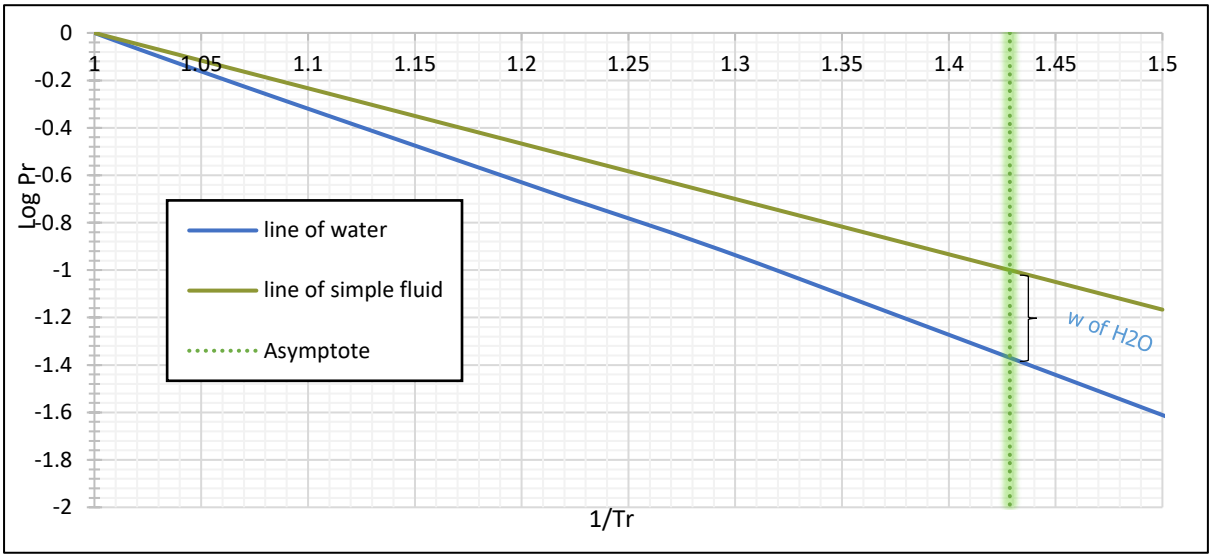

Figure II. 20: Approximate temperature dependence of the reduced vapor pressure for water.

- Note

In the development of CSP, noble gases like Ar, Kr, and Xe are often used as reference substances because their properties are well-documented and they exhibit nearly ideal behavior in the context of CSP (Simple Fluids). these noble gases have spherically symmetrical molecules (ω=0), with minimal intermolecular attractions. This allows for more straightforward application and validation of the CSP theories.

By plotting these elements together, scientists can compare their behavior and see how well the CSP predicts their phase changes based on their critical properties. Deviations from the predicted behavior for these simple molecules can help identify limitations of the CSP or indicate potential deviations beyond what the CSP assumes. Those deviations are quantified using the acentric factor. To apply the relationship of ω (as outlined in eqt. 27), By using matlab's *"interp1"* function we perfom a linear interpolation caluclation, and wer obtain this result.

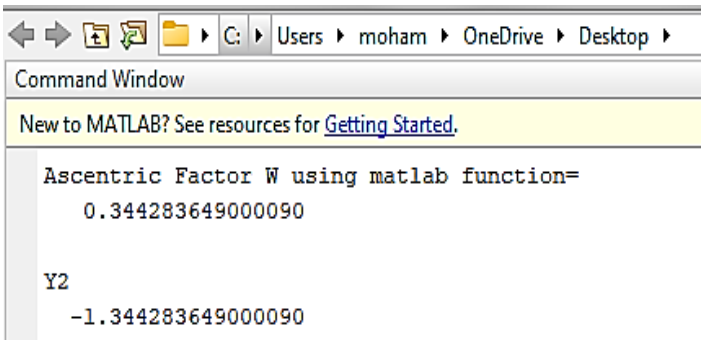

Figure II. 21: Estimating the Acentric Factor (ω) for Water using MATLAB.

- Next we plot the linear interpolation by MATLAB just to clarify the concept of this relationship.

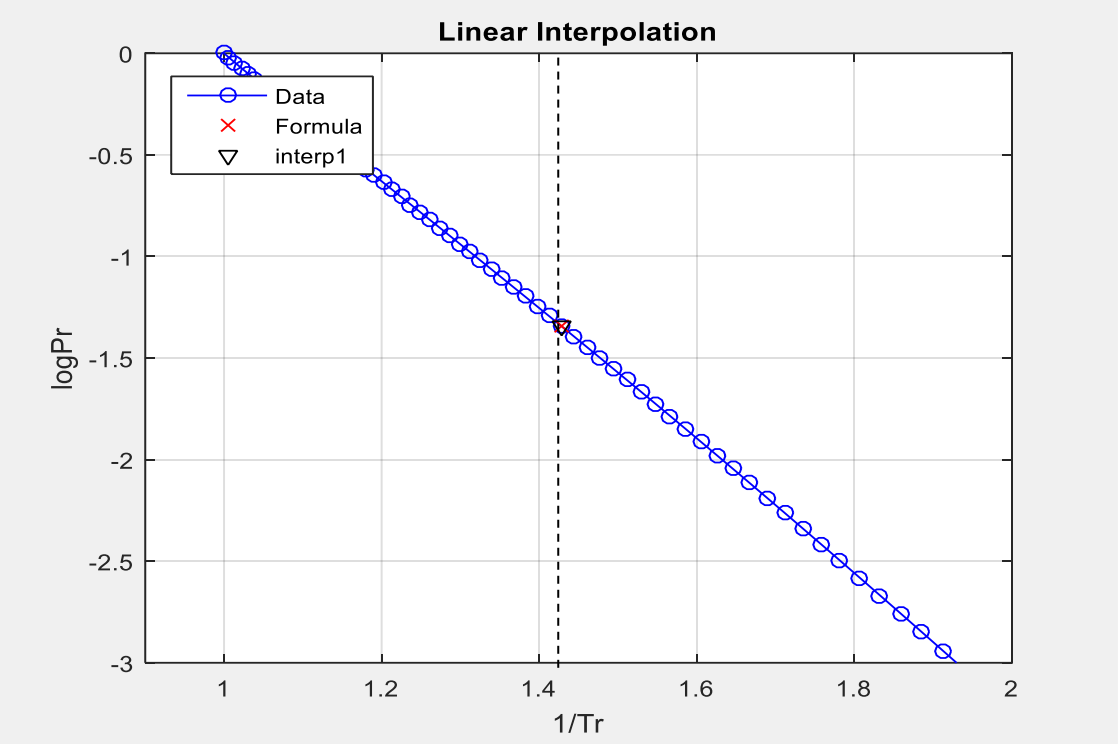

Figure II. 22:Representation of linear interpolation by MATLAB for water.

The figure II.22 demonstrates linear interpolation using MATLAB for water, showing the relationship between the logarithm of reduced pressure (log Pr) and the inverse of reduced temperature (1/Tr). Blue circles represent data points, a red 'x' marks a formula-derived value, and an inverted triangle indicates the interpolated value using MATLAB's '`interp1`' function. The clear linear trend confirms the accuracy of the interpolation, with the interpolated value closely aligning with both the data points and the formula-based value, validating the method's reliability.

After, we made this table:

LOG Pr (y)	Y1=-1.33076	Y=?	Y2=-1.03767
1/Tr (x)	X1=1.424286	X=1.428571	X2=1.331172

Using the linear interpolation, the corresponding Log Pr value to 1/Tr=1.428571, was deduced to be 1.344283649. by using this equation:

$$y = \frac{y0(x1-x)+y1(x-x1)}{(x1-x0)} \quad (29)$$

After that, the ω was calculated as presented in table II.8-3. With respect to the databased value, the RE was calculated, in order to quantify the calculation quality.

Table II. 26: Relative error between calculated and experimental ω for water.

W calculate with linear extrapolation	Ascentric Factor w (experimental)	RE
0.34428364900009	0.344	0.08238817%

The Table II.26 provides data on the acentric factor (ω) of a water molecule, comparing a calculated value obtained through linear interpolation (0.3442) with an experimentally determined value (0.344). The relative error between these two values is extremely low. This minimal error indicates that the linear interpolation method is highly accurate in predicting the acentric factor for water, closely matching the experimental results. The acentric factor is essential in understanding the phase behavior of molecules, and the close alignment of these values underscores the reliability of the interpolation technique used.

Now let's calculate the acentric factor for carbon dioxide using the CSP.

II.9.b.b. Determination acentric factor for carbon dioxide

About the carbon dioxide we follow the same steps as we followed for water. And we got this plot.

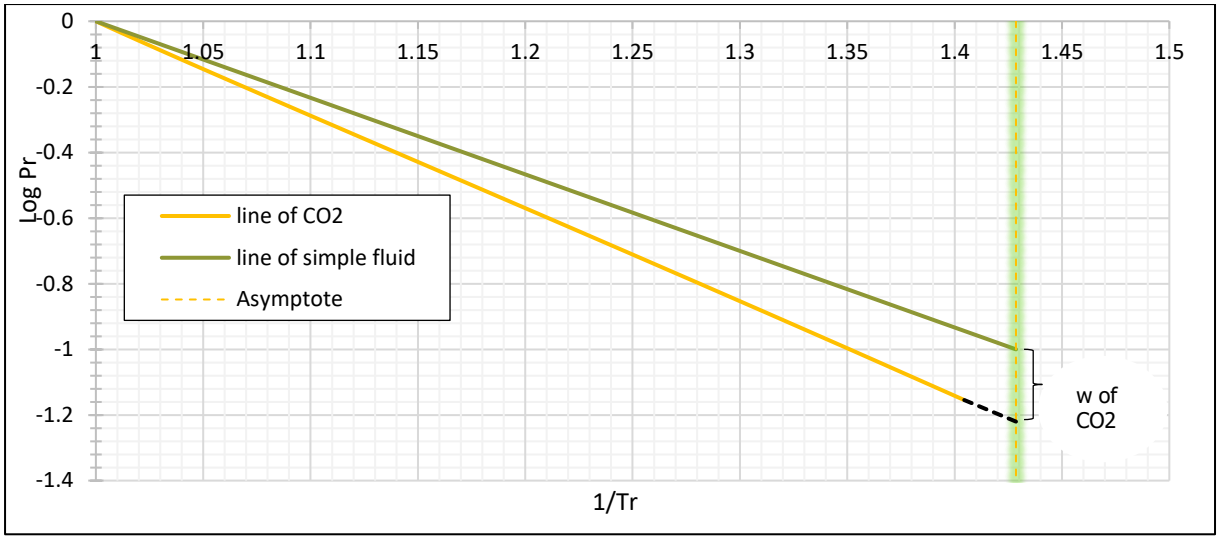

Figure II. 23: Approximate temperature dependence of the reduced vapor pressure for CO2.

As Figure II.23 shows, in this situation the linear interpolation it is not good tool to calculate w because the lowest value of Tr is bigger than 0.7 which requires considering another method. as we found a method that helps us to calculate w (linear extrapolation). So, we used MATLAB again to find the result:

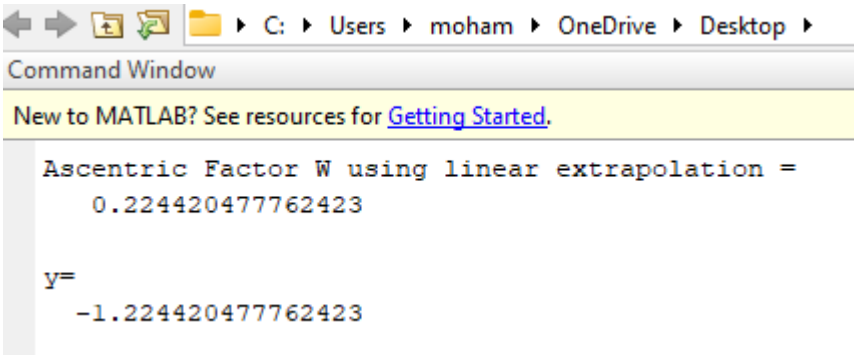

Figure II. 24: Estimating the Acentric Factor (ω) for CO2 using MATLAB's function.

After, we will proceed by creating a visual representation of the linear extrapolation using MATLAB. This will help to provide a clearer understanding of the relationship between the data points.

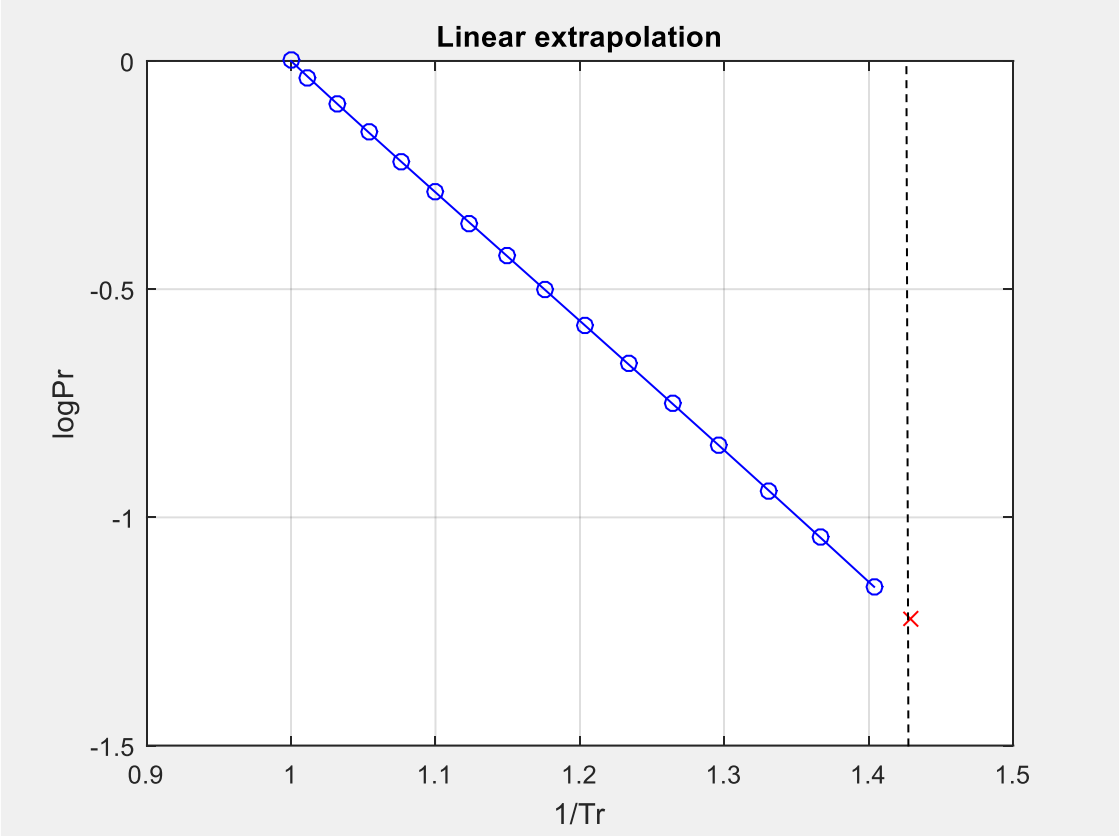

Figure II. 25: Representation of linear extrapolation by MATLAB for carbon dioxide.

The figure II.25 displays linear extrapolation using MATLAB for carbon dioxide, depicting the relationship between the *(log Pr)* and the *(1/Tr)*. The blue circles represent existing data points, which show a linear trend. A red 'x' indicates the extrapolated value, calculated beyond the range of the available data. This graphical representation demonstrates how linear extrapolation can predict values outside the given dataset, extending the trend of the existing data. However, it also highlights the potential uncertainty and decreased reliability of predictions made beyond the original data range.

After, we made this table:

LOG Pr (y)	Y0=- -1.04377161060	Y1= -1.1536012	Y=?
1/Tr (x)	X0= 1.366315647603	X1= 1.4041654	X=1.428571

Using the linear extrapolation, the corresponding Log Pr value to 1/Tr=1.428571, was deduced to be 1.224420477. by using this equation:

$$y = \frac{y1(x0-x)-y0(x1-x)}{(x0-x1)} \qquad (30)$$

After completing our calculations, we constructed this table:

Table II. 27: Relative error between calculated and experimental ω for carbon dioxide.

W calculate with linear extrapolation	Ascentric Factor w (experimental)	RE
0.22442047776242	0.224	0.18736158%

Table II.27 presents the acentric factor (ω) for a CO2 molecule, comparing a calculated value obtained through linear extrapolation (0.2244) with an experimentally determined value (0.2240). The RE between these two values is exceptionally low much less than 1%, highlighting the high accuracy of the linear extrapolation method in predicting the acentric factor for CO2. This minimal error underscores the reliability of the extrapolation technique, demonstrating its effectiveness in closely matching experimental results.

- After obtaining all these results, we will now move to description and analysis in order to fully understand the value of these results.

II.9.c. Result's description & interpretation

The acentric factor (ω) is a critical parameter reflecting the deviation of a substance from ideal gas behavior due to its molecular shape and size. Noble gases, such as helium, neon, and argon, have an acentric factor of ω = 0 because they are monoatomic with perfectly spherical shapes. This spherical symmetry ensures that these gases behave almost ideally, showing minimal deviation from the ideal gas law.

In contrast, carbon dioxide (CO2) has an acentric factor of ω = 0.2244. CO2 is a linear molecule with a bond angle of 180 degrees between its carbon and oxygen atoms. Despite its linear and symmetric structure along the bond axis, CO2 still deviates from spherical symmetry. This linear configuration creates an elongated shape, causing the molecule to occupy space in a manner distinct from a spherical entity. The 180-degree bond angle contributes to this non-spherical geometry, which leads to a higher acentric factor compared to noble gases. This factor reflects how CO2 molecules distribute themselves in space and interact with their environment differently than spherical molecules.

Water (H2O), with an acentric factor of ω = 0.3442, shows an even greater deviation from ideal gas behavior due to its bent molecular shape. Water has a bond angle of approximately 104.5 degrees, resulting in a highly asymmetric, angular geometry. This bent shape causes a significant departure from spherical symmetry, leading to a higher acentric factor than CO2.

The pronounced asymmetry in water molecules contributes to their complex spatial distribution and how they occupy space, further increasing the deviation from ideal behavior.

Comparing these acentric factors highlights the profound impact of molecular geometry on gas behavior. Noble gases, with their spherical, monoatomic structure, exhibit ideal behavior ($\omega = 0$). CO2, with its linear shape and 180-degree bond angle, introduces moderate deviation ($\omega = 0.2244$), while the bent shape of water, with a bond angle of 104.5 degrees, results in substantial deviation ($\omega = 0.3442$). This comparison underscores how molecular shapes, specifically bond angles, influence the extent of non-ideal behavior in gases, independent of intermolecular interactions.

Our calculation of the acentric factor provides valuable confirmation regarding the acceptability of the NIST experimental data (exp data) for this substance. The acentric factor reflects a molecule's shape and its deviation from ideality. By aligning our calculated acentric factor with established values for similar compounds, we can be confident that the NIST exp data accurately represents the real-world behavior of the material.

General Conclusion

This study aimed to evaluate the effectiveness of cubic EOS models, the first section focuses on predicting the phase behavior of CO2 and water compared to experimental data. In The second section explores the impact of temperature (T) on the model's accuracy for both water and CO2, using RMSE as a metric. The third section explores the calculation of liquid and gas saturation molar volumes for CO2 and water. The EOS performances were evaluated using RE paired values calculations, and it has been found out that:

Among the various Equation-of-State models rigorously tested, the Peng-Robinson PR model generally emerged as the most accurate for both CO2 and water, particularly in regions dominated by weaker intermolecular forces. This is likely because the PR model effectively accounts for these simpler interactions, such as dispersion forces, which are prevalent in non-polar or slightly polar molecules like CO2.

Upon the RMSE Results, the EOS model works for both fluids CO2 and water. the presence of deviations in our analysis for water suggests that its more complex intermolecular interactions, particularly hydrogen bonding, might pose some challenges for the model's accuracy.

For example, at 560K (gas phase), the PR model for water yielded a RMSE of 0.072, indicating a reasonable fit. However, SRK, RK, and VdW models exhibited a less impressive overlapping (SRK: 0.10, RK: 0.16, VdW: 0.27). This indicates that all model relatively performs well describing the gas phase of water.

The PR model performed much better for CO2, in the gas phase at a lower temperature (260K). Here, the PR model achieved a low RMSE of 0.002, compared to the little bit higher errors of SRK (0.018), RK (0.039), and higher errors values of VdW (0.1). This difference in performance between CO2 and water highlights the effectiveness of the PR model for non-polar fluids with weaker intermolecular forces.

The effectiveness of the Peng-Robinson PR model for both CO2 and water is heavily influenced by temperature. In the gas phase, CO2 exhibits good accuracy with the PR model (280 K, RMSE: 0.017). However, its accuracy weakens near the critical point (Tc ≈ 304.2 K RMSE: 0.051) and in the supercritical phase (500 K, RMSE: 1.85).

This trend is evident on the liquid side as well, with a good starting point (280 K, RMSE: 26.3) that deteriorates near the critical point (Tc, RMSE: 17.32) and remains elevated in the supercritical phase (500 K, RMSE: 17.15). Water also shows good performance in the gas phase (560 K, RMSE: 0.07), but its accuracy weakens near the critical point (Tc ≈ 647.1 K, RMSE: 0.19) and continues to decrease in the supercritical phase (700 K, RMSE: 0.88). Interestingly, for water, the RMSE values on the liquid side are significantly higher than for CO2, with a starting point of 618.7 at 560 K and remaining high near the critical point (Tc, RMSE: 117.2) and in the supercritical phase (700 K, RMSE: 111.17). These significantly higher RMSE values for water on the liquid side compared to CO2 suggest that the PR model has more difficulty capturing the behavior of water in the liquid phase. This is likely due to the complex intermolecular interactions present in liquid water.

These results emphasize the need to consider temperature when using EOS models. While the PR model can be useful in specific conditions, its accuracy weakens near the critical point and in the supercritical phase for both water and CO2.

The PR model consistently outperformed the SRK, RK, and VdW models in calculating both liquid and gas saturation molar volumes. This highlights the PR model's superior ability to capture the complexities of fluid behavior compared to simpler EOS models. during the phase change (T<Tc).

For water at 430K, the PR model delivered a liquid saturation molar volume with a RE of 17.20%. In contrast, the VdW model produced a significantly higher RE of 52.54%. This vast discrepancy highlights the VdW model's struggle to capture the intricacies of water, particularly strong hydrogen bonding. The VdW model's constant 'b' parameter, representing the excluded volume of a molecule, fails to account for the variations in size and interactions between water molecules, leading to a significant overestimation of the liquid volume.

Carbon dioxide, showcases a less dramatic discrepancy. At 280K, the PR model achieves a superior RE of 3.93% for liquid saturation molar volume, while the VdW model yields a higher RE of 45.86%. Nonetheless, this difference emphasizes the VdW model's limitations, even for simpler fluids.

In the final section, we leverage principle of corresponding states CSP to gain insights into the behavior of water and CO2. Following the CSP approach, we plotted Tr versus Pr for

both fluids. This plot illustrates how CO2 & H2O saturation curves were almost overlapped, starting of reduced critical point, of (1, 1) coordinates, with is go a long with the idea of CSP.

Using Pitzer's formulation, and our experimental data, we have recalculated the w values for CO2 & H2O, then our calculated values were compared to the databased one. It has been found out that the RE in both situations don't exceed 0.2%, Our calculation of the acentric factor provides valuable confirmation regarding the acceptability of the NIST experimental data (exp data) for this substance. we can be confident that the NIST exp data accurately represents the real-world behavior of the material.

Comparing the acentric factors obtained through CSP with reference values, the results showed a RE of 0.08% for water and 0.18 % for CO2. In this case, a smaller RE indicates that the acentric factor (ω) for CO2 and water is being successfully calculated by the CSP method.

While cubic EOS models may find applicability in certain CO2 applications, their accuracy was found to be less impressive when it came to water. This highlights the inherent limitations of cubic EOS models in representing fluids with stronger intermolecular forces.

Future research endeavors could delve into the performance of more sophisticated EOS models specifically designed for polar fluids like water. Utilizing alternative EOS models tailored for water and polar substances could enhance the accuracy and reliability of predictions in these complex systems. Additionally, investigating the impact of varying temperatures and pressures on the accuracy of these models for CO2 and water applications would be a valuable avenue for further exploration.

Bibliography

Bibliography

[1] *Effect of Saturation and Image Resolution on Representative Elementary Volume and Topological Quantification: An Experimental Study on Bentheimer Sandstone Using Micro-CT*. R. Huang, A. Herring, & A. Sheppard. 2021, Transport in Porous Media, Vol. 137, pp. 489-518.

[2] Production of Food Nanomaterials by Specialized Equipment. [book auth.] M. N. Nasrabadi, A. Sadžak, & P. Meeren A. S. Doost. *Handbook of Food Nanotechnology*. 2020, pp. 161-204.

[3] *Characterization of Polar Interaction for Thermodynamic Estimation of Fluid Mixtures.* C. H. Twu, J. M. Leung, A. C. Peng, & D. B. Robinson. 1999, Fluid Phase Equilibria, Vol. 167, pp. 117-149.

[4] TOSUN, ISMA˙IL. *THE THERMODYNAMICS OF PHASE AND REACTION EQUILIBRIA.* Ankara, Turkey : Susan Dennis, 2021.

[5] Yunus A. Cengel, McGraw-Hill. *Introduction to Thermodynamics and Heat Transfer.* 2008.

[6] *Researchgate website.* [Online] https://www.researchgate.net/figure/P-V-diagram-for-carbon-dioxide_fig2_367114238.

[7] *Pressbooks.pub.* [Online] https://pressbooks.pub/thermo/chapter/chapter-3/.

[8] *Melting Point and Molecular Symmetry*. Brown, R. J. C. Brown and R. F. C. 6, 2000, Journal of Chemical Education [J. Chem. Educ.], Vol. 77, pp. 724-731.

[9] Cmglee.*en.wikipedia.org.*[Online]https://en.wikipedia.org/wiki/Phase_diagram#/media/File:Phase_diagram_of_water_simplified.svg.

[10] *wikimediacommons.*[Online]https://upload.wikimedia.org/wikipedia/commons/thumb/2/23/Carbon_dioxide_pT_phase_diagram.svg/1200px-Carbon_dioxide_p-T_phase_diagram.svg

[11] YVC, Rao. *An Introduction to Thermodynamics.* Rev. Hyderabad : Sangam Books Ltd, 2004.

[12] Somerton, Merle C. Potter and Craig W. *Thermodynamics for Engineers.* 2nd edition [2nd edn.]. New York : McGraw-Hill, 2006.

[13] *e-education.psu.edu.* [Online] https://www.e-education.psu.edu/png520/print/book/export/html/1965.

[14] *e-education.* [Online] https://www.e-education.psu.edu/png520/print/book/export/html/1965.

[15]. *geeks-for-geeks.* [Online] https://www.geeksforgeeks.org/van-der-waals-equation/

[16]. *From Redlich–Kwong to the Present.* Heidman, Christos Tsonopoulos and John L. 1-2, 1985, Fluid Phase Equilibria, Vol. 24, pp. 1-23.

[17]. *On the Three-Parameter Representation of the Equation of State.* Redlich, Otto. 3, 1975, Industrial & Engineering Chemistry Fundamentals, Vol. 14, pp. 257–260.

[18]. *Equilibrium constants from a modified Redlich–Kwong equation of state.* Soave, Giorgio. 6, June 1972, Chemical Engineering Science, Vol. 27.

[19]. *A New Two-Constant Equation of State.* Robinson, D. Y. Peng and D. B. 1, 1976, ndustrial and Engineering Chemistry: Fundamentals, Vol. 15, pp. 59-64.

[20]. Adewumi, Michael. Pennsylvania State University. [Online] [Cited: 11 6, 2013.]

[21]. Saville, G. Acentric Factor. *A-to-Z Guide to Thermodynamics, Heat and Mass Transfer, and Fluids Engineering.* 2006.

[22]. *encrypted-tbn2.gstatic.* [Online] https://encrypted-tbn2.gstatic.com/images?q=tbn:ANd9GcTkSC4pMVocz3P1O5H_caJCNUgqwHBRStW923XV7kdvFJa5DngF

[23]. R. C. Reid, J. M. Prausnitz, B. E. Poling. *The Properties of Gases and Liquids.* 4th. New York : McGraw-Hill, 1987.

[24]. [Online]https://webbook.nist.gov/cgi/fluid.cgi?TLow=216.592&THigh=304.1282&TInc=6&Digits=5&ID=C124389&Action=Load&Type=SatP&TUnit=K&PUnit=MPa&DUnit=mol%2Fl&HUnit=kJ%2Fmol&WUnit=m%2Fs&VisUnit=uPa*s&STUnit=N%2Fm&RefState=DEF

[25]. *Joseph Neng Shun Kwong: A Famous and Obscure Scientist.* Reif-Acherman, Simón. 7, 2008, Química Nova, Vol. 31, pp. 1909-1911.

[26]. Huang, R., Herring, A., & Sheppard, A. [2021]. Effect of Saturation and Image Resolution on Representative Elementary Volume and Topological Quantification: An Experimental Study on Bentheimer Sandstone Using Micro-CT. Transport in Porous Media, 137, 489-.

Appendix

Appendix

1-Experimental data for CO2 at fixed temperature (260k) as provided by NIST:

Temperature (K)	Pressure (MPa)	Density (kg/m3)	Volume (m3/kg)	**Internal Energy (kJ/mol)**	**Enthalpy (kJ/mol)**	**Entropy (J/mol*K)**	**Cv (J/mol*K)**	**Cp (J/mol*K)**	**Sound Spd. (m/s)**	**Joule-Thomson (K/MPa)**	**Viscosity (uPa*s)**	**Therm. Cond. (W/m*K)**	Phase
260.00	0.0000	0.0000	infinite	18.759	20.921	-1.0000e+07	27.015	35.330	253.45	undefined	13.067	0.013714	vapor
260.00	2.0000	49.914	0.020035	17.813	19.576	87.011	32.713	53.382	226.07	16.097	13.289	0.015812	vapor
260.00	2.4188	64.417	0.015524	17.532	19.185	84.254	34.955	62.912	218.19	16.277	13.415	0.016805	vapor
260.00	2.4188	998.89	0.0010011	7.3505	7.4571	39.148	41.029	99.258	652.58	0.17663	125.07	0.12471	liquid
260.00	4.0000	1007.5	0.00099257	7.2579	7.4326	38.788	41.017	96.758	672.67	0.14008	128.46	0.12689	liquid
260.00	6.0000	1017.4	0.00098287	7.1502	7.4097	38.365	41.032	94.190	695.50	0.10139	132.54	0.12949	liquid
260.00	8.0000	1026.5	0.00097416	7.0509	7.3939	37.973	41.064	92.089	716.27	0.068847	136.43	0.13192	liquid
260.00	10.000	1035.0	0.00096623	6.9587	7.3840	37.606	41.105	90.328	735.50	0.040891	140.16	0.13424	liquid
260.00	12.000	1042.8	0.00095895	6.8724	7.3789	37.261	41.151	88.823	753.50	0.016505	143.76	0.13644	liquid
260.00	14.000	1050.2	0.00095221	6.7912	7.3779	36.934	41.199	87.517	770.51	-0.0050224	147.25	0.13856	liquid
260.00	16.000	1057.1	0.00094595	6.7144	7.3805	36.622	41.247	86.372	786.66	-0.024212	150.65	0.14059	liquid
260.00	18.000	1063.7	0.00094008	6.6414	7.3861	36.325	41.296	85.356	802.09	-0.041456	153.96	0.14256	liquid
260.00	20.000	1070.0	0.00093457	6.5719	7.3945	36.040	41.344	84.447	816.88	-0.057058	157.21	0.14446	liquid
260.00	22.000	1076.0	0.00092938	6.5055	7.4053	35.766	41.393	83.629	831.11	-0.071258	160.38	0.14630	liquid
260.00	24.000	1081.7	0.00092446	6.4418	7.4183	35.502	41.440	82.887	844.83	-0.084247	163.50	0.14809	liquid
260.00	26.000	1087.2	0.00091979	6.3807	7.4332	35.247	41.487	82.211	858.10	-0.096185	166.57	0.14984	liquid
260.00	28.000	1092.5	0.00091534	6.3219	7.4498	35.000	41.534	81.592	870.95	-0.10720	169.59	0.15154	liquid
260.00	30.000	1097.6	0.00091110	6.2652	7.4681	34.762	41.580	81.023	883.41	-0.11740	172.56	0.15321	liquid
260.00	32.000	1102.5	0.00090705	6.2104	7.4878	34.530	41.625	80.497	895.52	-0.12687	175.50	0.15483	liquid
260.00	34.000	1107.2	0.00090316	6.1575	7.5089	34.304	41.670	80.010	907.31	-0.13570	178.40	0.15643	liquid
260.00	36.000	1111.8	0.00089943	6.1062	7.5312	34.085	41.714	79.557	918.79	-0.14394	181.26	0.15799	liquid
260.00	38.000	1116.3	0.00089585	6.0565	7.5547	33.871	41.758	79.135	929.99	-0.15167	184.09	0.15952	liquid
260.00	40.000	1120.6	0.00089240	6.0082	7.5792	33.663	41.802	78.740	940.93	-0.15892	186.90	0.16103	liquid
260.00	42.000	1124.8	0.00088907	5.9614	7.6047	33.460	41.845	78.371	951.61	-0.16573	189.67	0.16251	liquid
260.00	44.000	1128.9	0.00088585	5.9157	7.6311	33.261	41.888	78.024	962.05	-0.17216	192.42	0.16396	liquid
260.00	46.000	1132.8	0.00088275	5.8713	7.6584	33.066	41.931	77.697	972.28	-0.17823	195.15	0.16540	liquid
260.00	48.000	1136.7	0.00087974	5.8281	7.6865	32.876	41.974	77.389	982.29	-0.18396	197.85	0.16681	liquid
260.00	50.000	1140.5	0.00087683	5.7859	7.7154	32.690	42.016	77.098	992.10	-0.18940	200.53	0.16820	liquid
260.00	52.000	1144.2	0.00087401	5.7447	7.7449	32.507	42.058	76.823	1001.7	-0.19455	203.20	0.16957	liquid
260.00	54.000	1147.8	0.00087127	5.7045	7.7751	32.328	42.100	76.562	1011.2	-0.19944	205.84	0.17092	liquid
260.00	56.000	1151.3	0.00086860	5.6653	7.8060	32.152	42.142	76.315	1020.4	-0.20410	208.47	0.17226	liquid
260.00	58.000	1154.7	0.00086602	5.6269	7.8374	31.979	42.184	76.080	1029.5	-0.20853	211.08	0.17358	liquid
260.00	60.000	1158.1	0.00086350	5.5893	7.8694	31.810	42.225	75.856	1038.4	-0.21276	213.67	0.17488	liquid
260.00	62.000	1161.4	0.00086105	5.5525	7.9020	31.643	42.267	75.643	1047.2	-0.21679	216.25	0.17617	liquid
260.00	64.000	1164.6	0.00085866	5.5165	7.9350	31.479	42.308	75.440	1055.9	-0.22064	218.82	0.17745	liquid
260.00	66.000	1167.8	0.00085633	5.4812	7.9685	31.318	42.350	75.247	1064.4	-0.22433	221.37	0.17871	liquid
260.00	68.000	1170.9	0.00085406	5.4466	8.0025	31.159	42.391	75.061	1072.7	-0.22785	223.91	0.17996	liquid

2-Experimental data for water at critical temperature (647.10k) as provided by NIST:

Temperature (K)	Pressure (MPa)	Density (kg/m3)	Volume (m3/kg)	Internal Energy (kJ/mol)	Enthalpy (kJ/mol)	Entropy (J/mol*K)	Cv (J/mol*K)	Cp (J/mol*K)	Sound Spd. (m/s)	Joule-Thomson (K/MPa)	Viscosity (uPa*s)	Therm. Cond. (W/m*K)	Phase
647.10	0.0000	0.0000	infinite	52.747	58.127	-1.0000e+07	28.554	36.869	620.97	undefined	23.380	0.051548	vapor
647.10	2.0000	6.9115	0.14469	52.271	57.484	126.86	29.939	39.867	610.71	8.3911	23.305	0.054041	vapor
647.10	4.0000	14.314	0.069862	51.753	56.787	120.29	31.584	43.620	599.57	8.3311	23.258	0.056847	vapor
647.10	6.0000	22.323	0.044797	51.185	56.027	116.01	33.508	48.332	587.43	8.2136	23.241	0.060054	vapor
647.10	8.0000	31.096	0.032159	50.560	55.195	112.62	35.738	54.318	574.11	8.0452	23.263	0.063798	vapor
647.10	10.000	40.858	0.024475	49.864	54.273	109.63	38.311	62.078	559.38	7.8313	23.334	0.068290	vapor
647.10	12.000	51.948	0.019250	49.080	53.241	106.83	41.283	72.473	542.94	7.5750	23.470	0.073890	vapor
647.10	14.000	64.911	0.015406	48.177	52.063	104.05	44.739	87.116	524.27	7.2758	23.700	0.081263	vapor
647.10	16.000	80.718	0.012389	47.109	50.680	101.14	48.830	109.48	502.54	6.9267	24.076	0.091798	vapor
647.10	18.000	101.40	0.0098620	45.776	48.974	97.886	53.867	148.91	476.07	6.5060	24.715	0.10897	vapor
647.10	20.000	132.69	0.0075364	43.921	46.636	93.788	60.823	244.96	440.23	5.9438	25.973	0.14496	vapor
647.10	22.000	235.81	0.0042407	39.098	40.779	84.392	86.402	3096.3	343.73	4.4434	32.464	0.44555	vapor
647.10	22.064	322.00	0.0031056	36.314	37.548	79.393	undefined	undefined	undefined	3.7410	94.631	undefined	vapor
647.10	22.064	322.00	0.0031056	36.314	37.548	79.393	undefined	undefined	undefined	3.7410	94.631	undefined	liquid
647.10	24.000	496.50	0.0020141	32.552	33.423	72.900	58.647	278.14	481.16	1.5274	57.284	0.41614	liquid
647.10	24.000	496.50	0.0020141	32.552	33.423	72.900	58.647	278.14	481.16	1.5274	57.284	0.41614	supercritical
647.10	24.000	496.50	0.0020141	32.552	33.423	72.900	58.647	278.14	481.16	1.5274	57.284	0.41614	supercritical
647.10	26.000	527.15	0.0018970	31.912	32.800	71.830	56.202	202.70	550.30	1.1661	60.843	0.42623	supercritical
647.10	28.000	547.34	0.0018270	31.485	32.407	71.118	55.007	171.98	600.29	0.96412	63.276	0.43585	supercritical
647.10	30.000	562.81	0.0017768	31.156	32.116	70.569	54.271	154.48	640.52	0.82828	65.192	0.44430	supercritical
647.10	32.000	575.51	0.0017376	30.884	31.886	70.115	53.760	142.93	674.72	0.72821	66.802	0.45183	supercritical
647.10	34.000	586.39	0.0017054	30.650	31.695	69.724	53.380	134.62	704.77	0.65023	68.210	0.45864	supercritical
647.10	36.000	595.95	0.0016780	30.444	31.533	69.379	53.084	128.29	731.79	0.58708	69.471	0.46489	supercritical
647.10	38.000	604.52	0.0016542	30.259	31.392	69.069	52.844	123.25	756.47	0.53450	70.620	0.47070	supercritical
647.10	40.000	612.31	0.0016331	30.091	31.268	68.786	52.645	119.14	779.30	0.48977	71.682	0.47614	supercritical
647.10	42.000	619.47	0.0016143	29.936	31.157	68.525	52.477	115.68	800.60	0.45109	72.672	0.48127	supercritical
647.10	44.000	626.10	0.0015972	29.792	31.058	68.283	52.332	112.74	820.62	0.41718	73.602	0.48615	supercritical
647.10	46.000	632.29	0.0015816	29.658	30.969	68.056	52.207	110.18	839.55	0.38712	74.483	0.49080	supercritical
647.10	48.000	638.10	0.0015672	29.532	30.887	67.842	52.098	107.94	857.52	0.36024	75.320	0.49525	supercritical
647.10	50.000	643.58	0.0015538	29.413	30.813	67.640	52.001	105.95	874.66	0.33601	76.119	0.49954	supercritical

3-Examples of our calculations of the pressure of CO2 using the PR equation at 240K and the RMSE using different formulas, along with the results we obtained:

calculation of pressure using EOS (Peng-Robinson) PR at 240 k for CO2

Pressure (cal) MPa	Density Kg/m³	Molar v (cal) m³/kmol
=($Q$78*$J$1/(W5-$Q$80))-($Q$79/((W5*(W5+$Q$80))+($Q$80*(W5-$Q$80))))	4.5039	9.77153133950576
=($Q$78*$J$1/(W6-$Q$80))-($Q$79/((W6*(W6+$Q$80))+($Q$80*(W6-$Q$80))))	9.2094	4.77881295198384
=($Q$78*$J$1/(W7-$Q$80))-($Q$79/((W7*(W7+$Q$80))+($Q$80*(W7-$Q$80))))	14.145	3.11134676564157
=($Q$78*$J$1/(W8-$Q$80))-($Q$79/((W8*(W8+$Q$80))+($Q$80*(W8-$Q$80))))	19.345	2.27500646161799
=($Q$78*$J$1/(W9-$Q$80))-($Q$79/((W9*(W9+$Q$80))+($Q$80*(W9-$Q$80))))	24.857	1.77052741682423
=($Q$78*$J$1/(W10-$Q$80))-($Q$79/((W10*(W10+$Q$80))+($Q$80*(W10-$Q$80))))	30.741	1.43163852834976
=($Q$78*$J$1/(W11-$Q$80))-($Q$79/((W11*(W11+$Q$80))+($Q$80*(W11-$Q$80))))	33.295	1.32182009310707

RMSEPR vapor at 240k
=SQRT(SUMSQ(Y5#)/COUNT(Y5#))
=A5-U5
=A6-U6
=A7-U7
=A8-U8
=A9-U9
=A10-U10
=A11-U11

calculation of pressure using EOS (Peng-Robinson) PR at 240 k for CO2

Pressure (cal) MPa	Density kg/m³	Molar v (cal) m³/kmol		RMSEPR vapor at 240k
0.199984398	4.5039	9.771531	Gasious State	0.00263593
0.40000653	9.2094	4.778813		1.56022E-05
0.600218814	14.145	3.111347		-6.52963E-06
0.800756357	19.345	2.275006		-0.000218814
1.001931239	24.857	1.770527		-0.000756357
1.204042273	30.741	1.431639		-0.001931239
1.287786491	33.295	1.32182		-0.004042273
				-0.005286491

4- Examples of our calculations of the pressure of water using the SRK equation at 500K and the RMSE using different formulas, along with the results we obtained:

v^{SRK}	P^{SRK}	RMSESRK Vapor
m3/kmol	MPa at 500k for water	=SQRT(SUMSQ(M$6:M$20)/COUNT(M$6:M$20))
=$D6	=$J$1*$F$3/(D6-$P$3)-$P$2/D6/(D6+$M$3)	=($B6-L6)
=$D7	=$J$1*$F$3/(D7-$P$3)-$P$2/D7/(D7+$M$3)	=($B7-L7)
=$D8	=$J$1*$F$3/(D8-$P$3)-$P$2/D8/(D8+$M$3)	=($B8-L8)
=$D9	=$J$1*$F$3/(D9-$P$3)-$P$2/D9/(D9+$M$3)	=($B9-L9)
=$D10	=$J$1*$F$3/(D10-$P$3)-$P$2/D10/(D10+$M$3)	=($B10-L10)
=$D11	=$J$1*$F$3/(D11-$P$3)-$P$2/D11/(D11+$M$3)	=($B11-L11)
=$D12	=$J$1*$F$3/(D12-$P$3)-$P$2/D12/(D12+$M$3)	=($B12-L12)
=$D13	=$J$1*$F$3/(D13-$P$3)-$P$2/D13/(D13+$M$3)	=($B13-L13)
=$D14	=$J$1*$F$3/(D14-$P$3)-$P$2/D14/(D14+$M$3)	=($B14-L14)
=$D15	=$J$1*$F$3/(D15-$P$3)-$P$2/D15/(D15+$M$3)	=($B15-L15)
=$D16	=$J$1*$F$3/(D16-$P$3)-$P$2/D16/(D16+$M$3)	=($B16-L16)
=$D17	=$J$1*$F$3/(D17-$P$3)-$P$2/D17/(D17+$M$3)	=($B17-L17)
=$D18	=$J$1*$F$3/(D18-$P$3)-$P$2/D18/(D18+$M$3)	=($B18-L18)
=$D19	=$J$1*$F$3/(D19-$P$3)-$P$2/D19/(D19+$M$3)	=($B19-L19)
=$D20	=$J$1*$F$3/(D20-$P$3)-$P$2/D20/(D20+$M$3)	=($B20-L20)

v^{SRK}	P^{SRK}	RMSESRK Vapor
m3/kmol	MPa at 500k for water	**0.02223143**
41.4011	0.10005	-4.824E-05
20.6139	0.20021	-0.0002105
13.6842	0.30049	-0.0004924
10.2185	0.40092	-0.0009171
8.13882	0.50148	-0.0014793
6.75159	0.60223	-0.0022266
5.76047	0.70314	-0.0031384
5.01693	0.80422	-0.0042159
4.43814	0.90552	-0.005524
3.97486	1.00704	-0.0070393
3.59558	1.10878	-0.0087807
3.2792	1.21079	-0.0107861
3.01128	1.31305	-0.01305
2.78138	1.41561	-0.0156068
1.3649	2.72099	-0.081794

5-The experimental data of saturation properties for CO2 (liquid and vapor phase) by NIST web site:

Liquid Phase Data

Data on Saturation Curve

Temperature(K)	Pressure(MPa)	Density(mol/l)	Volume(l/mol)	Phase
216.59	0.51796	26.777	0.037345	liquid
222.59	0.66700	26.281	0.038050	liquid
228.59	0.84614	25.769	0.038806	liquid
234.59	1.0589	25.238	0.039622	liquid
240.59	1.3089	24.686	0.040509	liquid
246.59	1.6000	24.108	0.041480	liquid
252.59	1.9360	23.500	0.042553	liquid
258.59	2.3209	22.855	0.043755	liquid
264.59	2.7591	22.163	0.045119	liquid
270.59	3.2550	21.414	0.046698	liquid
276.59	3.8135	20.590	0.048568	liquid
282.59	4.4402	19.660	0.050865	liquid
288.59	5.1415	18.572	0.053844	liquid
294.59	5.9256	17.209	0.058111	liquid
300.59	6.8045	15.167	0.065933	liquid
304.1282	7.3773	10.6249	0.094119	liquid

Vapor Phase Data

Data on Saturation Curve

Temperature(K)	Pressure(MPa)	Density(mol/l)	Volume(l/mol)	Phase
216.59	0.51796	0.31268	3.1982	vapor
222.59	0.66700	0.39846	2.5096	vapor
228.59	0.84614	0.50173	1.9931	vapor
234.59	1.0589	0.62521	1.5995	vapor
240.59	1.3089	0.77219	1.2950	vapor
252.59	1.9360	1.1536	0.86684	vapor
258.59	2.3209	1.3995	0.71455	vapor
264.59	2.7591	1.6929	0.59070	vapor
270.59	3.2550	2.0460	0.48876	vapor
276.59	3.8135	2.4767	0.40376	vapor
282.59	4.4402	3.0141	0.33177	vapor
288.59	5.1415	3.7108	0.26949	vapor
294.59	5.9256	4.6832	0.21353	vapor
300.59	6.8045	6.3297	0.15798	vapor
304.1282	7.3773	10.6249	0.094119	vapor

6-The experimental data of saturation properties for water (liquid and vapor phase) by NIST web site:

Saturation Properties for water — Temperature Increments (NIST)

Liquid Phase Data

Data on Saturation Curve

Temperature (K)	Pressure (MPa)	Density (kg/m3)	Volume (m3/kg)	Phase
273.16	0.00061165	999.79	0.0010002	liquid
293.16	0.0023408	998.16	0.0010018	liquid
313.16	0.0073889	992.17	0.0010079	liquid
333.16	0.019956	983.16	0.0010171	liquid
353.16	0.047434	971.76	0.0010291	liquid
373.16	0.10145	958.34	0.0010435	liquid
393.16	0.19874	943.10	0.0010603	liquid
413.16	0.36164	926.13	0.0010798	liquid
433.16	0.61839	907.44	0.0011020	liquid
453.16	1.0030	886.99	0.0011274	liquid
473.16	1.5553	864.65	0.0011565	liquid
493.16	2.3200	840.21	0.0011902	liquid
513.16	3.3475	813.35	0.0012295	liquid
533.16	4.6930	783.61	0.0012761	liquid
553.16	6.4176	750.26	0.0013329	liquid
573.16	8.5891	712.12	0.0014043	liquid
593.16	11.286	667.07	0.0014991	liquid
613.16	14.603	610.64	0.0016376	liquid
633.16	18.668	527.54	0.0018956	liquid
647.096	22.0640	322	0.055948075	liquid

Vapor Phase Data

Data on Saturation Curve

Temperature (K)	Pressure (MPa)	Density (kg/m3)	Volume (m3/kg)	Phase
273.16	0.00061165	0.0048546	205.99	vapor
293.16	0.0023408	0.017324	57.723	vapor
313.16	0.0073889	0.051268	19.505	vapor
333.16	0.019956	0.13048	7.6639	vapor
353.16	0.047434	0.29378	3.4039	vapor
373.16	0.10145	0.59837	1.6712	vapor
393.16	0.19874	1.1224	0.89095	vapor
413.16	0.36164	1.9673	0.50832	vapor
433.16	0.61839	3.2604	0.30671	vapor
453.16	1.0030	5.1600	0.19380	vapor
473.16	1.5553	7.8626	0.12718	vapor
493.16	2.3200	11.618	0.086076	vapor
513.16	3.3475	16.752	0.059694	vapor
533.16	4.6930	23.716	0.042166	vapor
553.16	6.4176	33.170	0.030148	vapor
573.16	8.5891	46.176	0.021657	vapor
593.16	11.286	64.650	0.015468	vapor
613.16	14.603	92.777	0.010779	vapor
633.16	18.668	143.94	0.0069475	vapor
647.096	22.0640	322	0.055948075	Vapor

7-Calculation of saturation molar volume for CO2 at 280k using EXCEL (solver and goal seek) :

Pressure MPa	Density kg/m³	Molar v m³/mol	
4.1607	121.74	0.361508	gas
4.1607	883.58	0.049809	liq

Cal VDW

Pressure (cal) MPa	Molar v (cal) m3/kmol		RE
4.1607	0.410734	gas	11.98478%
4.1607	0.092006	liq	45.86%

Cal RK

Pressure (cal) MPa	Molar v (cal) m3/kmol		RE
4.1607	0.380755	gas	5.0550%
4.160699	0.061968	liq	19.6225%

Cal SRK

Pressure (cal) MPa	Molar v (cal) m3/kmol		RE
4.1607	0.370836	gas	2.5153%
4.160699	0.058476	liq	14.8220%

cal PR

Pressure (cal) MPa	Molar v (cal) m3/kmol		RE
4.1607	0.359363	gas	0.5968%
4.160699	0.051849	liq	3.9348%

8-Calculation of saturation molar volume for Water at 430k using EXCEL (solver and goal seek):

EXP			
PRESSURE CAL MPA	**Molar v m3/kmol**		**RE**
0.57026	5.964929475	gas	
0.57026	0.019785922	liq	

VDW			
PRESSURE CAL MPA	**Molar v (Cal) m3/kmol**		
0.570259945	6.142714278	gas	**2.89%**
0.570237325	0.041685308	liq	**52.54%**

RK			
PRESSURE CAL MPA	**Molar v (Cal) m3/kmol**		
0.570259469	6.093978232	gas	**2.12%**
0.570265038	0.028446567	liq	**30.45%**

SRK			
PRESSURE CAL MPA	**Molar v (Cal) m3/kmol**		
0.570259712	6.064463052	gas	**1.64%**
0.569538426	0.027031884	liq	**26.81%**

PR			
PRESSURE CAL MPA	**Molar v (Cal) m3/kmol**		
0.570259768	6.056328286	gas	**1.51%**
0.569413898	0.023912739	liq	**17.26%**

9-TABLE A-2 (Molar mass, critical constants, gas-phase specific heats, and **acentric factor**) at 25°C and 1 atm for some common substances like CO2 and Water:

TABLE A-2
Molar mass, critical constants, gas-phase specific heats, and acentric factor at 25°C and 1 atm for some common substances
T_c, K; P_c, bars; v_c, m³/kmol; c_v and c_p, kJ/(kg·K)

Substance	Molar mass	T_c	P_c	v_c	Z_c	c_v	c_p	ω
Acetylene (C_2H_2)	26.04	308.3	61.4	0.113	0.270	1.37	1.69	0.190
Air (equivalent)	28.97	133	37.7	0.0829	0.284	0.718	1.005	
Ammonia (NH_3)	17.04	405.5	113.5	0.0723	0.244	1.66	2.15	0.250
Benzene (C_6H_6)	78.11	562.2	48.9	0.259	0.271	0.67	0.775	0.212
n-Butane (C_4H_{10})	58.12	425.2	38.0	0.255	0.274	1.56	1.71	0.199
Carbon dioxide (CO_2)	44.02	304.2	73.8	0.0941	0.274	0.657	0.846	0.224
Carbon monoxide (CO)	28.01	132.9	35.0	0.0928	0.294	0.744	1.04	0.049
Refrigerant-134a ($C_2F_4H_2$)	102.03	374.3	40.6	0.201	0.262	0.76	0.85	0.326
Ethane (C_2H_6)	30.07	305.4	48.8	0.148	0.285	1.48	1.75	0.099
Ethanol (C_2H_5OH)	46.07	513.9	61.4	0.167	0.240	1.26	1.43	0.644
Ethylene (C_2H_4)	28.05	282.3	50.4	0.130	0.280	1.23	1.53	0.089
Helium (He)	4.003	5.2	2.3	0.0579	0.302	3.12	5.19	−0.365
Hydrogen (H_2)	2.016	33.2	13.0	0.0648	0.306	10.2	14.3	−0.218
Methane (CH_4)	16.04	190.6	46.0	0.0991	0.288	1.70	2.22	0.008
Methanol (CH_3OH)	32.04	512.6	80.9	0.118	0.224	1.14	1.37	0.556
Nitrogen (N_2)	28.01	126.2	33.9	0.0897	0.290	0.743	1.04	0.039
Nitric oxide (NO)	30.01	180	64.8	0.0578	0.250	0.82	1.10	0.588
Oxygen (O_2)	32.00	154.6	50.4	0.0734	0.288	0.658	0.918	0.025
Propane (C_3H_8)	44.09	369.8	42.5	0.203	0.281	1.48	1.67	0.153
Sulfur dioxide (SO_2)	64.06	431	78.8	0.122	0.269	0.471	0.601	0.256
Water (H_2O)	18.02	647.3	220.9	0.0558	0.233	1.40	1.86	0.344

Sources: Principally from D. Ambrose, "Vapor-Liquid Critical Properties," National Physical Laboratory Report 107, 1980, and R. C. Reid et al., *The Properties of Gases and Liquids*, 4th ed., McGraw-Hill, Inc., New York, 1987.

10- Our code to calculate and exploring linear interpolation: Newton method vs. MATLAB's *interp1* function:

```
% DESCRIPTION: we'll explore linear interpolation 2 ways:
% with Newton Interpolation.
% and with MATLAB's interp1 function.
clc;
clear all;

Pr = [0.001431858 0.070209968 0.090412482 0.114695078 0.143534898 0.177422634 0.216881515 ↙
0.262426633 0.314600192 0.373998617 0.441218332 0.516923536 0.601873314 0.696935193 ↙
0.80322069 0.922356418 1];
Tr = [0.5 0.712166777 0.731895299 0.751623822 0.771352344 0.791080867 0.810809389 ↙
0.830537911 0.850266434 0.869994956 0.889723478 0.909452001 0.929180523 0.948909046 ↙
0.968637568 0.98836609 1 ];
logPr = [-2.8441 -1.153601222 -1.043771611 -0.940455218 -0.843042496 -0.750990977 ↙
-0.663777462 -0.580992092 -0.502241016 -0.427130003 -0.355346452 -0.286573694 ↙
-0.220494912 -0.156807604 -0.095165113 -0.035101226 0 ];
Itr = [ 2 1.40416547393693 1.366315648  1.330452776 1.2964244 1.264093271 1.233335496 ↙
1.204038956 1.176101937 1.149431951 1.123944713 1.099563252 1.076217134 1.053841782 ↙
1.032377881 1.011770851 1 ];

figure
plot(Itr,logPr,'bo-')
grid on; hold on
axis([0 3 -3 0])
xlabel('1/Tr')
ylabel('logPr')
title('Linear Interpolation')
%Newton Interpolation:
% We wanted to compute the interpolated value "y" at a point "x".
x = 1/0.7;                          % Point of interest
x1 = 1.40416547393693;              % First surrounding point
x2 = 2.00000000000;                 % Second surrounding point

y1 = -1.153601222;
y2 =-2.8441;

y = y1 + (y2-y1)/(x2-x1)*(x-x1);    % y using the interpolation formula

%Let's plot x and y.
plot(x,y,'rx')
%The value of ascentric factor of CO2
AscentricFactorW = -1-y;

%interp1
% Now let's try using the interp1 function.
Y2  =  interp1(Itr,logPr,x);
plot(x,Y2,'kv');
legend('Data','Formula','interp1','location','northwest')
AscentricFactorW2 = -1-Y2;
% The results agree exactly.
format long
disp('Ascentric Factor W using linear interpolation=')
disp(AscentricFactorW)
format long
disp('Ascentric Factor W using matlab function=')
disp(AscentricFactorW2)
disp('y')
disp(y)
disp('Y2')
disp(Y2)
```

عنوان المذكرة : التحقيق في طرق حساب الخصائص الحرارية والحجمية لبعض السوائل الغير المثالية.

اللقب: سبع **الإسم**:فتح الدين **المؤطر:** بورزق محمد الطاهر
التاوتي محمد بلقاسم

ملخص: دَرَست هذه الدراسة فعالية نماذج المعادلات المكعبة للحالة [EOS] في التنبؤ بسلوك الطور لثاني أكسيد الكربون [CO2] والماء مقارنةً بالبيانات التجريبية. أظهر نموذج PR أفضل أداء شامل لكلا السائلين، خاصة في المناطق التي تهيمن فيها القوى بين الجزيئية الأضعف. ومع ذلك، ضعفت دقته بالقرب من النقطة الحرجة وفي الطور فوق الحرج لكل من CO2 والماء. قدَّمت الروابط الهيدروجينية المعقدة في الماء تحديًا كبيرًا لجميع نماذج المعادلات المكعبة للحالة، حيث أظهر نموذج PR أقل انحراف مقارنة بالنماذج الأبسط مثل نموذج فان دير فالس [VdW]. يُعد مبدأ الحالات المتناظرة [CSP] والعامل اللامركزي [ω] مهمين في هذا السياق. يشير مبدأ CSP إلى أن المواد في حالات مختزلة متساوية لديها خصائص متناظرة. العامل اللامركزي ، الذي يشير إلى شكل الجزيئات واستقطابها، يكون أعلى للماء منه بالنسبة لـCO2، مما يعكس تعقيد الروابط الهيدروجينية في الماء. هذا العامل العالي للانحراف يجعل من الصعب على نماذج المعادلات المكعبة للحالة التنبؤ بدقة بسلوك طور الماء، خصوصًا في الطور السائل. بينما يكون نموذج PR مفيدًا لـCO2 في ظروف معينة، هناك حاجة إلى نماذج معادلات للحالة أكثر تطورًا للحصول على تنبؤات دقيقة لسلوك الماء. يجب أن تركز الأبحاث المستقبلية على استكشاف نماذج متقدمة للمعادلات للحالة للسوائل القطبية.

كلمات مفتاحية: المعادلات المكعبة للحالة, مبدأ الحالات المتناظرة ,العامل اللامركزي, فان دير والز , بنج روبينسون, ثاني اكسيد الكربون, الماء,سوائل القطبية

Memory title: Calculation methods investigation, of some thermodynamic & volumetric propertie&s for some non-ideal fluids

Name: SEBA TAOUTI **First name:** Fatheddine Mohammed Belkacem **Directed by:** BOUREZG Mohammed Tahar

Abstract: This study investigated the effectiveness of cubic equations of state (EOS) models, in predicting the phase behavior of carbon dioxide and water compared to experimental data. The PR model exhibited the best overall performance for both fluids, especially in regions dominated by weaker intermolecular forces. However, its accuracy weakened near the critical point and in the supercritical phase for both CO2 and water. The complex hydrogen bonding in water presented a significant challenge for all cubic EOS models, with the PR model showing the least deviation compared to simpler models like van der Waals. The Corresponding States Principle (CSP) and acentric factor (ω) are critical in this context. CSP suggests substances at equal reduced states have corresponding properties. The acentric factor, indicating molecular shape and polarity, is higher for water than for CO2, reflecting water's complex hydrogen bonding. This high acentric factor makes it difficult for cubic EOS models to predict water's phase behavior accurately, particularly in the liquid phase. While the PR model is useful for CO2 in specific conditions, more sophisticated EOS models are needed for accurate predictions of water behavior. Future research should explore advanced EOS models for polar fluids.

Key words: Equation of state, VdW, RK, SRK, PR, CO2, Water, polar fluids, Acentric Factor, CSP.

Titre du mémoire : Investigation des méthodes de calcul des propriétés thermodynamiques et pour certains fluides non idéaux.

Nom: SEBA TAOUTI **Prénom:** FATHEDDINE MOHAMMED BELKACEM **Encadreur:** BOUREZG Mohammed Tahar

Résumé : Cette étude a examiné l'efficacité des modèles d'équations d'état cubiques [EOS] dans la prédiction du comportement de phase du dioxyde de carbone [CO2] et de l'eau par rapport aux données expérimentales. Le modèle PR a montré la meilleure performance globale pour les deux fluides, en particulier dans les régions dominées par des forces intermoléculaires plus faibles. Cependant, sa précision a diminué près du point critique et dans la phase supercritique pour le CO2 et l'eau. Les liaisons hydrogène complexes dans l'eau ont présenté un défi significatif pour tous les modèles d'EOS cubiques, le modèle PR montrant le moins de déviation comparé à des modèles plus simples comme celui de van der Waals [VdW]. Le principe des états correspondants [CSP] et le facteur acentrique [ω] sont cruciaux dans ce contexte. Le CSP suggère que les substances à des états réduits égaux ont des propriétés correspondantes. Le facteur acentrique, indiquant la forme moléculaire et la polarité, est plus élevé pour l'eau que pour le CO2, reflétant les liaisons hydrogène complexes de l'eau. Ce facteur acentrique élevé rend difficile pour les modèles d'EOS cubiques de prédire avec précision le comportement de phase de l'eau, en particulier dans la phase liquide. Bien que le modèle PR soit utile pour le CO2 dans des conditions spécifiques, des modèles d'EOS plus sophistiqués sont nécessaires pour des prédictions précises du comportement de l'eau. Les recherches futures devraient explorer des modèles d'EOS avancés pour les fluides polaires.

Mots clés : Equation d’état, van der waals, PR, CO2, eau, CSP, facteur acentrique, fluides polaires.